Catalytic Ethylene Polymerization

Novel Reactors for Kinetics in Gas, Slurry and Solution Processes

Michiel F. Bergstra

Samenstelling promotiecommssie:

Prof. dr. U. Karst, voorzitter	Universiteit Twente
Prof. dr. -ing. habil G. Weickert, promotor	Universiteit Twente
Prof. dr. ir. W.P.M. van Swaaij	Universiteit Twente
Prof. dr. ir. J.W.M. Noordermeer	Universiteit Twente
Prof. dr. K.-H. Reichert	Technische Universität Berlin, Duitsland
Prof. dr. L.L. Böhm	Universität Aachen, Duitsland
Ir. G. Mei, deskundige	Basell Polyolefins, Ferrara, Italië
Dr. ir. F. Van Buren, deskundige	Dow Benelux b.v., Terneuzen

CATALYTIC ETHYLENE POLYMERIZATION

PROEFSCHRIFT

ter verkrijging van
de graad van doctor aan de Universiteit Twente,
op gezag van de rector magnificus,
prof. dr. F.A. van Vught,
volgens besluit van het College van Promoties
in het openbaar te verdedigen
op donderdag 28 oktober 2004 om 16.45 uur

door

Michiel Friso Bergstra

geboren op 23 maart 1976

te Ede

Dit proefschrift is goedgekeurd door de promotor
Prof. dr. -ing. habil G. Weickert

Contents

Summary

The worldwide annual total polyethylene production by catalytic polymerization processes is approximately 31 million tons of high-density polyethylene (HDPE) and 19.6 million tons of linear low-density polyethylene (LLDPE). Most polyethylene (PE) products are used for packaging (film, bags, sealings, bottles/drums etc), due to its low cost price. Other important markets are piping and tubing, due to good chemical resistance and strength of PE and the automotive industry. These and even more advanced products need superior polymer properties, which are highly influenced by the polymerization conditions, kinetics and catalyst. Despite all research, only few academic research groups were able to provide information about polymerization kinetics or polymer properties at industrial, controlled conditions.

In this work a multi purpose setup has been developed for homo- and co-polymerizations of ethylene and 1-hexene in slurry and gas phase. Polymerization experiments have been executed in semi-batch mode with a heterogeneous metallocene catalyst under industrial conditions. During the gas-phase polymerizations the monomer concentrations have been measured and controlled online. The activities for both monomers were measured with flow meter techniques.
The presented polymerization kinetics were measured in a very accurate way isothermal within 0.2°C and isobaric within 0.15 bar. The concentrations of monomer and co-monomer were kept constant within 5% of the set point. All polymerization kinetics were measured with high reproducibility. The co-monomer effect was observed, the activity for ethylene was 50% higher in the presence of 1 mol% 1-hexene compared to a homo-polymerization.

Homo-polymerizations

Ethylene homo-polymerizations were executed with the silica supported Ind_2ZrCl_2/MAO catalyst using a so-called Reactive Bed Preparation method. This RBP method combines a slurry polymerization followed by a gas phase polymerization with the same polymerizing particles, i.e. a reactive bed. Polymerization kinetics were measured with high accuracy and reproducibility. The slurry and gas phase polymerization rates showed the same dependency on monomer bulk concentration. A complexation model has been proposed to describe the observed non-first order behavior on the monomer bulk concentration. This model also explains non-Arrhenius temperature dependence with a concentration dependence of the activation energy of the commonly used polymerization rate model: $R_p = k_p \cdot C^* \cdot M$

Summary

Gas phase co-polymerizations

Ethylene/1-hexene co-polymerizations have been presented with the same silica supported Ind_2ZrCl_2/MAO catalyst in gas phase. The influence of the co-monomer was examined at industrial process conditions. The reaction rate profiles of both monomers were measured and showed increasing activity with increasing co-monomer. The complexation model was extended for the co-monomer. This model can describe the large reaction rate increase even when only a small amount of co-monomer is incorporated. The co-polymerization equation derived from this mechanism is dependent on the two reactivity ratios, the monomer ratio and a ratio of the homo-polymerization constants. This is in contrast to the co-polymerization equation derived from a first order Markov model, which is only dependent on the reactivity ratios and the monomer ratio. The complexation model described rather well the measured reaction rates for both monomers and also the incorporated 1-hexene weight fraction. The produced polymers were analyzed on properties such as density, molecular weight, melt point and incorporated co-monomer mass fraction, which were found to be all highly dependent on the 1-hexene gas concentration and consequently the weight fraction. In-situ sorption of the co-monomer could be determined by combining the kinetic information with the incorporated co-monomer mass fraction. The polymer properties have been compared with a LLDPE produced with a Ziegler-Natta catalyst.

Solution polymerizations

Next to the multi purpose setup for slurry and gas phase ethylene polymerizations, an experimental setup has been developed for solution polymerizations at high temperature, i.e. above the melting point of polyethylene. This setup has been equipped with a so-called isothermal-isoperibolic heat-compensation temperature control. This means that the reactor temperature is controlled by an internal heating element in such a way that the total heat production, chemical and electrical heat, in the reactor is kept constant before and after catalyst injection.

A kinetic study has been presented of high temperature solution ethylene homo- and co-octene-polymerizations with a highly active and fast deactivating catalyst. The used catalyst had an initial polymerization rate up to 30.000 kg·g(cat)$^{-1}$·h^{-1} and lost more than 80% of it's activity within 2 minutes at 180°C and 30 bar. The new reactor has enabled to measure reproducible polymerization rate profiles within a few seconds after catalyst injection even at initial heat production rates of 3.8 kW at isothermal (±1 K) and isobaric (±0.05 bar) conditions. Catalyst decay could be described as second order deactivation.

Chapter 1

Introduction

History

In 1935, Perrin discovered that ethylene could be polymerized at very high pressure into a semi crystalline solid. This discovery at the ICI laboratories led to the commercialization of low-density polyethylene in 1938. Low density polyethylene is produced in supercritical ethylene at high pressure (600 till 3500 bar) and high temperature (200 till 350°C). This radical polymerization leads to a highly branched polyethylene (Whiteley 2002).

In 1950 Hogan and Banks, at the Phillips Petroleum Company, discovered that highly crystalline polyethylene could be produced at moderate temperature (70 till 100°C) and pressure (30 till 40 bar) with a catalyst containing chromium oxide on a silica support: the Phillips catalyst. (Whiteley 2002).

In 1953, Ziegler, at the University of Mülheim, discovered that highly crystalline polyethylene could be synthesized under very mild conditions, atmospheric pressure and temperatures between 50 and 100°C. Ziegler used a catalyst of titaniumchloride and alkylaluminum compounds. This Ziegler catalyst can easily co-polymerize ethylene with α-olefins producing polyethylene with densities varying from 0.960 till 0.880 kg/L; from high-density polyethylene till linear low-density polyethylene. In the late 1950s the first low-pressure catalytic solution process was commercialized at Hoechst, Frankfurt.

Metallocene catalysts were already known since the 1950s, but the breakthrough came after Reichert and Meyer (1973) added small amounts of water to titanocene/alkyl aluminum chloride systems. This resulted finally in methylaluminoxane (MAO), which proved to be a good co-catalyst for metallocene catalysts. In 1976 Kaminsky and Sinn (Kaminsky 1996) obtained a highly active catalyst with a metallocene complex and MAO. The polymers produced with metallocene catalysts have narrower molecular weight distributions and more uniform incorporation of co-monomers than polymers produced with Ziegler catalysts.

Polyethylene Processes

Hoechst's catalytic ethylene solution polymerization process was a scale-up of the laboratory synthesis as presented in Ziegler's Nobel Prize lecture (1964). The activity of Ziegler's catalyst was so low that the catalyst compounds had to be removed from the polyethylene. The major objective was to develop high activity catalysts, which resulted in low catalyst residues in the polymer. Throughout the years, Ziegler-Natta catalysts have been developed with such high productivities that catalyst removal from the polymer is not required anymore (Böhm 2003).

In 1978 the Unipol process was introduced. This gas phase fluidized bed reactor is economically attractive because the solvent recovery is eliminated. These developments have changed the polyethylene processes tremendously.

More recent developed polymerization technologies, like Spherilene and Borstar PE, have been developed in order to produce polymers with better properties. These processes use slurry and gas-phase reactors in series.

Solution polymerization processes acquired new importance because of their shorter residence times and ability for using modern homogeneous catalysts exhibiting improved co-monomer incorporation, like metallocene catalysts.

Catalyst design for solution processes does not require supporting of the catalyst on carriers like silica, which often broadens molecular weight distributions and lowers catalyst activity. These processes can operate in a wide range of co-monomer types and concentrations providing a wide range of product densities, and they are suitable for the production of lower molecular weight resins.

Nowadays the annual worldwide capacity is approximately 31 million tons for HDPE and 19.6 million tons for LLDPE. The demand is expected to grow for HDPE 5%/year and for LLDPE 6.7%/year (Chemical Week, July21/28 2004: 37). The latest trends are tailor made polymers. Superior polymer properties can be obtained by manipulating kinetics with process conditions in single reactors with different reaction zones (Covezzi and Mei 2001) or using two different catalyst on one support, Univation (Liu 2003). Improving polymer properties by manipulating kinetics can only be successful if the dependency of polymer properties on required process conditions are known. Despite all research, only few academic research groups were able to provide information about polymerization kinetics at industrial conditions or properties of polymers produced under industrial conditions.

Outline of the thesis

The objective of this work has been to measure kinetics at industrial and constant conditions (i.e. constant temperature, pressure and monomer concentrations) in different catalytic ethylene polymerization processes. During these kinetic experiments sufficient amounts of polymer have been produced for analyses. This provides relations between process parameters, kinetics and polymer properties. Kinetics and polymer properties have been examined with a metallocene catalyst for ethylene homo-polymerizations in slurry and gas phase and for ethylene co-polymerizations with 1-hexene in gas phase.

Next to that also a Ziegler-Natta catalyst system has been used for ethylene homo- and co-octene-polymerizations in solution phase at high temperature, above the melting point of polyethylene.

The presented work has been realized within a four year co-operation with Basell Polyolefins and an one year co-operation with Dow Benelux and the IPP research

group of the University Twente. New tools have been developed to measure more precisely kinetics and a large amount of new data has become available.

Chapter 2 describes the experimental set up, which was designed and implemented for homo-polymerizations in gas and slurry phase and for gas phase co-polymerizations. The novelty of this reactor is that from both monomers independently the reaction rate can be measured. Slurry, gas phase homo- and gas phase co-polymerizations will be discussed on the basis of reproducibility, temperature, pressure control and monomer concentration control.

Chapter 3 presents ethylene homo-polymerization in slurry and gas phase with silica supported Ind_2ZrCl_2/MAO catalyst. The slurry and gas phase homo-polymerization kinetics are compared with each other. The reaction rate is modeled with a complexation model, which describes the non-lineair behavior at low ethylene bulk concentration and the linear behavior at high ethylene bulk concentration.

Chapter 4 discusses ethylene 1-hexene gas phase co-polymerizations with the silica supported Ind_2ZrCl_2/MAO catalyst. The 1-hexene and ethylene concentration have been varied. The obtained kinetics are described with the complexation model extended for the co-monomer. Polymer properties will be discussed to quantify the LLDPE.

Chapter 5 describes the experimental set up, which enables to measure kinetics of ethylene polymerizations in solution phase at high temperature (above the melting point of PE). This reactor has an isothermal isoperibolic compensation temperature control, which allows measuring reaction rates up to 1 g/s (3800 Watt) already 10 seconds after catalyst injection at constant temperature and pressure.

Literature

Böhm, L. L. (2003). "The Ethylene Polymerization with Ziegler Catalysts: Fifty Years after the Discovery." *Angew. Chem. Int. Ed.* **42**: 5010-5030.

Covezzi, M. and Mei, G. (2001). "The Multizone Circulating Reactor Technology." *Chem. Eng. Sci.* **56**: 4059-4067.

Kaminsky, W. (1996). "New Polymers by Metallocene Catalysis." *Macromol. Chem. Phys.* **197**: 3907-3945.

Liu, H. T. D., C.R.; Shirodkar, P.P. (2003). "Bimodal Polyethylene Productc from UNIPOL Single Gas Phase Reactor Using Engineered Catalysts." *Macromol. Symp.* **195**: 309-316.

Reichert, K.-H. and Meyer, K. R. (1973). "Zur Kinetik der Niederdruckpolymerisation von Äthylen mit löslichen Ziegler-Katalysatoren." *Macromol. Chem. Phys.* **169**(1): 163-176.

Whiteley, K. S. (2002). Polyolefins - Polyethylene. Ullmann's Encyclopedia of Industrial Chemistry, InterScience Wiley-VCH Verlag GmbH.

Ziegler, K. (1964). "Folgen und Werdegang einer Erfindung." *Angew. Chem.* **76**(13): 545-620.

Chapter 2

Semi-Batch Reactor for Highly Reproducible Kinetic Measurements of Catalyzed Gas and Slurry Phase Olefin Co-Polymerizations

Abstract

A multi purpose setup is presented for homo- and co-polymerizations of ethylene and 1-hexene in slurry and gas phase. Polymerization experiments have been executed semi-batch with a heterogeneous metallocene catalyst under industrial conditions. During the gas-phase polymerization the monomer concentrations have been measured and controlled online. The activities for both monomers have been measured with flow meter technique.

The presented polymerization kinetics have been measured in a very accurate way in isothermal (within 0.2°C) and isobaric mode (within 0.15 bar). The concentrations of monomer and co-monomer have been kept constant within 5% of the set point. All polymerization kinetics have been measured with high reproducibility. The co-monomer effect was observed, the activity for ethylene was 50% higher in the presence of 1-hexene compared to a homo-polymerization.

Chapter 2

Introduction

General slurry and gas phase polymerizations

HDPE and LLDPE are produced on industrial scale in solution, slurry or gas phase processes. Most processes can switch by changing co-monomer concentration between HDPE and LLDPE production (Whiteley 2002). Slurry processes are operated in loop reactors, vertical like the Phillips loop reactors or horizontal like Amoco, and in stirred tank reactors, like Basell's Hostalen slurry process. Slurry processes are still widely used, while slurry reactors have a very efficient heat removal and wide co-monomer range. But the product range is limited due to solubility of the produced polymer, e.g. low molecular weight PE and highly incorporated co-monomer LLDPE. Since the late 1960s gas phase reactors were introduced, like fluid bed reactors in the Unipol process, BASF's stirred tank reactors and Amoco's horizontal stirred tank reactors. Gas phase processes can be operated with 1-butene or 1-hexene as co-monomer. Most novel technologies are combinations of gas and slurry phase reactors, like Spherilene (Covezzi 1995; Galli 1995) and Borstar PE (Avela *et al.* 1998). Cascaded processes are suitable for bi-modal polyethylene production.

State of the art

Although research is performed for decades on metallocene catalyzed ethylene homo- and co-polymerizations (Hamielec and Soares 1996; Kaminsky 1996), only few academic research groups are able to measure kinetics and produce sufficient amounts of polymer, for property analyses, at industrial conditions with good reproducibility, temperature, pressure and gas phase co-monomer control. Most reports are on slurry polymerizations (Chien *et al.* 1998; Britto *et al.* 2001; Kappler *et al.* 2003). Some gas phase ethylene polymerization kinetics are measured at relative low pressure (5 bar) in a stirred bed 1.0 L glass reactor (Roos *et al.* 1997) and with optical microscopy in a mini reactor (20 mL) (Kallio *et al.* 2001). Only few (Han-Adebekun *et al.* 1997; Chakravarti and Ray 2001) were able to measure kinetics of highly active metallocene catalysts under industrial conditions, i.e. elevated pressures and temperatures at constant process parameters.

Some data is published about gas phase ethylene 1-hexene co-polymerizations in isoperibolic mode with 1-hexene fed batch wise (Kumkaew *et al.* 2003; Zhou *et al.* 2003). In their studies sharp decreases in reaction rate were observed in the presence of 1-hexene followed by a slower increase compared to homo-polymerizations. They explained this with temperature dependence on kinetics, temperature increases (2°C up to 15°C) were observed during long time periods (15 min). These non-isothermal conditions, during a long period, will change kinetics and polymer properties. Another explanation might be the presence of impurities in the 1-hexene. Impurities can react irreversibly and reversibly, so after a certain time a poisoned catalyst site can be reactivated (CO). With large amounts of impurities all sites will be deactivated

irreversibly, at high 1-hexene concentrations hardly any reaction rate was observed. However quasi-isothermal kinetics can be obtained in isoperibolic mode when the temperature remains within ± 1 K. This requires a small amount of catalyst, but sufficient activity is required to avoid poisoning effects. Very smooth temperature profiles will be obtained and smooth mass flow meter curves (Weickert 2003).

This work

The kinetic behavior of a catalyst is important for reactor design, process optimization, control and polymer properties like molecular weight, molecular weight distributions, density, co-polymer composition, etc. Yield measurements, often used to characterize the catalyst performance, are not sufficient, because very different polymerization rate profiles can result in the same yield, see Weickert (2003).

Laboratory scale reactors are required to measure polymerization rate profiles of HDPE and LLDPE in slurry and gas phase under industrial conditions. This means for gas phase polymerizations the presence of an inert gas (e.g. nitrogen, propane). Inert gasses are used in industrial reactors to improve heat transfer on particle and reactor scale. Because of scaling-up requirements, these reactors should produce PE's at constant reaction conditions within a 10% reproducibility in polymerization rate and reaction conditions (Böhm *et al.* 1990).

In this work we present a reactor system including temperature, pressure and gas composition control, which is able to measure rate profiles in a reproducible and accurate way at industrial conditions. Some polymerizations with an impurity sensitive metallocene catalyst will be presented in order to demonstrate the "kinetic potential" of the equipment.

Experimental

Setup

The experimental setup for gas-phase polymerizations is represented in Figure 1. The reactor is a jacketed, stainless steel 1600 mL reactor from Büchi, which operates up to pressures of 40 bar and temperatures of 120°C. The setup is equipped with two automatic catalyst injection systems, suitable for dry-powder and slurry injections. The suspended catalyst injection system described by Samson *et al.* (1998; 1999) has been automated and can be used for catalyst and/or scavenger injections.

The dry catalyst injection consists of a tube with a valve on both ends. The tube is placed on the reactor and the dead ends are flushed with nitrogen. The catalyst is injected by pressurizing the tube, up to maximum 60 bar, and opening the bottom valve. A 100 ml vessel is placed on the reactor for adding an inert seedbed to the reactor, to prevent the catalyst particles to stick to the wall and to each other (Meier *et al.* 2001). This bed injection vessel can also be used for adding large amounts of pre-polymerized catalyst into the reactor. The seedbed and produced polymer are mixed with a helical stirrer combined with a propeller on the tip, to obtain good powder circulation along the wall. This forced circulation improves the heat transfer from the

polymerizing particles to the cooled reactor wall. The stirrer speed can be varied up to 2000 rpm. The reaction temperature is measured above the helical stirrer, in contact with the circulating powder.
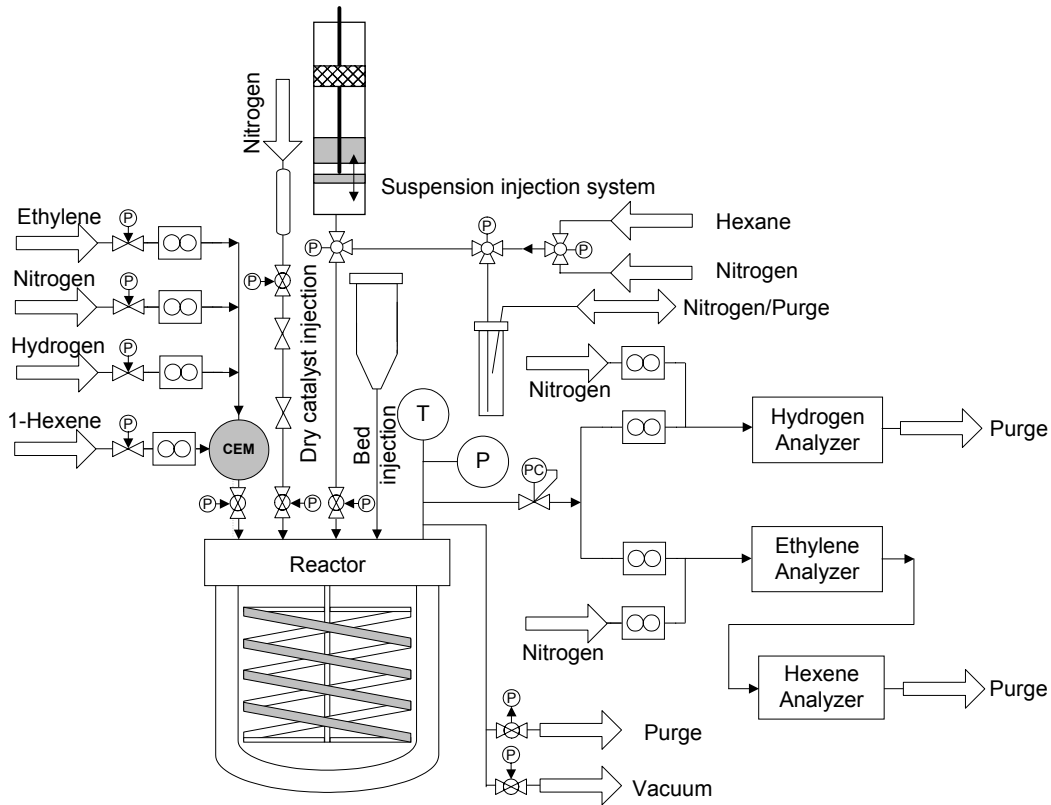
Figure 1: Experimental setup for gas and slurry phase ethylene homo- and co 1-hexene polymerizations

Ethylene, nitrogen and hydrogen can be added to the reactor by thermal mass flow controllers, 1-hexene is fed to the reactor by a thermal liquid mass flow controller. All components flow into the reactor via a Controlled Evaporator Mixer (CEM, Bronckhorst HiTech), wherein 1-hexene is dosed by a control valve in the gas mixture flow and evaporated in the CEM-system. A continuous flow can be withdrawn from the reactor over a pressure reducer via thermal mass flow controllers (Brooks Instruments) to analyzers. Three analyzers are used to measure online the concentrations of the monomers and hydrogen. The ethylene and 1-hexene concentrations are measured with two infrared analyzers (respectively Xendos 2550 and 2500, Servomex). The monomer concentrations can be diluted with nitrogen in order to get these concentrations in the range of the analyzers. This nitrogen is added to the sample flow by a thermal mass flow controller. The real concentration in the reactor is calculated with the ratio of the sample flow, the dilution with nitrogen and the measured concentration. The hydrogen concentration is measured by a modified thermal conductivity detector (TCD; Thermor 615, Maihak). After measuring the thermal conductivity of the sample in the measurement cell, the sample is flowing through a hydrogenation reactor; here all the hydrogen is converted by hydrogenating

a part of the ethylene on a palladium catalyst. This hydrogen free sample is measured in the reference cell and the original hydrogen concentration is calculated via a Wheatstone bridge. Note the conductivity of ethylene and ethane differs only slightly and the conductivity of hydrogen is 7 times higher, see Table 1 (Daubert *et al.* 1999). This is also the case for most other common olefins and their hydrogenated products. This enables to measure the hydrogen concentration in a multi-component system independent of the ethylene and co-monomer concentrations. The reaction gas contains besides the monomers and hydrogen also nitrogen (about 50 vol.%).

	Thermal conductivity (Relative to N2)	
	25°C	75°C
Ethylene	0.82	0.94
Ethane	0.85	0.98
1-Hexene	N/A	0.62
n-Hexane	N/A	0.62
Propylene	0.68	0.79
Propane	0.71	0.83
1-Butene	0.60	0.69
n-Butane	0.64	0.76
Hydrogen	6.8	6.7
Nitrogen	1.0	1.0

Table 1: *Thermal conductivities of most common olefins and products after hydrogenation (Daubert, AIChE and DIPPR, 1999)*

The modified-TCD has to be calibrated for each monomer / nitrogen ratio with zero and span hydrogen concentration. The dead time for this modified analyzer is 75 s. The analyzer is tested by feeding a constant hydrogen flow in a typical reaction mixture (52 vol.% ethylene and 48 vol.% nitrogen) at constant temperature (74.75 ± 0.05°C) and pressure (3.00 ± 0.02 bar). Figure 2 gives the calculated values from mass flow meters with a CSTR model versus the measured values with the modified TCD. Hydrogen concentrations above 0.1 vol.% can be measured accurately.

The polymerization reaction rate could be calculated by making a mass balance over the reactor for each component. For examination of the influences of various process parameters on the (co-) polymerization kinetics it is required to control parameters like pressure, temperature and concentrations of monomers, hydrogen and nitrogen.
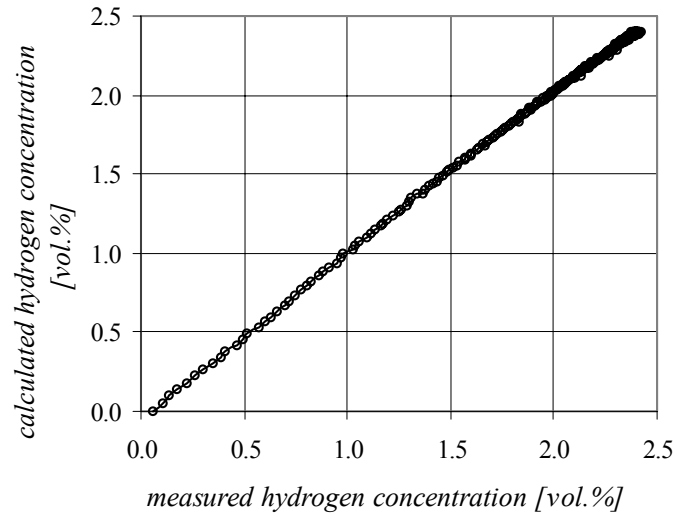
Figure 2: *Calculated hydrogen concentration versus measured hydrogen concentration with modified TCD*

Control

A HP 3852A Data Acquisition/Control Unit (DACU) measures all temperatures, pressures, concentrations and mass flows. This data is stored on a PC, which contains the operation software. The software, with proportional-integral-derivative (PID) algorithms, is controlling the concentrations and pressure.

Figure 3 shows the complexity of this control problem, different flows of the components influence directly the other flow-controlled parameters. The system parameters are coupled; furthermore one should notice that hexene could only be fed simultaneously with ethylene and/or nitrogen. Another control configuration might be with a fixed nitrogen flow and variable outgoing flow over the TCD for pressure controlling. In this case the ethylene, hexene and hydrogen flow controllers are used for their concentrations control. However the main consumption during the reaction is of ethylene and therefore a much more accurate pressure control is achieved with the configuration of Figure 3. Also variations in the outgoing flow result in small variations on the mass flow controller to the infrared analyzers; this results in large fluctuations in the concentration measurements. Therefore the control configuration of Figure 3 was chosen; thus the ethylene mass flow controller controls the pressure; the hexene and hydrogen mass flow controllers control respectively the hexene and the hydrogen concentration; the nitrogen flow controller is used for controlling the ethylene concentration. The relative ratios (C6/(C2+C6) and H2/C2) are automatically controlled, because all gas concentrations are controlled.
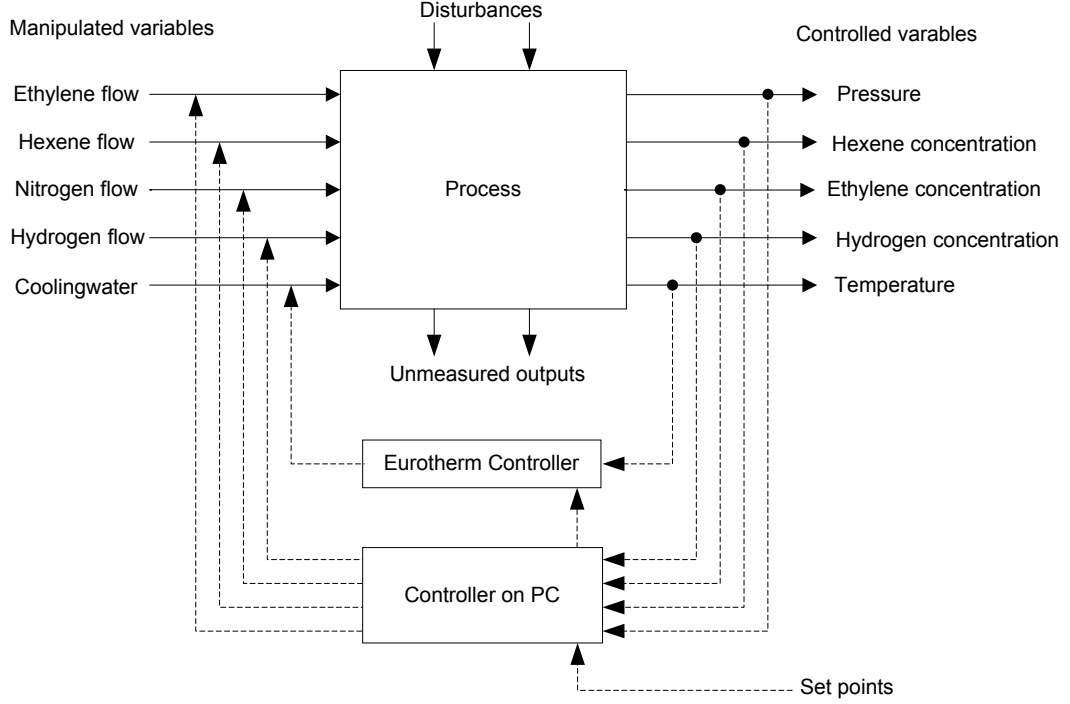
Figure 3: *Control scheme for semi batch co-polymerization in gas phase*

The co-polymerization reaction control system is time dependent and contains a time delay. A discrete PI algorithm (Stephanopoulos 1984) is used for controlling the concentrations and pressure:

$$c(nT) = K_c \varepsilon[nT] + \frac{K_c T}{\tau_I} \sum_{k=0}^{n} \varepsilon[kT] + c_s \qquad (1)$$

$$\text{with } \varepsilon[nT] = y_{sp}[nT] - y[nT] \qquad (2)$$

The input for the controller is the error ($\varepsilon[nT]$) between the set point ($y_{sp}[nT]$) and the measured value ($y[nT]$) at a certain time. The output ($c[nT]$) is calculated with proportional gain (K_c), integral time constant (τ_I) and controller's bias ($c_s = c(nT)$ when $\varepsilon = 0$). For the pressure and the nitrogen control the controller with a proportional and integral part is sufficient. For the 1-hexene control, with large time delay, a derivative part and a slave factor, on ethylene, are introduced:

$$c(nT) = K_c \varepsilon[nT] + \frac{K_c T}{\tau_I} \sum_{k=0}^{n} \varepsilon[kT] + \frac{K_c \tau_D}{T} \left(\varepsilon[nT] - \varepsilon[(n-1)T] \right) + c_s + \frac{y_{sp,2}}{y_{sp,1}} \cdot \Phi_{V,1} \cdot f \quad (3)$$

In this case the output ($c[nT]$) is calculated with the proportional gain (K_c), integral time constant (τ_I), derivative time constant (τ_D), controller's bias ($c_s = c(nT)$ when $\varepsilon = 0$) and a slave factor (f) on ethylene.

A fast temperature control is required for executing isothermal ethylene polymerizations, which are rather exothermic and therefore thermal run-away might arise. Figure 4 shows the reactor temperature control. The cover plate of the reactor is operated at a constant temperature slightly higher than the operating temperature to prevent condensation of 1-hexene. An oil bath is used for heating the connection between the CEM system and the reactor at approximately ten degrees higher than the operating temperature; here the hexene concentration reaches the highest values.
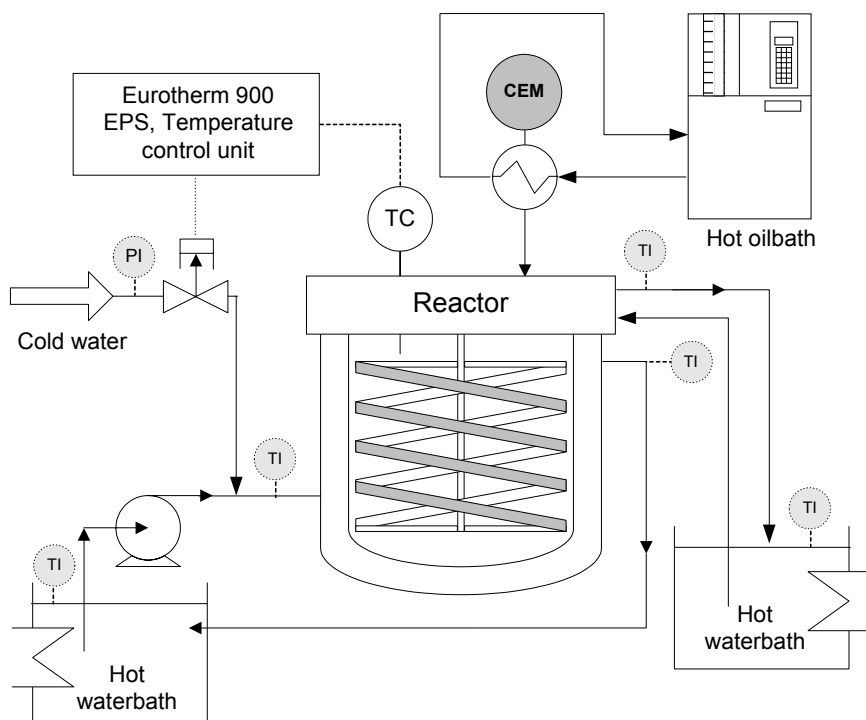
Figure 4: *Temperature control system for experimental set up*

The reactor temperature is controlled by the jacket temperature. Cold water is added to hot water by a control valve, which is operated by an Eurotherm 900EPS, PID cascade controller. The circulation time of the cooling water is shortened by a water pump (0.5 L/s). The reactor temperature can be kept constant within 0.2 K from one minute after catalyst injection onwards.

Chemicals and monomer purification

The metallocene catalyst (donated by Basell), used during the presented measurements, is a bisindenyl zirconium dichloride (Ind_2ZrCl_2). The zirconocene is supported on silica with an average particle diameter of 60 μm and a pore volume of about 1.6 ml/g. The catalyst contains 6.4 wt% Al and 0.2 wt% Zr. The Al / Zr molar ratio is 108. This catalyst system does not need pre-treatment.

Triisobutylalumina (TIBA) obtained from Akzo Nobel is used as scavenger during the slurry polymerizations. Triethylalumnina (TEA) supported on silica was used as scavenger during gas phase polymerizations. During the gas phase co-polymerizations

salt was used as seedbed. The salt is sieved and dried at 200°C under vacuum for 48 hours.

Ethylene (purity > 99.9%, C_2H_2 < 7 ppm, feed quality, Hoekloos) is further purified over a 1 L-column with oxidized BASF R3-16 catalyst, two 3.3-L packed columns one filled with reduced BASF R3-16 catalyst and one with molecular sieves (13X, 4A and 3A, Sigma-Aldrich) and a 1-L column with Selexsorb® COS (Alcoa, see Smith), see Figure 5a. This extended purification unit removes CO, oxygen, water, CO_2, H_2S and COS from the ethylene monomer. Nitrogen (purity >99.999%, O_2 < 1-10 ppm, H_2O < 1-10 ppm, Praxair) and hydrogen (purity >99.999%, Praxair) are purified over BASF R3-11 catalyst and molecular sieves (13X, 4A, 3A). For nitrogen two 19-L packed columns are used and for hydrogen four 0.5-L packed bed reactors are used.
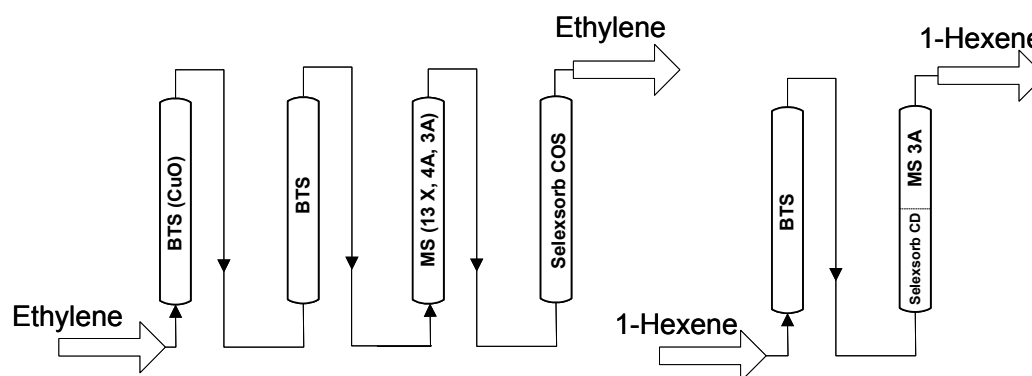
Figure 5: A. Purification scheme for ethylene, B. Purification scheme for 1-hexene

1-Hexene (purity 98%, Sigma-Aldrich) is pressurized and purged several times with purified nitrogen. Afterwards 1-hexene is purified (Figure 5b) over a 0.5-L column with reduced BASF R3-11 catalyst and a 0.5-L column with 50% Selexsorb® CD (Alcoa) and 50% molecular sieves (3A, Sigma-Aldrich). Hexane (purity > 99%, pro synthesis, Merck) is purified over reduced BASF R3-11 catalyst and molecular sieves (13X, 4A, 3A).

Procedures

The standard procedure for a gas phase polymerization is as follows:
1. Before each experiment the reactor is checked for any leakage.
2. The reactor is heated above 90°C and repeatedly pressurized with nitrogen, purged and evacuated (<10 mbar).
3. A seedbed is introduced into the reactor, typical 100 g sodium chloride with 1000 mg TEA supported on silica
4. The seedbed is mixed at 400 RPM at 10 bar nitrogen for 10 minutes.
5. The reactor is purged and evacuated for some minutes. The gas composition and temperature are installed, the ethylene and 1-hexene concentration 10% relative higher than the desired set point. This is done to achieve as soon as possible the desired set points after catalyst injection, which is accompanied with 2-3 bar pressure rise of nitrogen.

7. The catalyst is injected (typical 45 mg) together with 200 mg TEA supported on silica via the dry injection unit; this starts the gas phase homo/co-polymerization.
8. At the end of the experiment the data will be saved at the PC and the set points are lowered.
9. Purging the gas mixture and evacuation of the reactor stops the polymerization reaction.
10. The reactor is rinsed with nitrogen a couple of times, cooled down and opened. The polymer product is collected and washed with water, to separate the salt, and dried under vacuum.

In case of slurry polymerizations the steps 3-7 are different:
3. 400 mL hexane is added into the reactor.
4. The desired temperature is installed, standard 70°C.
5. Scavenger is injected, typical 125 mg TIBA, via the suspended injection and stirred for 10 minutes.
6. The catalyst is injected, 45 mg with 1.2 mL hexane, with the dry injection system and stirred for 10 minutes.
7. The reactor is pressurized till the desired operation pressure.

At the end of a slurry experiment the reactor will not be evacuated, the polymer/hexane mixture can be collected, filtrated and dried (instead of steps 9 and 11).

The operation of the setup is simplified by automation of all procedures to a large extent; the complete setup is operated from outside the concrete box. The operation program is written in HPVEE and includes flexible set points for all process parameters, which can be changed during the polymerization process. This enables to force temperature, pressure and/or concentration profiles, dynamic or step wise.

Reaction rate measurement

The polymerization rate can be derived for each component (i = 1 for ethylene and i = 2 for 1-hexene) from its mass balance:

$$\frac{\partial m_i}{\partial t} = \frac{\partial m_{g,i}}{\partial t} + \frac{\partial m_{s,i}}{\partial t} = \Phi_{M,in,i} - \Phi_{M,out,i} - R_{pi} \qquad (4)$$

With $\quad \dfrac{\partial m_{g,i}}{\partial t} = \dfrac{\partial \left(\rho_g (T,p) \cdot x_i \cdot V_g \right)}{\partial t} \quad$ with $\quad V_g = V_R - \dfrac{m_{bed}}{\rho_{bed}} - \dfrac{m_{PE}}{\rho_{PE}} \qquad (5, 6)$

The experiments are executed isothermal and isobaric, density changes can be neglected and the concentrations are also kept constant. The accumulation in the gas phase can be represented by:

$$\frac{\partial m_{g,i}}{\partial t} = -\frac{\rho_g (T_R, p_R)}{\rho_{PE}} \cdot x_i \frac{\partial m_{PE}}{\partial t} \qquad \text{with} \qquad \frac{\partial m_{PE}}{\partial t} = R_{Ptotal} = R_{P1} + R_{P2} \qquad (7, 8)$$

For experiments at low ethylene partial pressure (<15 bar) the relative change in mass production due to change in volume is less then 1.5%, for pressures of 40 bar, the

change in mass production is 4.5%. For the co-monomer this correction can be neglected; due to very low concentration and density of the co-monomer this correction is les then 0.1%.

$$\frac{\partial m_{s,i}}{\partial t} = \frac{\partial\left(\theta\left(T,p,x_i,\chi\right)\cdot m_{PE}\right)}{\partial t} = \theta\left(T_R,p_R,x_i,\chi\right)\cdot\frac{\partial m_{PE}}{\partial t} \tag{9}$$

The sorbed amount of the co-monomer cannot be neglected. This can be recalculated after polymer analyses, which will give the real amount of incorporated co-monomer. It is assumed that the co-monomer solubility (θ_2) will not change in time; after all the temperature, pressure and gas phase concentrations are constant resulting in a polymer production with constant properties (density, crystallinity, molecular weight etc.) in time.

$$\theta_2 = \frac{Yield_{2,MFM} - X_{2,PE}\cdot Yield_{PE}}{Yield_{PE}} \tag{10}$$

Finally the reaction rate can be calculated with:

$$R_{p1} = \rho_1^0\cdot\Phi_{V,in,1} - \rho_g^0\cdot x_1\cdot\left(\Phi_{V,out,a} + \Phi_{V,out,b}\right) + \frac{\rho_g^R}{\rho_{PE}}\cdot x_1\cdot\left(R_{p1} + R_{p2}\right) \tag{11}$$

$$R_{p2} = \Phi_{M,in,2} - \rho_g^0\cdot x_2\cdot\left(\Phi_{V,out,a} + \Phi_{V,out,b}\right) - \theta_2\cdot\left(R_{p1} + R_{p2}\right) \tag{12}$$

The reaction rate is obtained by substitution of R_{p2} in R_{p1}. R_{p2} is give by:

$$R_{p2} = \frac{1}{1+\theta_2}\cdot\left(\Phi_{M,in,2} - \rho_g^0\cdot x_2\cdot\left(\Phi_{V,out,a} + \Phi_{V,out,b}\right) - \theta_2\cdot R_{p1}\right) \tag{13}$$

Substitution results in:

$$R_{p1} = \frac{\rho_1^0\cdot\Phi_{V,in,1} - \rho_g^0\cdot x_1\cdot\left(\Phi_{V,out,a} + \Phi_{V,out,b}\right)}{1 - \dfrac{\rho_g^R\cdot x_1}{\rho_{PE}}\cdot\dfrac{1}{1+\theta_2}}$$
$$+ \frac{\dfrac{\rho_g^R\cdot x_1}{\rho_{PE}}\cdot\dfrac{1}{1+\theta_2}\cdot\left(\Phi_{M,in,2} - \rho_g^0\cdot x_2\cdot\left(\Phi_{V,out,a} + \Phi_{V,out,b}\right)\right)}{1 - \dfrac{\rho_g^R\cdot x_1}{\rho_{PE}}\cdot\dfrac{1}{1+\theta_2}} \tag{14}$$

For homo-polymerizations the equation R_{p1} is simplified because $R_{p2} = 0$ and the second term completely disappears.

This equation can also be simplified when the relative change in mass production due to change in volume is very small, i.e. when the gas density is low compared to the polymer density. In that case the second term can be neglected and the denominator approaches 1.

Examples and Discussion

Slurry homo-polymerizations

Figure 6 shows the reaction rate profile (a), the temperature of the reactor and cooling jacket (b) and the pressure in time (c) respectively.
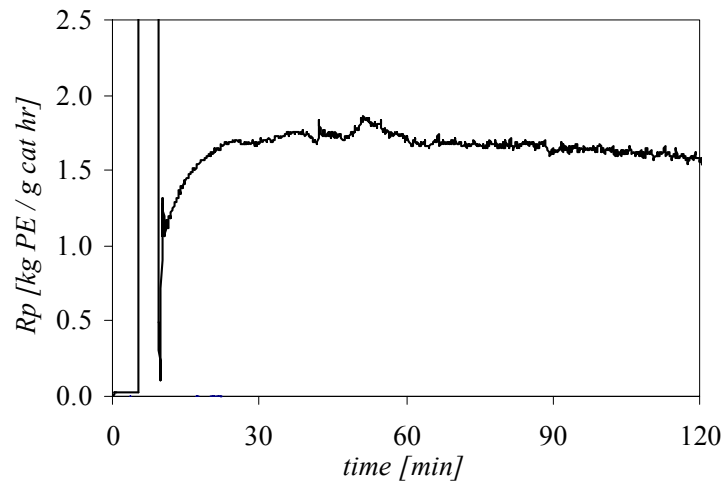

Figure 6a: Polymerization rate profile of homo-polymerization in slurry phase at 70°C and 13.7 bar with 65 mg catalyst (incl. support)
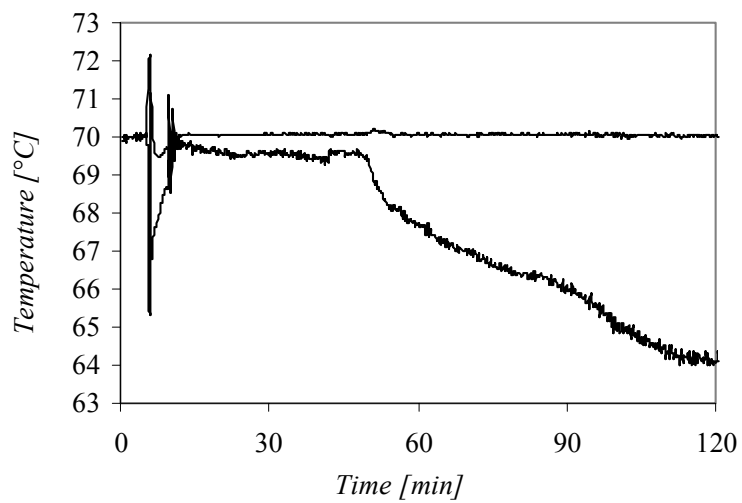

Figure 6b: Temperature profile of homo-polymerization in slurry phase at 70°C and 13.7 bar with 65 mg catalyst (incl. support)
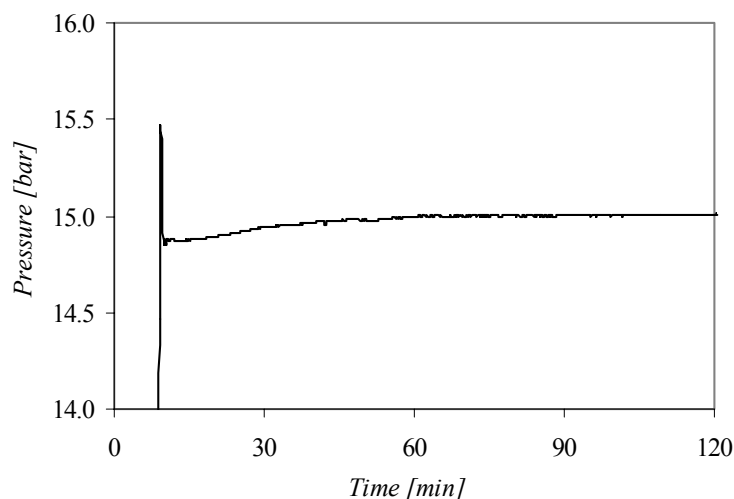
Figure 6c: *Pressure profile of homo-polymerization in slurry phase at 70°C and at an ethylene partial pressure of 13.7 bar with 65 mg catalyst (incl. support)*

The reactor is pressurized after 5 minutes; it takes about 4 minutes to reach the desired pressure, afterwards the pressure is kept constant within 0.15 bar. The catalyst reaches maximum activity 20 minutes after reaching the set point and shows low deactivation rate. The temperature control in slurry experiments is good due to the good heat transfer. During pressurizing the temperature increases 2°C, but during the rest of the experiment the temperature is kept stable within 0.2°C. After 50 minutes the heat transfer is changing, due to the increased amount of polymer in the diluents mixture a sharp decrease of the temperature in the cooling jacket is observed.

Exp	T	P	R_{pmax}[1]	Deviation
	°C	bar	$kgPE/g_{cat}hr$	
S1	69.74	10.14	1.83	3.8%
S2	69.89	9.92	1.93	1.3%
S3	69.96	9.82	1.96	2.9%
S4	69.95	9.87	1.79	6.1%
S5	69.96	9.80	2.04	6.9%
S6	69.94	9.92	1.81	5.2%
S7	69.94	9.88	2.03	6.6%
S8	70.05	9.94	1.86	2.7%
Average			1.91	

[1] Activity is per gram catalyst including support material.

Table 2*: Maximum activity for several homo-polymerizations in slurry phase*

Table 2 shows the maximum activity for 8 slurry homo-polymerizations at 70°C and a partial pressure of 9.9 bar; the average maximum activity for these experiments is 1.9 $kgPE \cdot g_{cat}^{-1} \cdot hr^{-1} \pm 7\%$.

Gas phase homo-polymerizations

Gas phase homo-polymerizations are executed at several temperatures and pressures (see chapter 3). Table 3 represents the maximum activity for several experiments at 70°C and 15 bar; the average maximum activity is 0.88 kgPE·g_{cat}^{-1}·hr^{-1} ± 6.5%.

Exp	T	P	R_{pmax} [1]	Deviation
	°C	bar	kgPE/g_{cat}hr	
G1	70.06	14.87	0.93	6.3%
G2	70.02	14.98	0.82	6.2%
G3	70.10	14.95	0.88	0.0%
G4	70.04	14.99	0.93	5.5%
G5	70.05	14.99	0.83	5.5%
Average			0.88	

[1] Activity is per gram catalyst including support material.

Table 3*: Maximum activity for several homo polymerizations in gas phase*

Gas phase co-polymerizations

Figure 7 shows the reaction rate curves for ethylene (R_{p1}) and for 1-hexene (R_{p2}) of two almost identical experiments (GEH2 and GEH4). Both experiments are executed at 90°C, 20 bar with 50 vol.% ethylene, 1.0 vol.% hexene and 49 vol.% nitrogen, with respectively 45 mg and 46 mg catalyst (incl. support) at 400 rpm. The reaction rates for ethylene and 1-hexene, the activation and deactivation behavior show a large similarity.

The experiments show some difference during the activation phase, this is due to the initial "disturbance" by the injection of catalyst with nitrogen, which slightly differs for each experiment (see also Figure 8a and 8b). Table 4 shows for several co-polymerization experiments at almost identical reaction conditions the maximum activity for ethylene and 1-hexene, the reproducibility is less than for homo-polymerizations but is still within 10% for ethylene, for the low concentrations of 1-hexene the reproducibility is within 17%.

The presented co-polymerization experiments are executed at a monomer bulk concentration of 10.6 kg·m^{-3}, at this monomer bulk concentration the expected homo-polymerization rate will be about 1.0 kgPE·g_{cat}^{-1}·hr^{-1} at 90°C. The measured activity for ethylene in the presence of 1-hexene is 50% higher.
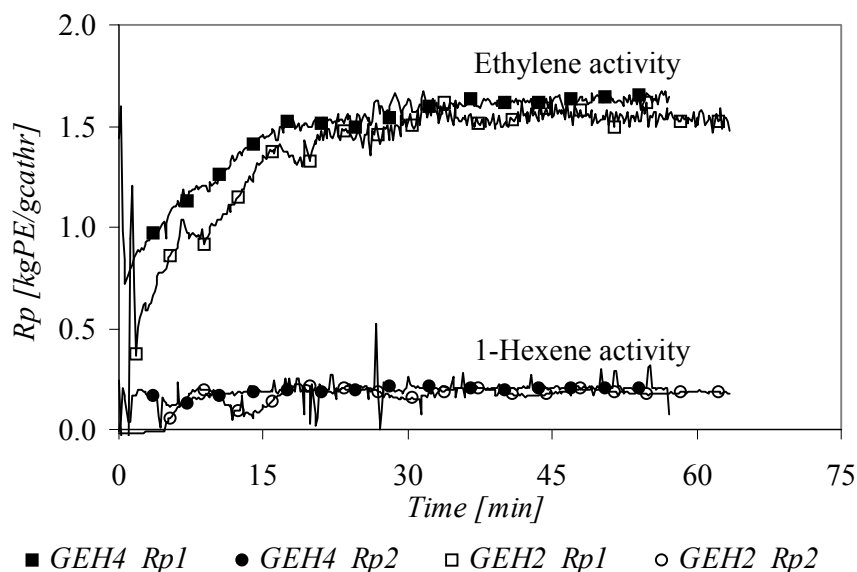
Figure 7: *Ethylene and 1-hexene activity for two gas-phase co-polymerizations (GEH4 and GEH2) at 90°C and 20 bar with 45 mg catalyst (incl. support)*

Exp	T	P	M1	M2	N2	R_{pmax1}[1]	Dev.	R_{pmax2}[1]	Dev.
	°C	bar	vol.%	vol.%	vol.%	$kgPE/g_{cat}hr$		$kgPE/g_{cat}hr$	
GEH1	91.64	19.98	50.16	0.99	48.85	1.44	3.8%	0.16	10.6%
GEH2	90.01	19.98	50.29	0.99	48.72	1.53	2.0%	0.18	1.3%
GEH3	90.03	19.96	50.06	0.99	48.95	1.49	0.4%	0.18	2.9%
GEH4	90.05	19.98	50.01	1.01	48.98	1.63	8.9%	0.21	16.8%
GEH5	89.93	20.88	52.77	1.10	46.13	1.47	1.9%	0.18	0.2%
GEH6	89.10	20.94	53.38	0.99	45.63	1.43	4.8%	0.18	2.1%
Average						1.50		0.18	

[1] Both activities are per gram catalyst including support material.

Table 4: Maximum activities of monomer 1 (ethylene) and monomer 2 (1-hexene) for several co-polymerizations in gas phase

Figure 8a and 8b represent the online measured concentrations of the monomers and nitrogen of experiment GEH4 and GEH2 respectively. In these two experiments the catalyst is injected with a large amount of nitrogen. This results in a huge drop in the ethylene and 1-hexene concentrations. But as can be observed from these figures for each experiment the initial concentration profile is slightly different. The PID controllers stabilize the concentrations quite fast, the deviations from the set point is less than 5%. Figure 8b shows that after 20 minutes still an oscillating 1-hexene-concentration profile compared to Figure 8a, which shows a constant 1-hexene-concentration profile. The 1-hexene concentration oscillations are not observed in the reaction rate curves; the activities for both experiments are nearly the same. This could be explained due to slow sorption and desorption behavior of 1-hexene resulting an average constant 1-hexene concentration near the active site.
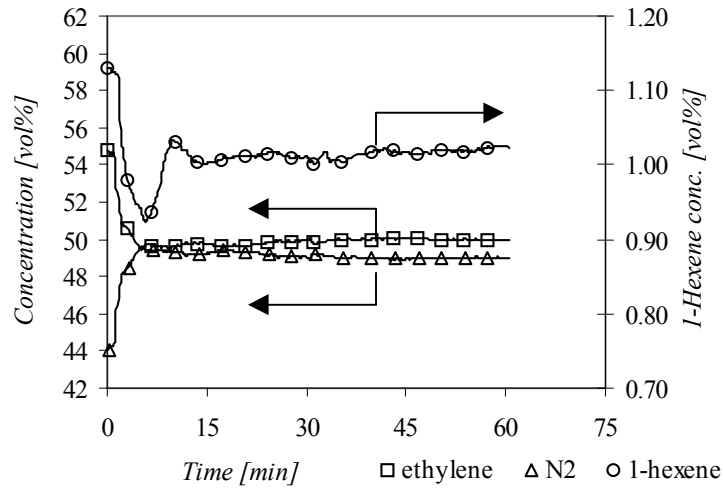
Figure 8a: *Gas concentration profile during gas-phase co-polymerization of experiment GEH4*
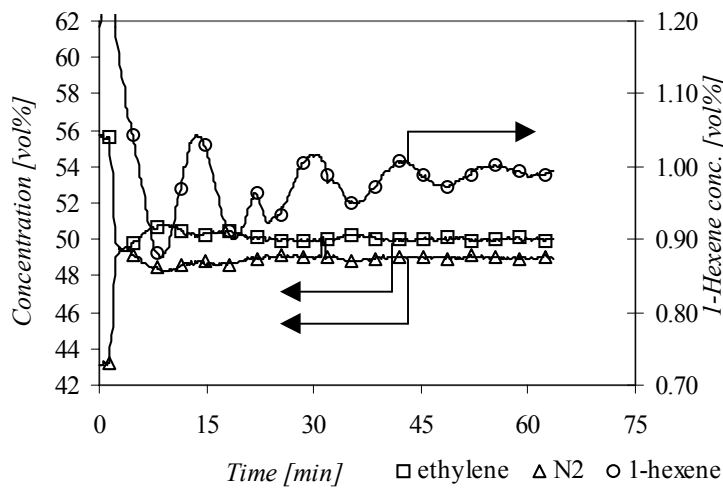
Figure 8b: *Gas concentration profile during gas-phase co-polymerization of experiment GEH2*

By manipulating the PID control, forced concentration profiles can be achieved, like oscillating concentrations or using different steps of high co-monomer and low co-monomer concentrations.

Figure 9 shows the temperature and pressure profile during experiment GEH4. The catalyst injection also causes here the deviation at the start, the pressure is increased by the nitrogen pulse and also the temperature increases fast due to the polymerization heat, however when the set points are reached the control is very accurate.
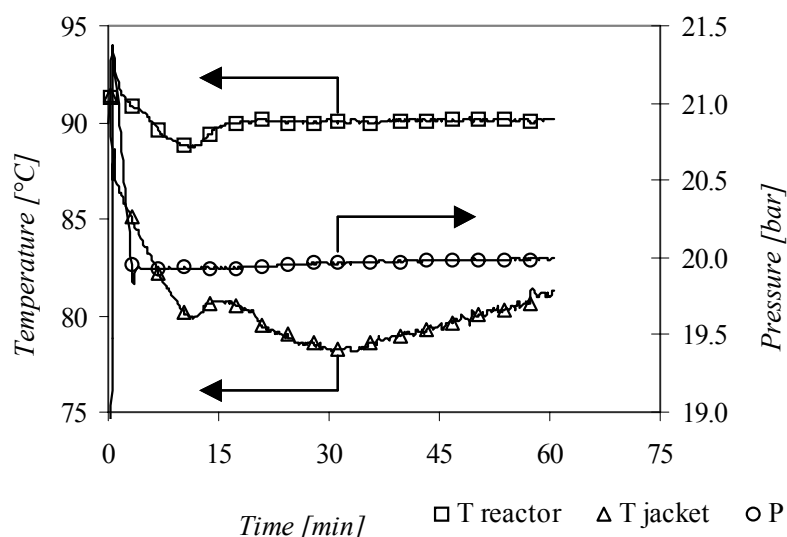
Figure 9: *Temperature profile of reactor and cooling jacket (left) and pressure profile (right) of experiment GEH4*

Conclusions

A multi purpose reactor has been developed for ethylene homo- and co-1-hexene-polymerizations in slurry and gas phase, which can operate at isothermal and isobaric conditions and in gas phase at constant monomer concentrations. With the presented experiments it has been demonstrated that the reactor is able to measure kinetics of a poison sensitive supported metallocene catalyst. The polymerization rate profiles are obtained under controlled conditions, all within 10% of the set point. The temperature is controlled within 0.2°C, the pressure within 0.15 bar, the ethylene concentrations is controlled within 2% and the 1-hexene concentration within 5%.

Furthermore it has been showed that ethylene 1-hexene co-polymerizations can be measured in an accurate and reproducible way. For both monomers the activity is measured with mass flow techniques and both monomer concentrations are measured online. The acceleration effect for ethylene activity in the presence of 1-hexene has been observed.

In the next two chapters extensive kinetic studies will be presented.

Acknowledgement

Notation

c	Output of controller	
c_s	Controller's bias signal	
C2	Ethylene concentration	vol.%
C6	1-Hexene concentration	vol.%
f	Slave factor	
m	Mass	kg
n	nth sample instant	
K_c	Proportional gain of controller	
P	Pressure	bara
R_{pi}	Polymerization rate for monomer i	$kg(PE) \cdot min^{-1}$
T	Temperature	°C
t	Time	min
x_i	Fraction of gas component i	
X_i	Fraction in polymer of monomer i	
y	Sampled value	
Yield	Polymer produced	kg(PE)

Greek letters

ε	Discrete error	
τ_I	Integral time constant	min
τ_D	Derivative time constant	min
T	Sample time period	min
Φ_m	Mass flow	$kg \cdot min^{-1}$
Φ_V	Volume flow	$m^3 \cdot min^{-1}$
ρ	Density	$kg \cdot m^{-3}$
θ	Solubility	$g \cdot g^{-1}$
χ	Crystallinity	-

Subscript

1	Monomer ethylene
2	Co-monomer 1-hexene
g	Gas
in	In flowing
m	Mass
M	Monomer
MFM	Mass Flow Meter
out	Out flowing
PE	Polymer
R	Reactor
s	Sorbed
sp	Set point

Superscript

0	Standard conditions, atmospheric pressure and room temperature
R	Reaction conditions

Abbreviations

CEM	Controlled Evaporator Mixer
HDPE	High density polyethylene
LLDPE	Linear low-density polyethylene
PE	Polyethylene
TCD	Thermal Conductivity Detector
TEA	Tri-ethylaluminum
TIBA	Tri-isobutylaluminum

Literature

Avela, R., Karling, R. and Takaharhu, J. (1998). "Borstar- The Enhanced Bimodal Polyethylene Technology". 6th International Workshop on Polymer Reaction Engineering, Berlin, DECHEMA Monographs Wiley-VCH.

Böhm, L. L., Göbel, P. and Schöneborn, P.-R. (1990). "Detailed Reaction Engineering as a Basis of Modern Slurry Technology for PE-HD-Production." *Angew. Makromol. Chem.* **174**: 189-203.

Britto, M. L., Galland, G. B., dos Santos, J. H. Z. and Forte, M. C. (2001). "Copolymerization of Ethylene and 1-Hexene with Et(Ind)2ZrCl2 in Hexane." *Polymer* **42**: 6355-6361.

Chakravarti, S. and Ray, W. H. (2001). "Kinetic Study of Olefin Polymerization with a Supported Metallocene Catalyst. II. Ethylene/1-Hexene Copolymerization in Gas Phase." *J. Appl. Polym. Sci.* **80**: 1096-1119.

Chien, J. C. W., Yu, Z., Marques, M. M., Flores, J. C. and Rausch, M. D. (1998). "Polymerizations of Olefins and Diolefins Catalyzed by Monocyclopentadienyltitanium Complexes Containing a (Dimethylamino) ethyl Substituent and Comparison with ansa-Zirconocene Systems." *J. Polym. Sci. A: Polym. Chem.* **36**: 319-328.

Covezzi, M. (1995). "The Spherilene Process: Linear Polyethylenes." *Macromol. Symp.* **89**: 577-586.

Daubert, T. E., Danner, R. P., Sibul, H. M., Stebbins, C. C., Rowley, R. L., Wilding, W. V., Oscarson, J. L., Adams, M. E. and Marshall, T. L., Eds. (1999). Physical and Thermodynamic Properties of Pure Chemicals, Part 1. AIChE & DIPPR. Columbus, OH, Greyden Press.

Galli, P. (1995). "The 'Spherilene' Process." *Plast., Rub. Comp. Proces. Appl.* **23**(1): 1-10.

Hamielec, A. E. and Soares, J. B. P. (1996). "Polymerization Reaction Engineering - Metallocene Catalysts." *Prog. Polym. Sci.* **21**: 651-706.

Han-Adebekun, G. C., Debling, J. A. and Ray, W. H. (1997). "Polymerization of Olefins Through Heterogeneous Catalysis. XVI. Design and Control of a Laboratory Stirred Bed Copolymerization Reactor." *J. Appl. Polym. Sci.* **64**: 373-382.

Kallio, K., Wartmann, A. and Reichert, K.-H. (2001). "Effect of Light on the Activity of Metallocene Catalysts in the Gas-Phase Polymerisation of Ethylene." *Macromol. Rapid Commun.* **22**(16): 1330-1334.

Kaminsky, W. (1996). "New Polymers by Metallocene Catalysis." *Macromol. Chem. Phys.* **197**: 3907-3945.

Kappler, B., Tuchbreiter, A., Faller, D., Liebetraut, P., Horbelt, W., Timmer, J., Honerkamp, J. and Mülhaupt, R. (2003). "Real-time Monitoring of Ethylene/1-Hexene Copolymerizations: Determination of Catalyst Activity, Copolymer Composition and Copolymerization Parameters." *Polymer* **44**: 6179-6186.

Kumkaew, P., Wu, L., Praserthdam, P. and Wanke, S. E. (2003). "Rates and Product Properties of Polyethylene Produced by Copolymerization of 1-Hexene and Ethylene in the Gas Phase with (n-BuCp)2ZrCl2 on Supports with Different Pore Sizes." *Polymer* **44**: 4791-4803.

Meier, G. B., Weickert, G. and van Swaaij, W. P. M. (2001). "Comparison of Gas- and Liquid-Phase Polymerization of Propylene with Heterogenous Metallocene Catalyst." *J. Appl. Polym. Sci.* **81**: 1193-1206.

Roos, P., Meier, G. B., Samson, J. J. C., Weickert, G. and Westerterp, K. R. (1997). "Gas Phase Polymerization of Ethylene with a Silica-Supported Metallocene Catalyst: Influence of Temperature on Deactivation." *Macromol. Rapid Commun.* **18**: 319-324.

Samson, J. J. C., Middelkoop, B. v., Weickert, G. and Westerterp, K. R. (1999). "Gas-Phase Polymerization of Propylene with a Highly Active Ziegler-Natta Catalyst." *AIChE Journal* **45**(7): 1548-558.

Samson, J. J. C., Weickert, G., Heerze, A. E. and Westerterp, K. R. (1998). "Liquid-Phase Polymerization of Propylene with a Highly Active Catalyst." *AIChE Journal* **44**(6): 1424-1437.

Smith, D. L. "Applications for Selective Adsorbents in Polymer Production Processes." *ALCOA, Technical Bulletin* **USA/6040-R00/0198**.

Stephanopoulos, G. (1984). Chemical Process Control - An Introduction to Theory and Practice. Englewood Cliffs, New Jersey, PTR Prentice Hall.

Weickert, G. (2003). High Precision Polymerization Rate Profiles. Ziegler Natta Catalysts. Terano, M. and Busico, V. Kanazawa, JAIST.

Whiteley, K. S. (2002). Polyolefins - Polyethylene. Ullmann's Encyclopedia of Industrial Chemistry, InterScience Wiley-VCH Verlag GmbH.

Zhou, J. M., Li, N. H., Bu, N. Y., Lynch, D. T. and Wanke, S. E. (2003). "Gas Phase Ethylene Polymerization over Polymer Supported Metallocene Catalysts." *J. Appl. Polym. Sci.* **90**: 1319-1330.

Chapter 2

Chapter 3

Ethylene Homo-Polymerization Kinetics with a Heterogeneous Metallocene Catalyst - A Comparison between Gas and Slurry Phase

Abstract

Ethylene homo-polymerizations were executed with a supported Ind_2ZrCl_2/MAO catalyst using a so-called Reactive Bed Preparation method. This RBP method combines a slurry polymerization with a gas phase polymerization with the same polymerizing particles, i.e. a reactive bed. Polymerization kinetics have been measured with high accuracy and reproducibility. The slurry and gas phase polymerization rates showed the same dependency on monomer bulk concentration. A complexation model has been proposed to describe the observed non-first order behavior on the monomer bulk concentration. This model also explains the non-Arrhenius temperature dependence and pressure dependence of the activation energy of the commonly used polymerization rate model: $R_p = k_p \cdot C^* \cdot M$.

Chapter 3

Introduction

General

Comparing slurry phase with gas phase catalytic polymerizations is important for some industrial processes, which consist of a slurry (pre-) polymerization followed by a gas phase polymerization, like Spherilene and Borstar PE technologies. But also when a good model is available for comparing gas with slurry phase polymerizations, it can be highly preferable to measure kinetics in slurry phase and use this for gas phase processes. This is because measuring batch wise kinetics in slurry phase has several advantages over gas phase.

One of the major differences in batch polymerizations is the requirement of a seedbed in gas phase polymerizations and diluent in slurry phase polymerizations. The diluent in slurry phase processes can easily be purified with additions of a scavenger. A seedbed has however a large specific surface and therefore a high potential for adsorbing impurities.

Continuous gas phase reactors use a reactive bed, which still contains the active catalyst. Before start up, a seedbed is added; afterwards no extra powder has to be added to the reactor. However continuous operation on lab scale needs a much higher experimental effort and provides much less kinetic data. Continuous process operation at lab scale can also differ from batch due to the presence of impurities.

Another difference is the heat transfer and temperature control. In slurry phase the temperature is much easier controlled due to good heat transfer. During batch wise polymerizations, the almost instantaneous increase in activity after catalyst injection can lead to a large temperature increase and even to local run-aways especially in gas phase. In continuous processes the polymer production is kept constant by controlling the catalyst feed. A constant polymer production results in a constant heat production and therefore easy temperature control.

Also the temperature control on local particle scale differs between slurry and gas phase polymerizations. The heat transfer coefficient for solid-liquid is higher than for solid-gas, therefore the temperature in the polymerizing particles in gas phase increases much more. Especially after catalyst injection, the temperature of the polymerizing particles can increase dramatically in gas phase (Hutchinson and Ray 1987). At moderate conditions already temperature increases up to 20°C were observed with infrared thermography during gas phase propylene-ethylene polymerizations in a micro reactor (Pater *et al.* 2003).

Other differences are caused by the possibility for leaching of the catalyst, solubility of low molecular weight polymer and highly modified copolymers in slurry phase and by fouling due to fines in gas phase. All these differences are also very catalyst and product dependent.

In general the absence of a seedbed and good temperature control makes it more favorable to study homo-polymerization kinetics in slurry phase than in gas phase. These slurry kinetic data can be used in gas phase, provided that the basic kinetics is

the same and that the differences between slurry and gas phase can be explained by differences on micro-scale.

State of the Art

Kissin *et al.* (1999) measured homo-polymerizations of a Ziegler-Natta system in a pressure range of 3.4-12.3 bar at 85°C in gas phase and in slurry phase, resulting in a reaction rate order on the ethylene concentration of 1.6-1.7 in gas phase and 1.8-1.9 in slurry phase.

Xu *et al.* (2001) performed gas phase ethylene homo-polymerizations with a supported metallocene catalyst in a pressure range of 2-6.9 bars and varied the temperature between 62 and 80°C. Chakravarti and Ray (2001) used the kinetics measured by Xu *et al.* for comparing the behavior of the same catalyst in slurry phase. They analyzed the slurry kinetics taking into account:

1. Gas-liquid mass transfer limitations
2. Monomer equilibrium concentration in diluent and polymer
3. Diffusion limitations at macro particle scale

According to Chakravarti and Ray the model predictions are much better when diffusion limitations on particle scale are taken into account. Especially the activation behavior of the catalyst is much better predicted. However, Xu showed clearly that the activation behavior of the used catalyst is very dependent on the temperature profile during the initial polymerization phase after catalyst injection. Another issue, which could change the kinetics, is the concentration of scavenger. Xu claimed that the scavenger is removed from the reactor before the polymerization starts, while Chakravarti injected the catalyst 15 min after scavenger injection.

This Work

In this work gas and slurry phase polymerization kinetics will be compared using a heterogeneous metallocene catalyst. Ethylene homo-polymerizations will be executed in wide ranges of pressure and temperature. The temperature and pressure have values comparable with industrial polymerization process conditions.

The observed kinetic behavior will be described with a model, which explains monomer concentration and temperature dependence. In chapter 4 this model will be extended for co-polymerizations.

The produced high-density polyethylenes were analyzed for molecular weight and density.

Experimental

Setup

The experimental equipment has been described in the Chapter 2. Figure 1 gives a schematic representation of the experimental setup. The reactor is a jacketed, stainless steel 1600 mL reactor from Büchi, which operates at pressures up to 40 bar and temperatures till 120°C. The setup is equipped with two automatic catalyst injection systems, suitable for dry-powder and slurry injections. The slurry catalyst injection system (Samson *et al.* 1998) can also be used for addition of liquids (e.g. hexane). The reaction mixture is mixed with a helical stirrer combined with a propeller on the tip, to obtain good powder circulation along the wall. This forced circulation improves the heat transfer from the polymerizing particles to the cooled reactor wall (Meier *et al.* 2001).
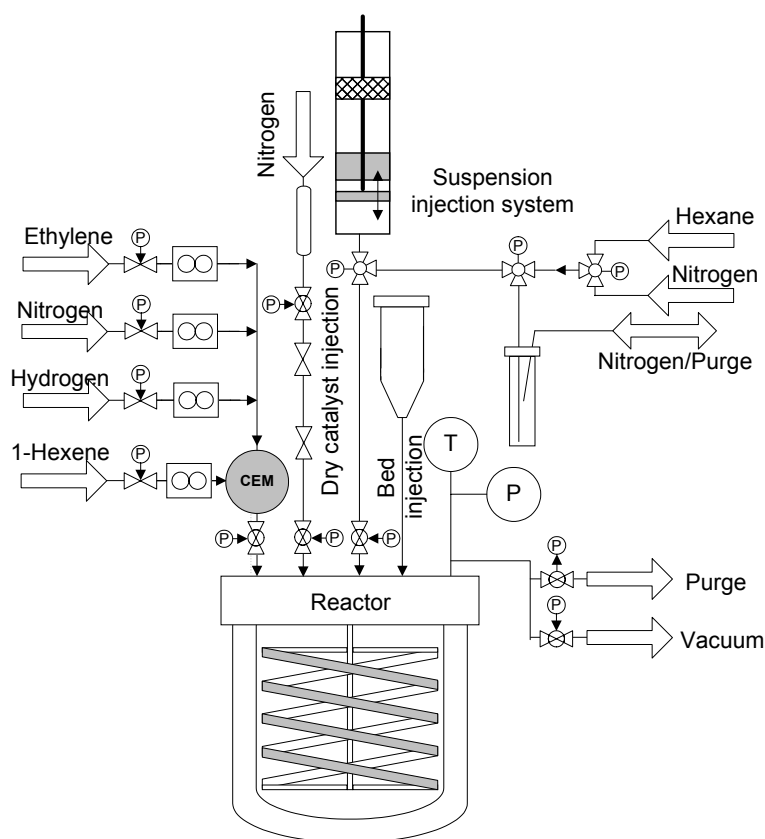
Figure 1: Experimental setup for gas and slurry phase ethylene polymerizations.

The stirrer speed can be varied up to 2000 rpm. The reaction temperature is measured above the helical stirrer, in contact with the circulating powder. A HP 3852A Data Acquisition/Control Unit (DACU) measures all temperatures, pressures and mass flows. This data is stored on a PC, which contains the operation software. A fast temperature control is required for doing isothermal ethylene polymerizations, which are rather exothermic and therefore thermal run-away might arise. The reactor temperature is controlled by the jacket temperature. Cold water is added to hot water

by a control valve, which is operated by a PID cascade controller. The reactor temperature can be kept constant within 0.2°C from one minute after catalyst injection onwards.

Chemicals

The used metallocene catalyst is bisindenylzirconiumdichloride (Ind_2ZrCl_2) with MAO as co-catalyst and was donated by Basell Polyolefins. The metallocene catalyst is supported on silica with an average particle diameter of 60 μm and a pore volume of about 1.6 ml/g. The catalyst contains 6.4 wt% Al and 0.2 wt% Zr. The molar ratio between Al / Zr is 108. This zirconocene does not need any extra pre-treatment before the catalyst is injected into the reactor.

Triisobutylalumina (TIBA) obtained from Akzo Nobel is used as scavenger during the slurry polymerizations. Ethylene (purity > 99.9%, C_2H_2 < 7 ppm, Hoekloos) is further purified over oxidized BASF R3-16 catalyst, reduced BASF R3-16 catalyst, molecular sieves (13X, 4A and 3A, Sigma-Aldrich) and Selexsorb® COS (Alcoa). Nitrogen (purity >99.999%, O_2 < 1-10 ppm, H_2O < 1-10 ppm, Praxair) and hexane (purity > 99%, pro synthesis, Merck) are purified over BASF R3-11 catalyst and molecular sieves (13X, 4A, 3A). Chapter 2 describes the chemical purification in detail.

Reactive Bed Preparation Procedure

In order to measure homo-polymerization kinetics in a reproducible way, a so-called reactive bed preparation method has been developed for ethylene polymerizations. The reactive bed preparation method combines a (pre-) polymerization in slurry phase with a gas phase polymerization, without intermediately introducing fresh catalyst. The reactive bed preparation method was developed in the High Pressure Laboratories of the University of Twente for propylene polymerizations (Putten 2004).

In that case a liquid pool propylene homo-polymerization is executed at a moderate temperature. After this pre-polymerization the reactor is heated to the desired temperature for the main polymerization. The liquid propylene will evaporate and the polymerization will continue in the gas phase. Complete evaporation can be achieved either by using a small amount of propylene or less favorable by purging propylene. This small amount should be enough to have liquid at low temperature, but after pre-polymerizing (≈10 g) and heating up to 70°C the partial pressure should stay below saturation pressure.

The main advantages of this method are that no additional bed material is required, if enough polymer is produced during the liquid phase, and that a good contact of scavenger with monomer and diluent takes place. Another advantage is that the catalyst is allowed to pre-polymerize under mild conditions with a good heat transfer, due to the use of a a liquid bulk instead of a gas.

The RBP-method was adapted for ethylene homo-polymerizations. As diluent hexane was added for obtaining a slurry polymerization initially. After the reactive bed

production this diluent should be taken out of the reactor without influencing the activity. Thereafter the main gas phase polymerization can be started.

The complete reactive bed preparation procedure is as follows:

1. The preparation and starting up of the experiment is the same as a standard slurry experiment (see chapter 2)
2. The catalyst (45 mg) is injected (via the dry injection system) together with 1.2 ml hexane and stirred for 10 min.
3. The reactor is pressurized with ethylene till a partial pressure of 2.5 bar in order to perform a pre-polymerization.
4. After 10 minutes the reactor is pressurized (at once or step by step till the desired pressure).
5. After production of a sufficient amount of polymer (roughly 50 g), the reactor is purged and evacuated under a small nitrogen flow (20 Nml/min) for 45 min, without opening the reactor and without deactivating the catalyst, in order to evaporate all liquid hexane.
6. The reactor is pressurized again with ethylene till the desired pressure (in one step or in several small steps) and the gas phase polymerization starts.

The homo-ethylene polymerizations are executed in semi-batch, isobaric and isothermal mode. In most experiments pressure or temperature steps were applied. The partial ethylene pressure has been varied for slurry phase experiments till 20 bar and for gas phase experiments till 30 bar. Temperature has been varied between 50 and 90°C during the gas phase experiments.

Reaction Rate Measurement

The ethylene reaction rate is determined with a mass flow technique. The following quasi-steady-state assumptions are used for ethylene in gas and liquid phase during slurry polymerizations:

$$\frac{\partial m_g}{\partial t} = \Phi_{m,in} - \Phi_{m,liq} = \delta \tag{1}$$

$$\frac{\partial m_{liq}}{\partial t} = \Phi_{m,liq} - R_p^* = \delta \tag{2}$$

the reaction rate is estimated from the mass flow directly:

$$R_p^* = \Phi_{m,in} \tag{3}$$

The following quasi-steady-state assumption is used during gas phase polymerizations:

$$\frac{\partial m_g}{\partial t} = \Phi_{m,in} - R_P^* = \delta \tag{4}$$

The reaction rate during gas phase polymerizations is also represented by equation 3.

Results and Discussion

Slurry Phase Polymerization

As an example, Figure 2 shows the rate profile of a standard slurry phase polymerization at 70°C and 13.7 bar ethylene partial pressure. Note that the catalyst activity is described in kg polyethylene per gram catalyst including support per hour. A reaction rate of 1.0 kgPE/g_{cat}hr corresponds to a rate of 45,600 kgPE/mol_{Zr}hr.
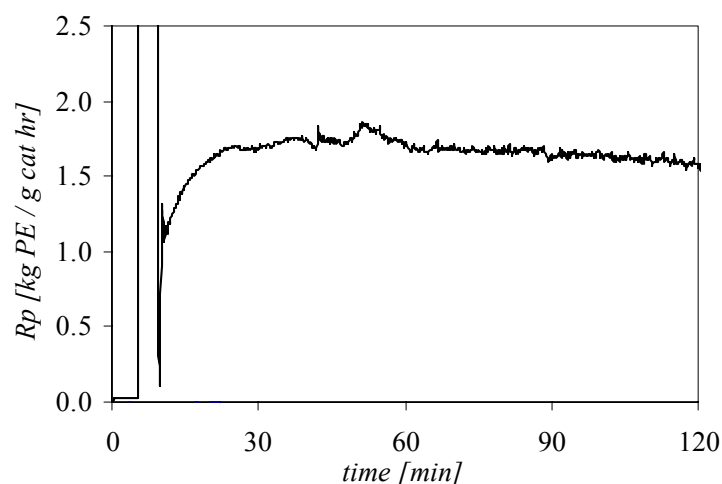

Figure 2: *Polymerization rate profile of slurry experiments at 13.7 bar and 70°C with 65 mg catalyst (incl. support)*

Figure 3: *Maximum polymerization rate vs. ethylene partial pressure in slurry phase at 70°C (□ S1 and ○ S2) and at 60°C (● S7 and ■ S8) with 45 mg catalyst (incl. support)*

Blom *et al.* (2002) used the same catalyst and measured a reaction rate at 80°C of 37 kg PE/($mmol_{Zr}$·hr·mol_E/L) at 31 bar in isobutane. At 70°C and 15 bar in this series an activity was measured of about 145 kg PE/($mmol_{Zr}$·hr·mol_E/L). Due to low deactivation of the catalyst (k_d in the order of 10^{-3} min^{-1}), experiments can be continued for several hours without loss of much activity. Figure 3 shows the results

of step experiments, which were executed at 60 (S7 and S8) and 70°C (S1 and S2). The maximum activity increases almost linearly with the increasing ethylene partial pressure. However when first order behavior is assumed the curve will not cross (0,0), which is the most reliable data point. Figure 3 shows the strong dependence of the maximum activity on temperature. The reaction rate could only be measured until 5 NL/min (maximum capacity of flow meter); this means for 70°C till 17 bar.

Gas Phase Polymerization

Figure 4 shows the maximum reaction rate during gas phase polymerizations measured at different ethylene partial pressures at 60 and 70°C. These gas phase polymerizations are executed after (pre-)polymerization in slurry phase with the Reactive Bed Preparation method. The maximum reaction rate is also more or less linearly dependent on the ethylene partial pressure. However also here linear behavior does not describe the reaction rate at low ethylene partial pressures correctly. The gas phase polymerizations also show a strong dependency on the temperature.
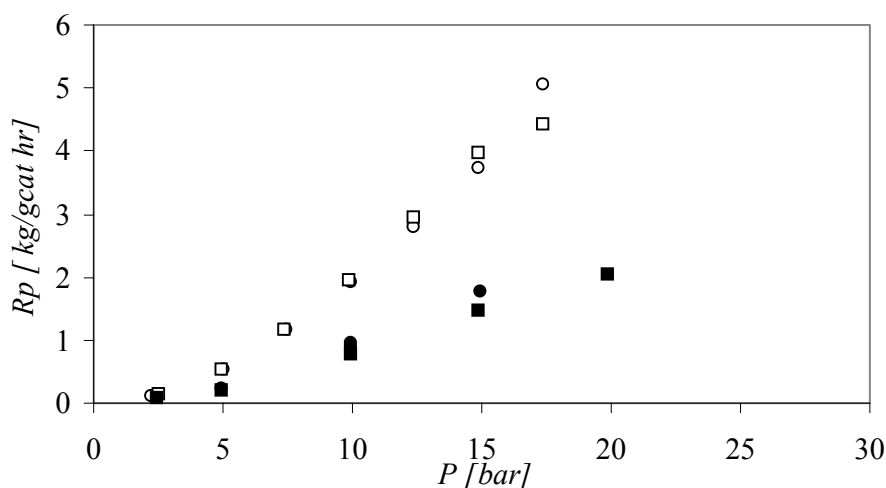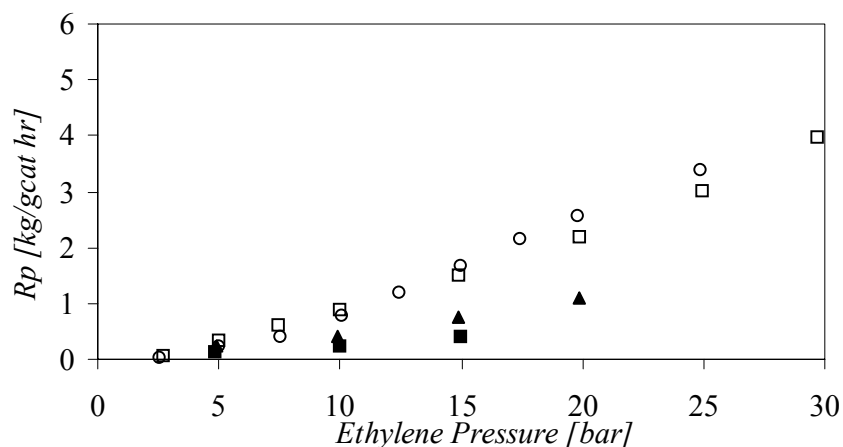

Figure 4: Maximum polymerization rate vs. ethylene partial pressure in gas phase at 70°C (□ G1 and ○ G2) and at 60°C (▲G7 and ■G8) with 45 mg catalyst (incl. support)

Comparison between Gas and Slurry Phase Polymerization

Figure 5 represents the slurry and gas phase experiments at 70°C for the given catalyst taken from Figure 3 and Figure 4; all this information can be extracted from only two RBP experiments. The reactor was first pressurized in steps during slurry phase polymerization and after purging and evacuation the reactor was pressurized in steps during gas phase polymerization. The slurry polymerizations show higher maximum activities at ethylene partial pressure than the gas phase polymerizations. The difference in activity can be explained by the driving force, i.e. the monomer concentration.

Figure 5: *Polymerization rate of two slurry (△S1 and □S2) and gas-phase (▲G1 and ■G2) experiments vs. ethylene partial pressure, at 70°C*
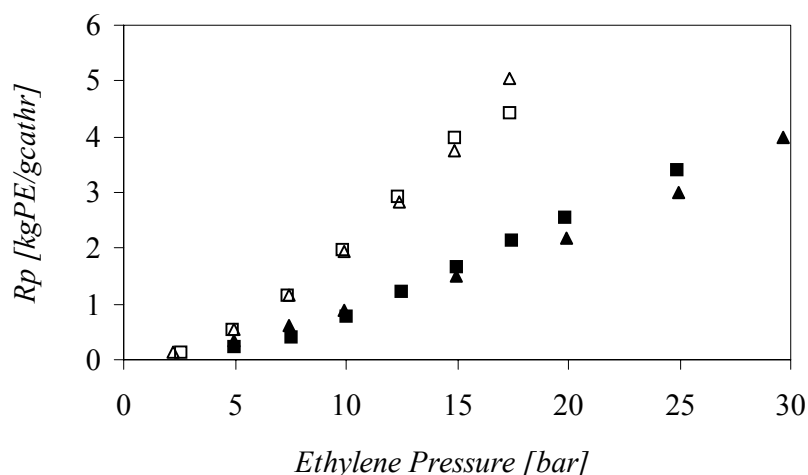
The following assumptions are made:

- Gas liquid mass transfer limitations will not be taken into account because mass transfer limitations will only cause problems at high absolute polymerization rates (g/min). The experiments are done at low absolute reaction rates (< 5 g/min).

- The monomer concentration in the pores equals the bulk concentration (Weickert *et al.* 1999) in gas phase. In this case convection plays an important role, the reaction creates the driving force for the monomer to flow through the pores.

- Diffusion limitations on particle scale can be neglected.

- Monomer concentration near active site is assumed to be the monomer bulk concentration.

With this simplified approach, the reaction rate is assumed to be dependent on the monomer bulk concentration. In slurry polymerization the monomer bulk concentration is given by the ethylene solubility in hexane. Experimental solubility data of ethylene in n-hexane at 20, 40 and 60°C (Konobeev and Lyapin 1967) was modeled with PC-SAFT EOS and extrapolated to 70°C with an interaction coefficient of 0.028 in all cases, see Figure 6 (Banat 2004). The monomer bulk concentration in gas phase polymerization is determined by the ethylene gas density, which is calculated with the second virial coefficient (Daubert *et al.* 1999). Figure 7 shows that slurry and gas phase experiments have the same maximum polymerization rate as function of the monomer bulk concentration, i.e. same propagation rate constant and reaction order. Also RBP experiments at 60°C show the same results when the maximum activity is plotted versus monomer bulk concentration (Figure 8).
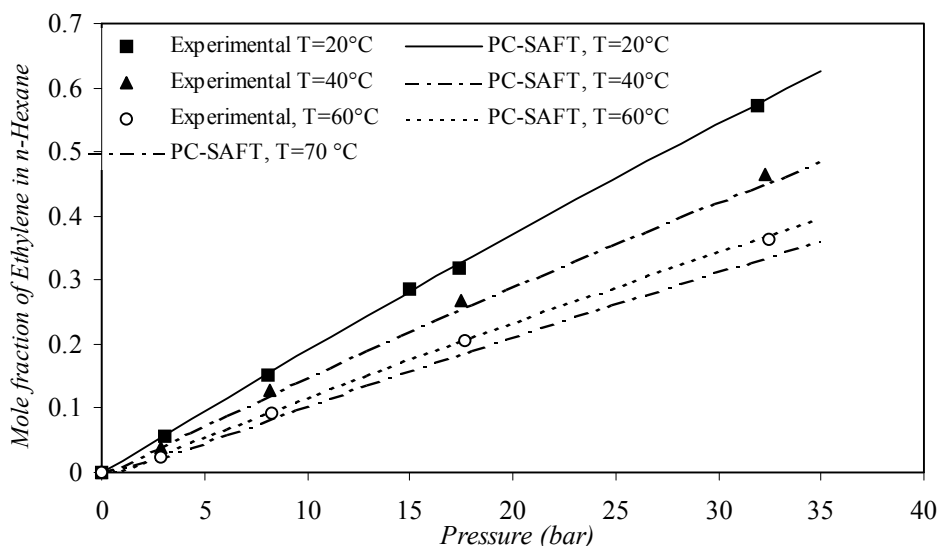
Figure 6: *Experimental solubility data of ethylene in n-hexane at 20 (■), 40 (▲) and 60°C (○) (IUPAC) modeled with PC-SAFT EOS and extrapolated to 70°C, with interaction coefficient of 0.028 (Banat)*
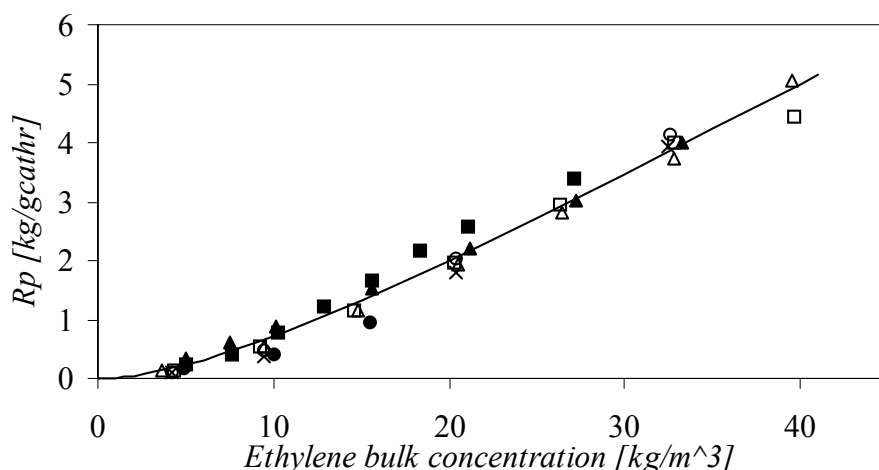
Figure 7: *Polymerization rate of several slurry (△S1, □S2, ×S3 and ○S4) and gas-phase (▲G1, ■G2 and ●G4) experiments vs. bulk concentration, all experiments at 70°C*

For the used heterogeneous metallocene catalyst under these reaction conditions, the following conclusions can be drawn:

- The basic kinetics for ethylene homo-polymerizations in slurry and gas phase is the same.
- No activity loss was observed when changing from slurry to gas phase polymerizations and therefore the reactive bed preparation method is not changing the measured kinetics. This is in contrast to propylene polymerizations, where van Putten (2004) found a 45% decrease in activity when propylene was purged before changing from liquid pre-polymerization to gas phase main-polymerization. Pater *et al.* (2004) could explain this by measuring propylene sorption in-situ. They found that propylene sorption behavior in polypropylene is changing irreversible when the polymer is

degassed and/or dried. The freshly produced polypropylene has a much higher propylene sorption in-situ, i.e. a higher concentration of monomer near the active site, than after degassing and/or drying.

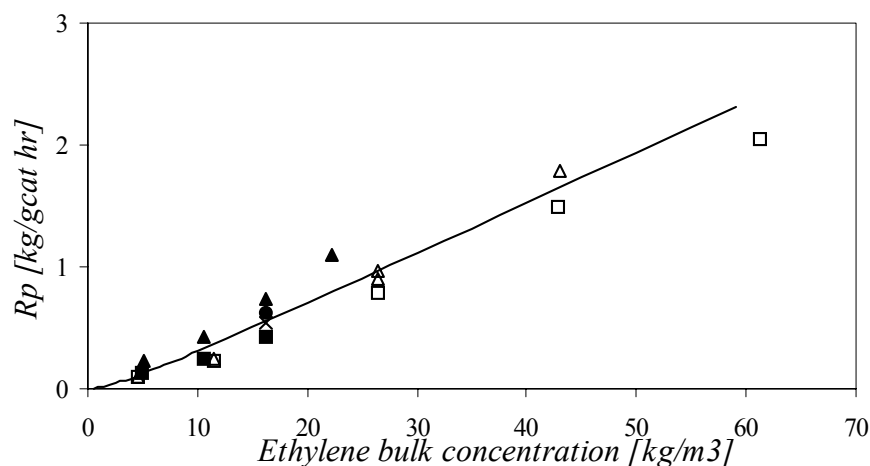**Figure 8:** *Polymerization rate of slurry ($\triangle$S7 and $\square$S8) and gas-phase ($\blacktriangle$G7, $\blacksquare$G8, $\bullet$G9 and $\times$G10) experiments vs. bulk concentration at 60°C*

### *Influence of Monomer Concentration*

Figure 7 shows clearly the non-first order dependency on monomer bulk concentration at low monomer concentration. Also Chakravarti and Ray (2001), Chien *et al.* (1998), Karol *et al.* (1993) and Kissin *et al.* (1999) reported a higher order and/or broken order dependency of the ethylene polymerization rate on the monomer concentration; 1.24, 2.0, 2.0 and 1.8 respectively. A conclusion from literature can be that measuring kinetics at low partial pressures results in higher reaction orders.

Karol *et al.* (1993) found for a Ti-based catalyst second order behavior both for slurry phase and gas phase polymerizations, until pressures of 7.5 bar and 9.5 bar respectively. They interpreted the observed behavior with a dynamic equilibrium kinetic model, wherein ethylene or alpha-olefins are acting as coordinating ligands at the active center during the polymerization process.

Chien *et al.* (1998), using metallocene catalysts, explained the observed non-first order dependency on monomer concentration by complex formation of one or two monomer molecules with the active site. Reversible complex formation from an active site with one monomer molecule is generally accepted (Böhm 1984; Schnauss and Reichert 1990; Shaffer and Ray 1997). Marques *et al.* (1997) proposed the double coordination mechanism for Ziegler-Natta catalyzed polymerizations based on the trigger mechanism by Ystenes (1991). In the trigger mechanism a monomer molecule forms a complex with the active site and the insertion takes place after incoming of a second monomer molecule. Ystenes assumed that the complexed monomer is inserted and not the incoming monomer. Weickert (2004a) showed an enormous increase of activity for propylene polymerizations only by addition of a small amount of ethylene in the presence of hydrogen. This phenomenon cannot only be explained by reactivity ratios and dormant site theories. Shimizu (2001) proposed that in the trigger

mechanism not the complexed monomer is inserted in the polymer chain but the incoming monomer. He based his hypothesis on the increased activity, small amount of insertions of ethylene and NMR data. A 2,1-propylene insertion leads to a dormant site; reactivating such a dormant site by ethylene should show a peak (34.8 –35.6 ppm) on NMR. This peak was not observed in the specific range. Obviously, complex formation between metal and monomer plays an important role for very different monomer catalyst combinations.

In this work the complex formation mechanism is represented as follows:

Complex formation: $\qquad C^0 + M \underset{k_2}{\overset{k_1}{\rightleftarrows}} C^M$ (5)
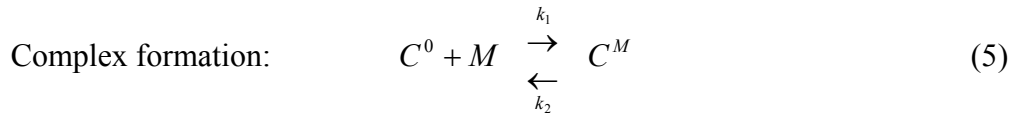
The uncomplexed active site (C^0) is complexed with monomer M (C^M).

Propagation reaction: $\qquad C_j^M + M \xrightarrow{k_p} C_{j+1}^M$ (6)
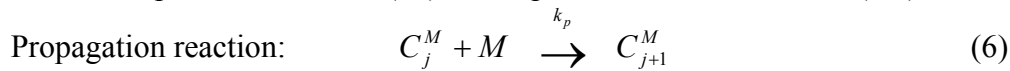
C_j^M is a complexed active site with a growing polymer chain of length j. The deactivation of the catalyst (see Figure 2, $k_d < 10^{-3}$ min^{-1}) is occurring at a different time scale than the complex formation, which is assumed to occur at a much smaller time scale. Therefore the deactivation is not changing the complexation and a steady state approach can be applied for the mechanism.

With: $\qquad\qquad\qquad C^M = \sum_j C_j^M$ (7)

The polymerization rate: $\qquad R_P = k_p \cdot C^M \cdot M$ (8)

Using steady-state approach:

$$\frac{dC^M}{dt} = k_1 C^0 \cdot M - k_2 C^M = 0 \quad \rightarrow \quad C^M = \frac{k_1}{k_2} C^0 \cdot M$$ (9)

Total amount of active sites: $\quad C_t = C^0 + C^M \quad \rightarrow \quad C^0 = \frac{k_2}{k_2 + k_1 M} \cdot C_t$ (10)

Combining (9) and (10): $\qquad C^M = \frac{k_1}{k_2} \cdot \frac{k_2 C_t}{k_2 + k_1 M} \cdot M = \frac{k_1 \cdot M}{k_2 + k_1 M} \cdot C_t$ (11)

Combining (8) and (11): $\qquad R_P = k_p \cdot C_t \cdot \frac{k_1 \cdot M^2}{k_2 + k_1 \cdot M}$ (12)

This simplified complexation model can explain first and second order behavior as presented in Figure 7. This means that for low monomer concentration the reaction rate is second order on monomer bulk concentration, and for high monomer concentrations the reaction rate dependency becomes first order on monomer bulk concentration.

Two extreme cases are distinguished:

- *Case I:*

The monomer concentration is very low: $\qquad k_1 \cdot M \ll k_2$

The reaction rate can be described by: $\qquad R_P = k_p \cdot \dfrac{k_1}{k_2} \cdot C_t \cdot M^2$ $\qquad$ (13)

For low monomer concentration the reaction rate is second order on monomer bulk concentration.

- *Case II:*

The monomer concentration is high: $\qquad k_1 \cdot M \gg k_2$

The reaction rate can be described by: $\qquad R_P = k_p \cdot C_t \cdot M$ $\qquad$ (14)

For high monomer concentrations the reaction rate dependency becomes first order on monomer bulk concentration and the commonly used polymerization rate model is obtained.

Influence of Temperature

The reaction rate constants k_1 and k_2 in reaction 5 and k_p in reaction 6 are assumed to be temperature dependent according to the Arrhenius equation. The ratio of k_1 and k_2 is the equilibrium constant K_A:

$$K_A = \frac{k_1}{k_2} = \frac{k_{1,0} \cdot e^{-E_{Act,1}/RT}}{k_{2,0} \cdot e^{-E_{Act,2}/RT}} = K_{A,0} \cdot e^{\Delta H/RT} \qquad (15)$$

And for the propagation constant: $\qquad k_p = k_{p,0} \cdot e^{-E_{Act,p}/RT}$ $\qquad$ (16)

Pressure series were executed at 60, 70 and 90°C resulting in three values for K_A. $k_p C_t$ is calculated with this temperature dependent K_A for a temperature series between 55 and 90°C at constant pressure.

K_{A0}	$1.03 \cdot 10^{-12}$	$m^3 \cdot kg^{-1}$
ΔH	71.7	$kJ \cdot mol^{-1}$
$C_t k_{p0}$	$2.49 \cdot 10^{10}$	$m^3 \cdot hr^{-1}$
$E_{act,p}$	74.9	$kJ \cdot mol^{-1}$

Table 1: *Parameters of complexation and propagation constant*

Figure 9 shows the Arrhenius plot for the equilibrium constant K_A, resulting in an enthalpy of 71.7 kJ/mol. Figure 10 shows the Arrhenius plot for the propagation constant; the activation energy for the propagation is 74.9 kJ/mol. Table 1 summarizes these enthalpies and the values for the initial constants.
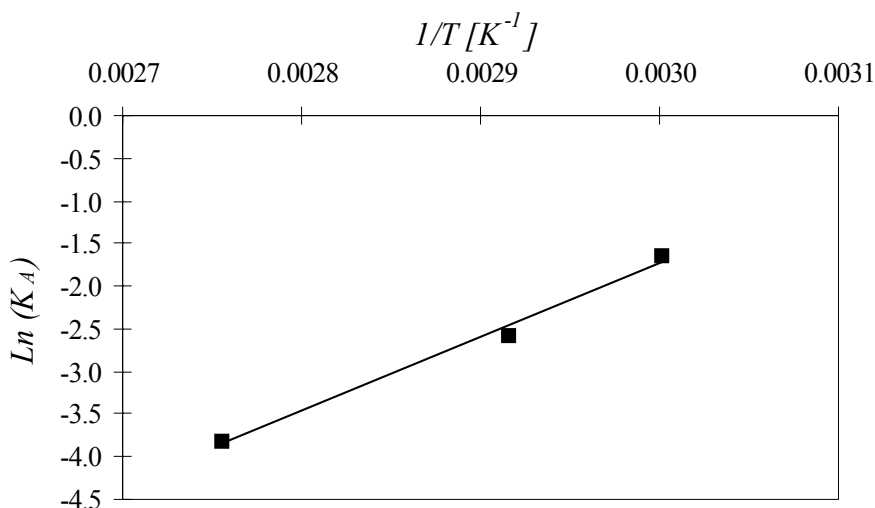
Figure 9: *Arrhenius plot of equilibrium constant K_A between 90°C and 60°C*
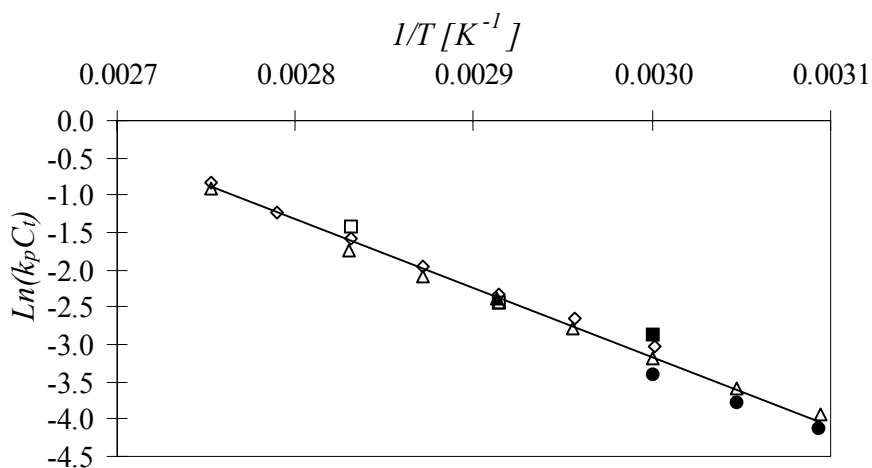
Figure 10: *Arrhenius plot of propagation constant (including Ct) of gas phase experiments (□G5, ▲G6, ■G7, ●G8, ○G9 and △G10) between 90°C and 50°C, at 15 bars with 45 mg catalyst (incl. support)*

This value is much higher then is often reported in literature; therefore the two extreme cases are considered again:

- **Case I:** $k_2 >> k_1 \cdot M$

Using a classical reaction rate model of $R_p = k_p \cdot C_t \cdot M^n$, the activation energy in this case will be:

$$-E_{Act,I} = -E_{Act,1} + E_{Act,2} - E_{Act,p} = \Delta H - E_{Act,p} = 71.7 - 74.9 = -3.2 \, kJ/mol \qquad (17)$$

The temperature will have only small influence on the reaction rate.

- **Case II:** $k_2 << k_1 \cdot M$

A classical reaction rate model of $R_p = k_p \cdot C_t \cdot M^n$ (with n=1) will predict in this case an activation energy of:

$$-E_{Act,II} = -E_{Act,p} = -74.9 \, kJ/mol \qquad (18)$$

At high monomer concentration the activation energy is high and therefore the reaction rate is strongly dependent on the temperature.

The two extreme cases show that the activation energy is dependent on the monomer concentration. This will be illustrated with literature data.

Roos et al. (1997) measured a propagation activation energy of 39.2 kJ/mol for a supported rac-Me$_2$Si[Ind]$_2$ZrCl$_2$/MAO catalyst at low ethylene partial pressure of 5 bar between 40 and 80°C.

Kaminsky (1994) measured ethylene polymerization activities with a Cp$_2$Zr(CH$_3$)$_2$/MAO catalyst in toluene at 8 bar ethylene. His data is presented in Table 2. The monomer bulk concentration, which is calculated with solubility data (Konobeev and Lyapin 1967), is not constant during the presented experiments (see Table 2). However an activation energy is calculated, assuming classical 1st order reaction model. The obtained activation energy for the propagation reaction is 75 kJ/mol.

T °C	P_e bar	Activity gPE/gZr·hr·bar	Rate kg PE/gZr·hr	x C2 in tol. mole/mole	Cm kg/m^3
20	8	9000	72	0.1113	33.04
70	8	70000	560	0.0644	17.19
90	8	3100000	24800	0.0550	14.18

Table 2: *Slurry polymerization data of Kaminsky (1994) with recalculated monomer bulk concentration*

Reaction rates are calculated at the conditions of Roos *et al.* (1997) and Kaminsky (1994) with the complexation model. Figure 11 shows the standard Arrhenius plot using a classical reaction rate model, so one combined activation energy. The activation energies, calculated from these data, are respectively 38 kJ/mol and 59 kJ/mol. Figure 11 also shows the activation energy for the two extreme cases; case I at 0.2 kg/m^3 results in $E_{act,I}$ = 5 kJ/mol and for case II at 50 kg/m^3 $E_{act,II}$ =60 kJ/mol.

Simon *et al.* (2001) presented ethylene polymerization kinetics with a nickeldiine catalyst. Table 3 presents their data; here the activation energies are calculated for each pressure interval. For this nickel-diine catalyst the same trend is observed as for the used zirconocene; the activation energy increases with increasing monomer concentration.
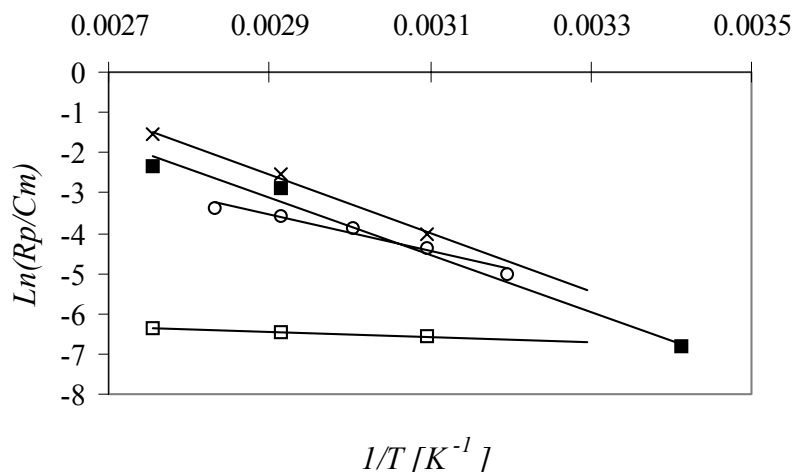
Figure 11: *Modified Arrhenius plot calculated from complexation model: ■ based on concentrations of Kaminsky E_{act} = 59 kJ/mol, ○ based on concentrations of Roos et al. E_{act} = 38 kJ/mol, □ Case I, at low, constant monomer concentration of 0.2 kg/m^3 E_{act} = 5 kJ/mol and × Case II, high, constant monomer concentration of 50 kg/m^3 E_{act} = 60 kJ/mol*

T	P	Cm	Rp	E_{act}
°C	bar	mol/L	kgPE/molNihr	kJ/mol
30	2	0.42	1360	
40	2	0.35	1460	16.7
50	2	0.32	1560	
30	4.8	0.97	2890	
40	4.8	0.81	3970	20.0
50	4.8	0.74	3590	
30	11.6	2.35	2950	
40	11.6	1.97	3680	39.8
50	11.6	1.80	6020	
30	18.4	3.74	2060	
40	18.4	3.13	3120	58.7
50	18.4	2.87	6710	

Table 3: *Polymerization data of Simon et al. (2001)*

The proposed complexation model with two Arrhenius dependent constants would not predict an exponential increasing propagation rate with increasing temperature. This is dependent on the values for ΔH and $E_{Act,p}$ and would lead to a maximum (see Figure 12).

Lower activities can also be explained by increasing deactivation, the lumped deactivation constant can also be expected to be Arrhenius dependent. Xu *et al.* (2001) and Chakravarti and Ray (2001) showed for the same catalyst an increasing deactivation from 60°C to 80°. Kumkaew *et al*. (2003) observed in their

measurements a increasing deactivation with increasing temperature resulting in a decreasing activity at 90°C and 100°C.
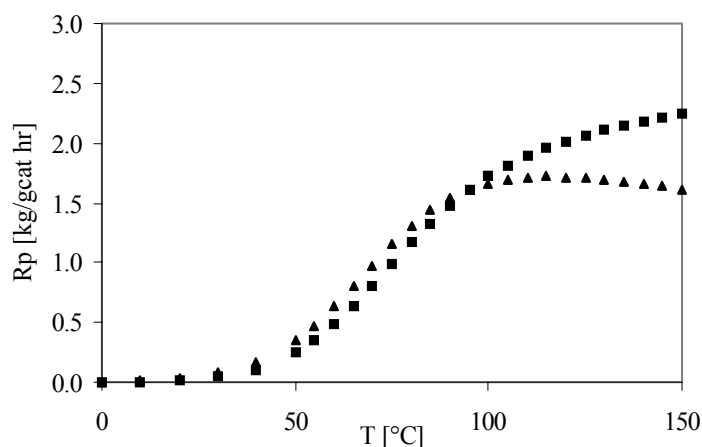

Figure 12: *Maximum reaction rate versus reaction temperature,* ▲ *Eact,p = 67kJ/mol and* ■ *Eact,p = 75 kJ/mol, ΔH in both simulations 71 kJ/mol*

Polymer Properties

For catalyst characterization, several polymers were analyzed for density and molecular weight distribution (MWD); Table 4 shows this data. Due to the changing process conditions within each experiment the MWD's are quite broad. Polydispersity indexes (PDI) are obtained varying from 3.4 till 5.1. Due to the changing process conditions different high-density polyethylenes are produced.

	Slurry		Gas					
Run	T	P	T	P	Mw	Mn	PDI	Density
	°C	bar	°C	bar	kg/mol	kg/mol	-	g/ml
1	70	2.5-17	70	2.5-30	429	107	4.01	0.9475
2	70	2.5-17	70	2.5-25	450	94	4.77	0.9479
7	60	2.5-20	60	2.5-20	453	89	5.08	0.9456
9	70	2.5-15	60-90	15	327	78	4.17	0.9466
11	70	15	70	15	363	74	4.90	0.9452
12[1]	70	15	70	15	271	68	3.96	0.9519
13a[2]	70	15	-	-	214	57	3.78	0.9538
13b[2]	70	15	-	-	241	72	3.35	0.9547

[1]During the gas phase part of run 12 three pulses of hydrogen were added.
[2]13a and b are duplicate analyzes of the same polymer produced in slurry phase.

Table 4: *Polymer properties: Molecular weights and densities of slurry and gas phase polymerizations with their polymerization conditions*
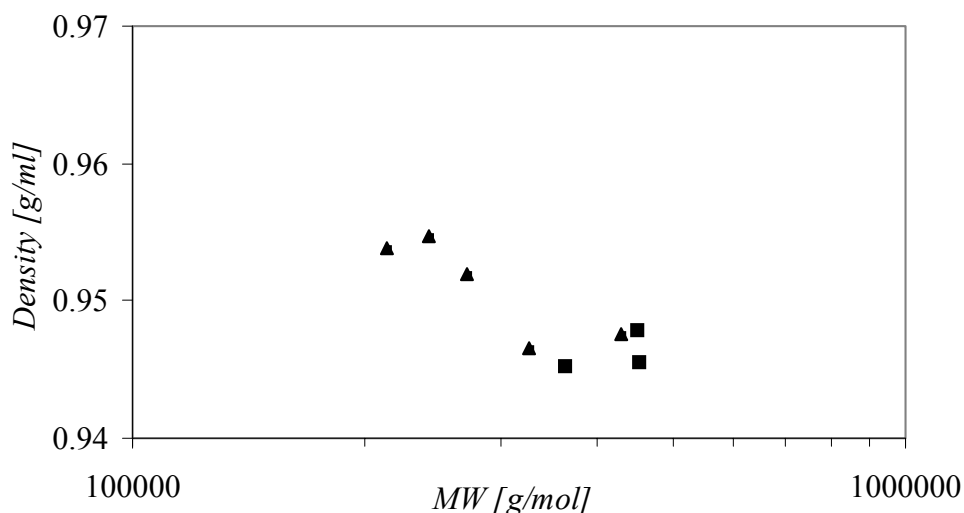
Figure 13: *Density vs. weight average Molecular Weight of homo-polymers produced during RBP experiments, T and P were varied, ▲ homo-polymers with PDI of 3.4-4.2 and ■ homo-polymers with PDI of 4.7-5.1*

Figure 13 shows that the density decreases with increasing molecular weight. This is in agreement with that for lower molecular weight polymer molecules a higher crystallinity is observed. Note that Figure 13 is not a straight line. This is a result of different polydispersity indexes and measurement uncertainties in the polymer analyses. Polymers with higher polydispersity index but same average molecular weight will have a higher density. The molecular weight obtained in this series at constant temperature (70°C) and pressure (15 bar) in hexane is 240 kg/mol. Blom *et al.* (2002) produced homo-polyethylene with a molecular weight of 260 kg/mol (PDI = 2.4) with a supported Ind_2ZrCl_2/MAO catalyst at 80°C in isobutane at 31.4 bar without hydrogen.

Conclusions

The following conclusions can be drawn taken into consideration that those are valid for the used supported Ind_2ZrCl_2/MAO catalyst under the presented polymerization conditions:

- The measured maximum polymerization rates show for gas and slurry phase an equal dependency on the monomer bulk concentration, the same propagation rate and reaction order
- Gas liquid mass transfer limitation does not play a significant role
- Diffusion limitations can be neglected
- The presented complexation model describes the non-linear dependency at low monomer bulk concentration (<10 kg·m^{-3}) and the linear dependency at high monomer bulk concentration (>10 kg·m^{-3}) on the maximum reaction rate.
- Due to the complexation model two activation energies are obtained one for the propagation reaction and one for the complexation. The combined activation energy is therefore monomer concentration dependent.

- The RBP method was successfully implemented for ethylene homo-polymerizations; the activity did not decrease during the evaporation of hexane.

Acknowledgement

Notation

C^0	Un-complexed active site	$mol \cdot g_{cat}^{-1}$
C^M	Complexed active site with monomer M	$mol \cdot g_{cat}^{-1}$
C_t	Total amount of active sites	$mol \cdot g_{cat}^{-1}$
$E_{act,i}$	Activation energy from reaction i	$kJ \cdot mol^{-1}$
ΔH	Enthalpy of complexation	$kJ \cdot mol^{-1}$
K_A	Equilibrium reaction constant of complexation	$m^3 \cdot kg^{-1}$
k_1	Reaction constant of complex forming	$m^3 \cdot kg^{-1} \cdot s^{-1}$
k_2	Reaction constant of de-complexing	s^{-1}
k_p	Propagation reaction constant	$m^3 \cdot mol^{-1} \cdot hr^{-1}$
M	Monomer concentration	$kg \cdot m^{-3}$
m	Mass	g
P	Pressure	bara
R	Gas constant	$J \cdot mol^{-1} \cdot K^{-1}$
R_p	Polymerization rate (activity)	$kg(PE) \cdot g_{cat}^{-1} \cdot min^{-1}$
R_p^*	Polymerization rate	$g(PE) \cdot min^{-1}$
T	Temperature	K
t	Time	min

Greek letters

Φ_m	Mass flow	$g \cdot min^{-1}$
δ	Small order symbol, negligible compared to other terms	

Subscript

0	Initial condition
1	Complex forming reaction
2	Reverse of complex forming reaction
g	Gas
in	Flowing into the reactor
liq	Flowing to liquid phase
p	Propagation reaction
PE	Polyethylene

Abbreviations

G	Gas phase experiment
Mn	Number average molecular weight
Mw	Weight average molecular weight
MWD	Molecular weight distribution
PDI	Polydispersity
PE	Polyethylene
RBP	Reactive Bed Preparation

S   Slurry phase experiment
TIBA   Tri-isobutylaluminum

Literature

Banat, Y. A. I. (2004). in press, Enschede, University of Twente.

Blom, R., Swang, O. and Heyn, R. H. (2002). "Semi-Batch Polymerizations of Ethylene with Metallocene Catalysts in the Presence of Hydrogen, 3 Correlation between Hydrogen Sensitivity and Molecular Parameters." *Macromol. Chem. Phys.* **203**(2): 381-387.

Böhm, L. L. (1984). "Homo- and Copolymerization with a Highly Active Ziegler-Natta Catalyst." *J. Appl. Polym. Sci.* **29**: 279-289.

Chakravarti, S. and Ray, W. H. (2001). "Kinetic Study of Olefin Polymerization with a Supported Metallocene Catalyst. II. Ethylene/1-Hexene Copolymerization in Gas Phase." *J. Appl. Polym. Sci.* **80**: 1096-1119.

Chakravarti, S. and Ray, W. H. (2001). "Kinetic Study of Olefin Polymerization with a Supported Metallocene Catalyst. III. Ethylene Homopolymerization in Slurry." *J. Appl. Polym. Sci.* **81**: 2901-2917.

Chien, J. C. W., Yu, Z., Marques, M. M., Flores, J. C. and Rausch, M. D. (1998). "Polymerizations of Olefins and Diolefins Catalyzed by Monocyclopentadienyltitanium Complexes Containing a (Dimethylamino) ethyl Substituent and Comparison with ansa-Zirconocene Systems." *J. Polym. Sci. A: Polym. Chem.* **36**: 319-328.

Daubert, T. E., Danner, R. P., Sibul, H. M., Stebbins, C. C., Rowley, R. L., Wilding, W. V., Oscarson, J. L., Adams, M. E. and Marshall, T. L., Eds. (1999). Physical and Thermodynamic Properties of Pure Chemicals, Part 1. AIChE & DIPPR. Columbus, OH, Greyden Press.

Hutchinson, R. A. and Ray, W. H. (1987). "Polymerization of Olefins through Heterogeneous Catalysis. VII. Particle Ignition and Extinction Phenomena." *J. Appl. Polym. Sci.* **34**(2): 657-676.

Kaminsky, W. (1994). "Zirconocene Catalysts for Olefin Polymerization." *Catalysis Today* **20**: 257-271.

Karol, F. J., Kao, S. C. and Cann, K. J. (1993). "Comonomer Effects with High-Activity Titanium- and Vanadium -Based Catalysts for Ethylene Polymerization." *J. Polym. Sci. A: Polym. Chem.* **31**: 2541-2553.

Kissin, Y. V., Mink, R. I. and Nowlin, T. E. (1999). "Ethylene Polymerization Reactions with Ziegler-Natta Catalysts. I. Ethylene Polymerization Kinetics and Kinetic Mechanism." *J. Polym. Sci. A: Polym. Chem.* **37**: 4255-4272.

Kissin, Y. V., Mink, R. I., Nowlin, T. E. and Brandolini, A. J. (1999). Kinetics and Mechanism of Ethylene Polymerization and Copolymerization Reactions with Heterogeneous Titanium-Based Ziegler-Natta Catalysts. Metalorganic catalysts for synthesis and polymerizations. Kaminsky, W., Springer Verlag**:** 60-75.

Konobeev, B. I. and Lyapin, V. V. (1967). IUPAC Solubility Data Series. Ethylene. Hayduk, W. Oxford, Oxford University Press. **1994 Volume 57**.

Kumkaew, P., Wanke, S. E., Praserthdam, P., Danumah, C. and Kaliaguine, S. (2003). "Gas-Phase Ethylene Polymerization Using Zirconocene Supported on Mesoporous Molecular Sieves." *J. Appl. Polym. Sci.* **87**(7): 1161-1177.

Marques, M. M., Dias, A. R., Costa, C., Lemos, F. and Ribeiro, F. R. (1997). "Homogeneous Ziegler-Natta Polymerisation: a Kinetic Approach 1. Steady-State Kinetics." *Polym. Int.* **43**: 77-85.

Meier, G. B., Weickert, G. and van Swaaij, W. P. M. (2001). "Comparison of Gas- and Liquid-Phase Polymerization of Propylene with Heterogenous Metallocene Catalyst." *J. Appl. Polym. Sci.* **81**: 1193-1206.

Pater, J. T. M., Weickert, G., Fait, A. and Mei, G. (2004). "Measurement of In-Situ Monomer Sorption in Poly(propylene)." *Macromol. Rapid Commun.* **25**: 1638-1642.

Pater, J. T. M., Weickert, G. and van Swaaij, W. P. M. (2003). "Propene Bulk Polymerization Kinetics: Role of Prepolymerization and Hydrogen." *AIChE Journal* **49**(1): 180-193.

Putten, I. C. v. (2004). Propylene Polymerization in a Circulating Slugging Fluidized Bed Reactor. Enschede, University of Twente**:** 73-90.

Roos, P., Meier, G. B., Samson, J. J. C., Weickert, G. and Westerterp, K. R. (1997). "Gas Phase Polymerization of Ethylene with a Silica-Supported Metallocene Catalyst: Influence of Temperature on Deactivation." *Macromol. Rapid Commun.* **18**: 319-324.

Samson, J. J. C., Weickert, G., Heerze, A. E. and Westerterp, K. R. (1998). "Liquid-Phase Polymerization of Propylene with a Highly Active Catalyst." *AIChE Journal* **44**(6): 1424-1437.

Schnauss, A. and Reichert, K.-H. (1990). "Modeling the Kinetics of Ethylene Polymerization with Ziegler-Natta Catalysts." *Makromol. Chem., Rapid Commun.* **11**: 315-320.

Shaffer, W. K. A. and Ray, W. H. (1997). "Polymerization of Olefins Through Heterogeneous Catalysis. XVIII. A Kinetic Explanation for Unusual Effects." *J. Appl. Polym. Sci.* **65**: 1053-1080.

Shimizu, F. (2001). Liquid Pool Polymerization of Propylene and Ethylene Using a Highly Active Ziegler-Natta Catalyst - Kinetics and Polymerization Mechanism. Enschede, University of Twente**:** 77-91.

Simon, L. C. W., C.P.; Soares, J.B.P.; Souza R.F. de (2001). "Kinetic Investigation of Ethylene Polymerization Catalyzed by Nickel-Diimine Catalysts." *J. Mol. Cat. A: Chem.* **165**: 55-66.

Weickert, G. (2004a). High Precision Polymerization Rate Profiles. Ziegler Natta Catalysts. Busico, V. Kanazawa, JAIST.

Weickert, G., Meier, G. B., Pater, J. T. M. and Westerterp, K. R. (1999). "The Particle as Microreactor: Catalytic Propylene Polymerizations with Supported Metallocene and Ziegler-Natta Catalysts." *Chem. Eng. Sci.* **54**: 3291-3296.

Xu, Z. G., Chakravarti, S. and Ray, W. H. (2001). "Kinetic Study of Olefin Polymerization with a Supported Metallocene Catalyst. I. Ethylene/Propylene Copolymerization in Gas Phase." *J. Appl. Polym. Sci.* **80**: 81-114.

Ystenes, M. (1991). "The Trigger Mechanism for Polymerization of a-Olefins with Ziegler-Natta Catalysts: A New Model Based on Interaction of Tweo Monomers at the Transition State and Monomer Activation of the Catalytic Center." *J. Catal.* **129**: 338-401.

Chapter 4

Metallocene Catalyzed Gas Phase Ethylene Co-Polymerizations: Kinetics and Polymer Properties

Abstract

A kinetic study of ethylene/1-hexene co-polymerization with a supported Ind_2ZrCl_2/MAO catalyst in gas phase is presented. The influence of the co-monomer was examined at industrial process conditions. For both monomers reaction rate profiles were measured. A complexation model is presented which is able to describe a large reaction rate increase due to a small amount of incorporated co-monomer. This complexation model results in a co-polymerization equation, which depends on the two reactivity ratios, the monomer concentration ratio and a ratio of the homo-polymerization kinetic constants. This kinetic model was able to describe the observed reaction rates for ethylene and 1-hexene and also the incorporated co-monomer weight fraction.

The produced polymers were analyzed on properties such as density, molecular weight, melt temperature and incorporated co-monomer mass fraction. In-situ sorption of the co-monomer could be determined by combining the kinetic information with the incorporated co-monomer mass fraction. The in-situ 1-hexene sorption is following Henry's law, but was found to be much higher than reported in literature. At increasing 1-hexene gas concentration the density, melting point and molecular weight of the produced polyethylene decreased, while the melt index increased with increasing hexene concentration.

The polymer properties have been compared with a typical LLDPE produced with a Ziegler-Natta catalyst.

Chapter 4

Introduction

General gas phase co-polymerizations

Metallocene catalysts have been investigated already for decades. Kaminsky (1996), Hamielec and Soares (1996) published reviews on metallocene catalyzed ethylene homo- and co-polymerizations. The potential of metallocene catalysts is high, but still most commercial HDPE and LLDPE are produced with Ziegler-Natta and Chromium (HDPE) catalysts. HDPE and LLDPE are often produced in gas phase reactors like fluidized bed reactors, e.g. in processes like Unipol, Spherilene (Covezzi 1995) and Borstar PE (Avela *et al.* 1998).

Besides the polymerization kinetics of the catalyst, also the polymer properties should be known before a catalyst can be introduced in an industrial reactor. Kinetics are important for optimizing reactor control. Combining kinetics with polymer properties gives tools to control polymer properties like molecular weight, molecular weight distribution, density, co-polymer composition, etc. The final mechanical properties of the polymer are highly influenced by these properties.

Essential differences between metallocene and Ziegler-Natta catalyst produced polymers are the molecular weight and incorporated co-monomer distribution. Metallocene catalysts produce narrower molecular weight distributions due to their single site behavior. Moreover, metallocenes will distribute the co-monomer much more homogeneous over the polymer chains. Ziegler-Natta catalysts produce polymers with the co-monomer built in preferably in the lower molecular weight part.

The co-monomer incorporation behavior and molecular weight distribution of metallocene catalysts provides the chance to produce superior polymer properties by manipulating kinetics with process conditions. This can be done in single reactors with different zones, Multi Zone Circulating Reactor (Covezzi and Mei 2001) or using two different catalyst on one support, Univation (Liu 2003). Two catalysts on one support is especially suitable for single site catalysts. So also in single reactors, bi-modal molecular weight distributions and/or bi-modal co-monomer compositions can be produced.

State of the art

Only a few academic research groups are able to measure kinetics and to produce sufficient amounts of polymer for property analyses, at industrial conditions with good reproducibility, temperature control, pressure control and gas phase co-monomer control. Most reports deal with slurry polymerizations (Quijada *et al.* 1995; Britto *et al.* 2001; Kappler *et al.* 2003). Only Kappler *et al.* measured the 1-hexene concentration in solution.

Ray's group (Han-Adebekun *et al.* 1997; Chakravarti and Ray 2001) was able to measure kinetics of highly active metallocene catalysts under industrial conditions, i.e. elevated pressures and temperatures at constant process parameters. They

observed immediately an increased activity due to 1-hexene; the so-called co-monomer effect. Polymer properties were not reported.

Kumkaew *et al*. (2003) and Zhou *et al*. (2003) performed gas phase ethylene 1-hexene co-polymerizations in isoperibolic mode with batch 1-hexene feed. The 1-hexene gas phase concentration decreased with 66% during the polymerization and the temperature increased sometimes with 25°C. These changing process conditions will inevitably change kinetics and polymer properties. Kumkaew observed a sharp decrease in initial reaction rate followed by a slow increase.

Industrial gas phase processes are operated in the presence of an inert gas (e.g. nitrogen, propane) to improve heat transfer on particle and reactor scale. At very high polymerization rates diffusion limitations can cause enrichment of inert gasses in the polymerizing particle and lower the monomer concentration (Parasu Veera *et al.* 2001).

This work

In this work ethylene 1-hexene co-polymerizations will be investigated with a supported Ind_2ZrCl_2/MAO catalyst at industrial, process conditions. Note that during the experiments all process conditions (temperature, pressure and ethylene and 1-hexene concentrations) are kept constant. This kinetic study will focus especially on the influence of 1-hexene on the polymerization rate, but also the ethylene concentration will be varied. The kinetic behavior will be described by a complexation model, which should be able to describe the co-monomer effect.

The influence of 1-hexene on polymer properties like density, molecular weight, melting point and melt flow index is measured. The incorporated co-monomer fraction is measured via IR in order to differentiate between sorption and real reaction rate.

Finally these polymer properties are compared with a commercial Ziegler-Natta LLDPE product.

Kinetic model

Table 1 represents three mechanisms to describe the co-polymerization kinetics. The complex physical and chemical effects during initiation and deactivation are described by semi empirical equations and assumed to be first order (Meier *et al.* 2001).

Model I: 1st order Markov	Model II: Trigger Mechanism	Model III: Complexation
Activation		
$C \xrightarrow{k_i} C^*$	See model I	$C \xrightarrow{k_i} C^0$
Complex formation		
-	$C^* + A \; \overset{k_{a1}}{\underset{k_{a2}}{\rightleftarrows}} \; P_0^*$	$C^0 + A \; \overset{k_{a1}}{\underset{k_{a2}}{\rightleftarrows}} \; C^A$
-	$C^* + B \; \overset{k_{b1}}{\underset{k_{b2}}{\rightleftarrows}} \; Q_0^*$	$C^0 + B \; \overset{k_{b1}}{\underset{k_{b2}}{\rightleftarrows}} \; C^B$
Start j=0		
$C^* + A \xrightarrow{k_{sa}} P_1^*$	$P_j^* + A \xrightarrow{k_{saa}} P_1^*$	$C_j^A + A \xrightarrow{k_{saa}} C_1^A$
$C^* + B \xrightarrow{k_{sb}} Q_1^*$	$P_j^* + B \xrightarrow{k_{sab}} Q_1^*$	$C_j^A + B \xrightarrow{k_{sab}} C_1^A$
	$Q_j^* + A \xrightarrow{k_{sba}} P_1^*$	$C_j^B + A \xrightarrow{k_{sba}} C_1^B$
	$Q_j^* + B \xrightarrow{k_{sbb}} Q_1^*$	$C_j^B + B \xrightarrow{k_{sbb}} C_1^B$
Propagation		
$P_j^* + A \xrightarrow{k_{paa}} P_{j+1}^*$	See model I	$C_j^A + A \xrightarrow{k_{paa}} C_{j+1}^A$
$P_j^* + B \xrightarrow{k_{pab}} Q_{j+1}^*$		$C_j^A + B \xrightarrow{k_{pab}} C_{j+1}^A$
$Q_j^* + A \xrightarrow{k_{pba}} P_{j+1}^*$		$C_j^B + A \xrightarrow{k_{pba}} C_{j+1}^B$
$Q_j^* + B \xrightarrow{k_{pbb}} Q_{j+1}^*$		$C_j^B + B \xrightarrow{k_{pbb}} C_{j+1}^B$
Deactivation		
$P^* \xrightarrow{k_{da}} D$	See model I	$C_t^A \xrightarrow{k_{da}} D$
$Q^* \xrightarrow{k_{db}} D$		$C_t^B \xrightarrow{k_{db}} D$

Table 1: *Kinetic Models*

Model I, first order Markov, is often used in literature (Böhm 1981; Fink and Richter 1999) to describe catalytic co-polymerizations. In model I P_j^* is an active site with a growing polymer chain of length j and with the last inserted monomer of type A. Q_j^* is an active site with a growing polymer chain of length j and with the last inserted monomer of type B. Model I, without further modifications, is not able to explain during homo-polymerizations the observed non-first order dependency of the reaction rate on the monomer concentration (see Chapter 3). Model I explains the increased reaction rate directly as a consequence of the incorporation of the co-monomer. An enormous increase of activity was observed during propylene polymerizations with a small amount of ethylene present in the reactor (Weickert 2003). Reactivity ratios of the first order Markov mechanism without further modifications, a reduced crystallinity of the produced polymer and dormant site theories cannot explain this increased activity.

Model II, the Trigger mechanism (Ystenes 1991), assumes a complex formation between the active site and a monomer. Ystenes assumed that the complexed monomer is inserted after incoming of a second monomer (triggering). In model II, P_j^* is an active site with a growing polymer chain of length j and with a complexed monomer of type A. Q_j^* is an active site with a growing polymer chain of length j and with a complexed monomer of type B.
Model II is able to describe the non-first order dependency of the reaction rate on the monomer concentration during homo-polymerizations (see Chapter 3). However, model II is also not able to describe the increased activity due to small additions of co-monomer. Also in Model II the increased activity is explained as a direct consequence of the incorporation of the co-monomer. In fact, the sequence control of A and B in model I and II are the same. The insertion of a complexed active site with monomer A triggered by B leads to a complexed site with monomer B. This complexed monomer B will be the next inserted monomer.

Complexation Model
The in this work proposed kinetic model, model III, for the co-polymerization of ethylene with 1-hexene is based on the trigger mechanism. However, now the incoming monomer is assumed to be inserted (see also Chapter 3), as was proposed by Shimizu (2001). Reversible complex formation has been reported more often in literature (Böhm 1984; Schnauss and Reichert 1990; Shaffer and Ray 1997).
This complexation model can describe the non-first order dependency of the reaction rate on monomer concentration and the increased activity due to small additions of co-monomer. The sequence of the monomers in the polymer chains is not controlled by the complexed monomer.
In model III C_j^A is an active site complexed with a monomer of type A and with a growing polymer chain of length j. C_j^B is an active site complexed with a monomer B and a growing polymer chain of length j. C^0 is an active site without a complexed

monomer. The propagation constant k_{pbb} is correlated to an insertion of monomer of type B within a polymer chain and a metal site complexed with a monomer of type B.

The reaction rate will be derived as follows:

The reaction rate for ethylene (A) is: $\quad R_{pA} = k_{paa} \cdot C^A \cdot A + k_{pba} \cdot C^B \cdot A \qquad$ (1)

And for 1-hexene (B): $\qquad\qquad\qquad R_{pB} = k_{pab} \cdot C^A \cdot B + k_{pbb} \cdot C^B \cdot B \qquad$ (2)

With $\qquad\qquad C^A = \sum_j C_j^A \quad$ and $\quad C^B = \sum_j C_j^B \qquad\qquad$ (3a, 3b)

The long chain hypotheses allows to neglect the first insertion of a monomer after a chain transfer for the reaction rate derivation. The following quasi steady state assumptions are used, assuming that these equilibriums are fast:

$$\frac{dC^A}{dt} = k_{a1}C^0 \cdot A - k_{a2}C^A = 0 \quad \rightarrow \quad C^A = K_A \cdot C^0 \cdot A \qquad (4)$$

$$\frac{dC^B}{dt} = k_{b1}C^0 \cdot B - k_{b2}C^B = 0 \quad \rightarrow \quad C^B = K_B \cdot C^0 \cdot B \qquad (5)$$

with: $\quad K_A = \dfrac{k_{a1}}{k_{a2}} \qquad$ and $\qquad K_B = \dfrac{k_{b1}}{k_{b2}} \qquad\qquad$ (6a, 6b)

At small time scale the total amount of active sites is constant:

$$C_t = C^0 + C^A + C^B \qquad (7)$$

$$C_t = C^0 + K_A \cdot A \cdot C^0 + K_B \cdot B \cdot C^0 \rightarrow \quad C^0 = \frac{1}{1 + K_A \cdot A + K_B \cdot B} \cdot C_t \qquad (8)$$

Combining (4) and (8): $\qquad C^A = \dfrac{K_A \cdot A}{1 + K_A \cdot A + K_B \cdot B} \cdot C_t \qquad$ (9)

And (5) and (8): $\qquad\qquad C^B = \dfrac{K_B \cdot B}{1 + K_A \cdot A + K_B \cdot B} \cdot C_t \qquad$ (10)

The total amount of active sites is not constant during the complete reaction time. The deactivation constants (k_{da} and k_{db}) are assumed to be equal (k_d).

$$\frac{dC}{dt} = -k_i C \qquad\qquad\qquad\qquad \text{at } t = 0, \, C = C_0 \qquad (12)$$

$$\frac{dC_t}{dt} = k_i C - k_d C_t \qquad\qquad\qquad \text{at } t = 0, \, C_t = 0 \qquad (13)$$

Simultaneous integration of (12) and (13) leads to:

$$C_t(t) = \frac{k_i}{k_i - k_d}\left(e^{-k_d t} - e^{-k_i t}\right) \cdot C_0 \qquad (14)$$

This results in the reaction rate for ethylene:

$$R_{pA}(t) = \frac{k_i}{k_i - k_d}\left(e^{-k_d t} - e^{-k_i t}\right) \cdot C_0 \cdot \frac{k_{paa} \cdot K_A \cdot A + k_{pba} \cdot K_B \cdot B}{1 + K_A \cdot A + K_B \cdot B} \cdot A \qquad (15)$$

and a reaction rate for 1-hexene:

$$R_{pB}(t) = \frac{k_i}{k_i - k_d}\left(e^{-k_d t} - e^{-k_i t}\right) \cdot C_0 \cdot \frac{k_{pab} \cdot K_A \cdot A + k_{pbb} \cdot K_B \cdot B}{1 + K_A \cdot A + K_B \cdot B} \cdot B \qquad (16)$$

The co-polymerization equation has been derived for predicting the instantaneous mass fraction of the incorporated co-monomer ($y_B{}^d$).

Mass fraction of hexene:
$$y_B^d = \frac{R_{pB}}{R_{pA} + R_{pB}} = \frac{1}{\dfrac{R_{pA}}{R_{pB}} + 1} \qquad (17)$$

with the reactivity ratios: $\quad r_A = \dfrac{k_{paa}}{k_{pab}} \quad$ and $\quad r_B = \dfrac{k_{pbb}}{k_{pba}} \qquad$ (18a, 18b)

and monomer ratio:
$$X = \frac{A}{B} \qquad (19)$$

$$\frac{R_{PA}}{R_{pB}} = \frac{k_{paa} \cdot K_A \cdot A + k_{pba} \cdot K_B \cdot B}{k_{pab} \cdot K_A \cdot A + k_{pbb} \cdot K_B \cdot B} \cdot \frac{A}{B} = \frac{k_{paa} \cdot \dfrac{K_A}{K_B} \cdot X + \dfrac{k_{pbb}}{r_B}}{\dfrac{k_{paa}}{r_A} \cdot \dfrac{K_A}{K_B} \cdot X + k_{pbb}} \cdot X =$$

$$= \frac{\dfrac{k_{paa}}{k_{pbb}} \cdot \dfrac{K_A}{K_B} \cdot X + \dfrac{1}{r_B}}{\dfrac{k_{paa}}{k_{pbb}} \cdot \dfrac{K_A}{K_B} \cdot \dfrac{1}{r_A} \cdot X + 1} \cdot X = \frac{K_X \cdot X + \dfrac{1}{r_B}}{K_X \cdot \dfrac{1}{r_A} \cdot X + 1} \cdot X \qquad (20)$$

with $K_X = \dfrac{K_A}{K_B} \cdot \dfrac{k_{paa}}{k_{pbb}}$ (21)

The standard co-polymerization equation for a first order Markov mechanism has the following rate ratio:

$$\frac{R_{pA}}{R_{pB}} = \frac{A}{B} \cdot \frac{r_A \cdot A + B}{A + r_B \cdot B} = X \cdot \frac{r_A \cdot X + 1}{X + r_B} \qquad (22)$$

This co-polymer equation (22) is only dependent on the reactivity ratios and the monomer ratio. The co-polymer equation obtained from the complexation mechanism (20) is next to the reactivity ratios and the monomer ratio also dependent on the homo-polymerization reaction constants (K_X).

Parameter estimation

Equation 15 is exactly the same equation as was obtained in case B = 0, during an ethylene homo-polymerization (see Chapter 3). The only difference here is the time dependency. Because the activation behavior of the catalyst was very fast and the deactivation rate of the catalyst was very slow ($k_d = 10^{-3}$ min^{-1}), the rate of the homo-polymerization model could be described independent of time. The values obtained for K_A and k_p ($=k_{paa}$) are assumed to be still valid in the co-polymerization model because: $k_i \gg k_d$. Therefore k_i and k_d do not influence the value of the maximum reaction rate because: $\dfrac{k_i}{k_i - k_d} \approx 1$

This means that the propagation constant and equilibrium constant (K_A) found for homo-ethylene polymerizations can be used in the co-polymerization model.

The reaction rate curves have been fitted with the activation–deactivation model:

For ethylene: $R_{pA}(t) = \dfrac{k_i}{k_i - k_d}\left(e^{-k_d t} - e^{-k_i t}\right) \cdot C_0 \cdot k_{pa} \cdot A$ (23)

For 1-hexene: $R_{pB}(t) = \dfrac{k_i}{k_i - k_d}\left(e^{-k_d t} - e^{-k_i t}\right) \cdot C_0 \cdot k_{pb} \cdot B$ (24)

The activation and deactivation constants are in both equations the same; only the propagation parameters are different. These propagation parameters ($k_{pa}C_0$ and $k_{pb}C_0$) are no constants but dependent on the monomer concentrations:

$$k_{pa}C_0 = C_0 \cdot \frac{k_{paa} \cdot K_A \cdot A + k_{pba} \cdot K_B \cdot B}{1 + K_A \cdot A + K_B \cdot B}$$ (25)

$$k_{pb}C_0 = C_0 \cdot \frac{k_{pab} \cdot K_A \cdot A + k_{pbb} \cdot K_B \cdot B}{1 + K_A \cdot A + K_B \cdot B}$$ (26)

The proposed complexation model (model III) contains six constants: K_A, K_B, k_{paa}, k_{pab}, k_{pbb} and k_{pba}. The ethylene homo-polymerizations provided the input values for k_{paa} and K_A (see Chapter 3). The other four parameters are fitted with the dependency of the propagation parameters provided by experimental series.

Experimental

Setup

The experimental setup has been described extensively in Chapter 2. Figure 1 shows a schematic overview of the setup. The reactor is a jacketed, stainless steel 1.6-L reactor from Büchi, which operates at pressures up to 40 bar and temperatures till 120°C. The setup is equipped with two automatic catalyst injection systems, suitable for dry-powder and slurry injections (Samson *et al.* 1998). The reaction components are mixed with a helical stirrer (up to 2000 rpm) combined with a propeller on the tip, to obtain good powder circulation along the wall. This forced circulation improves the heat transfer from the polymerizing particles to the cooled reactor wall (Meier *et al.* 2001). The reaction temperature is measured above the helical stirrer, in contact with the circulating powder. The reaction temperature can be kept constant within 0.2°C from one minute after catalyst injection onwards.
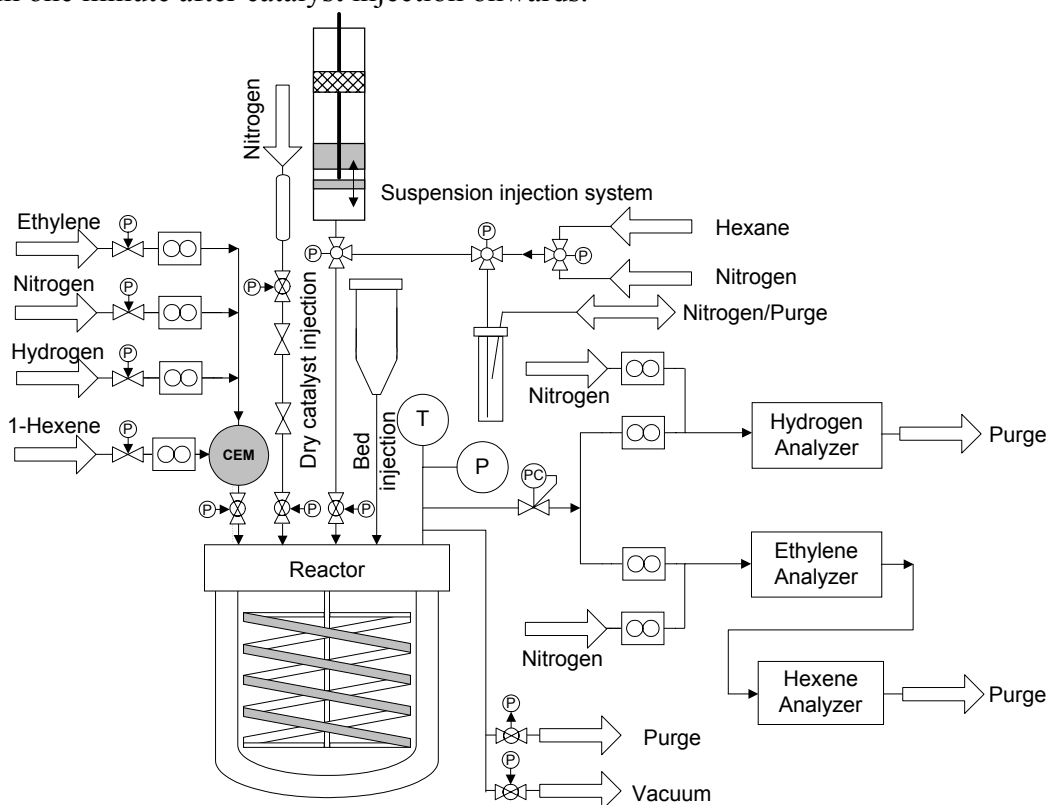

Figure 1: *Experimental setup for gas phase ethylene/1-hexene co-polymerizations*

Ethylene and nitrogen are added to the reactor by thermal mass flow controllers and 1-hexene is fed to the reactor by a thermal liquid mass flow controller. All components flow into the reactor via a Controlled Evaporator Mixer (CEM, Bronkhorst Hi-Tec), wherein 1-hexene is dosed by a control valve and is evaporated in the gas mixture flow. A continuous flow is withdrawn from the reactor over a pressure reducer via thermal mass flow controllers (Brooks Instruments) to analyzers. The ethylene and 1-hexene concentrations are measured online with two Infrared analyzers (respectively Xendos 2550 and 2500, Servomex). A Data

Acquisition/Control Unit (HP 3852A) measures all temperatures, pressures, mass flows and concentrations. This data is stored on a PC, which contains the operation software. From this data the polymerization rate for both monomers can be derived as discussed in Chapter 2.

Chemicals

The used metallocene catalyst is silica supported bisindenylzirconiumdichloride (Ind_2ZrCl_2) with MAO as co-catalyst (donated by Basell Polyolefins). The catalyst contains 6.4 wt% Al and 0.2 wt% Zr. The Al / Zr molar ratio is 108. This zirconocene does not need any extra pre-treatment before the catalyst is injected into the reactor. Triethylalumina (TEA) supported on silica is used as scavenger during the gas phase co-polymerizations. Salt, used as seedbed, was sieved and dried at 200°C under vacuum for 48 hours. Ethylene (purity > 99.9%, Hoekloos) is further purified over oxidized BASF R3-16 catalyst, reduced BASF R3-16 catalyst, molecular sieves (13X, 4A and 3A, Sigma-Aldrich) and Selexsorb® COS (Alcoa). 1-Hexene (purity 98%, Sigma-Aldrich) is pressurized and purged several times with purified nitrogen. Afterwards 1-hexene is purified over reduced BASF R3-11 catalyst, Selexsorb® CD (Alcoa) and molecular sieves (3A, Sigma-Aldrich). Nitrogen (purity >99.999%, Praxair) is purified over BASF R3-11 catalyst and molecular sieves (13X, 4A, 3A). Chapter 2 described the chemical purification in detail.

Polymerization Procedure

The polymerization procedure was discussed in Chapter 2. A short summary follows here. The salt bed (100 g) is injected with 1.00 g TEA supported on silica. Then the desired gas concentrations are set. The catalyst (45 mg incl. support) is injected together with 280 mg TEA supported on silica via the dry catalyst injection unit; this starts the polymerization reaction. After the polymerization, the polymer is washed with water to separate the salt from the polymer. Afterwards the polymer is dried under vacuum at 60°C for 4 hours.

Run	C2 mol%	C6 mol%	C6/(C2+C6) -	Incorpor. C6 wt%	Yield g	Yield by C6 MFM g	Yield by C6wt% g	Correct %	Density kg/L	Cryst. -	Sorption C6 g/g a-PE	P_{C6} bar
0	100	0	0	0	-	-	-	-	0.9547	0.700	0.000	0
1	49.92	0.52	0.0103	3.6	35.9	2.4	1.29	54%	0.9296	0.538	0.067	0.104
2	50.03	0.52	0.0102	3.3	76.6	4.8	2.53	53%	0.9299	0.540	0.064	0.103
3	56.63	0.77	0.0134	3.3	144.5	9.3	4.77	51%	0.9289	0.533	0.067	0.154
4	49.95	0.74	0.0147	4.4	67.1	6.5	2.95	45%	0.9246	0.504	0.107	0.149
8	50.01	1.01	0.0198	6.1	75.4	8.6	4.60	53%	0.9199	0.473	0.101	0.202
11	51.31	0.99	0.0190	6.1	59.8	6.3	3.65	58%	0.9204	0.476	0.083	0.199
12	49.84	1.36	0.0266	8.5	71.9	13.7	6.11	45%	0.9140	0.432	0.186	0.272
13	30.17	0.94	0.0302	8.8	50.7	12.0	4.46	37%	0.9133	0.428	0.260	0.188
14	72.23	0.97	0.0132	4.14	79.1	7.1	3.27	46%	0.9249	0.506	0.098	0.193

Table 2: *Data for 1-hexene sorption calculation.*

Results and Discussion

In-situ sorption of 1-Hexene

Knowing the mass flow rate of 1-hexene and the hexene weight fraction in the polymer, the in-situ sorption during the polymerization can be determined.

Table 2 shows the yields and mass fraction of 1-hexene of the produced co-polymers at 90°C and 20 bar. Obviously a large difference is present between the 1-hexene yield obtained by mass flow meters (MFM) and derived by polymer IR-analyses and total yield (C6wt%). The differences are about 50%. These differences cannot be explained by errors in the flow meters, IR gas analyzers or in the polymer IR-analyses, which could explain differences up to 10-20%. Assuming that these errors in the measurement techniques are small, the differences between flow meter yield and IR-analyses yield can be explained by absorption of 1-hexene in the amorphous part of the polyethylene.

Table 2 also shows the densities of the produced co-polymers. From these densities the crystallinity could be calculated. It is assumed that the density for 100% crystalline PE is 1.005 kg/L and for 100% amorphous PE is 0.855 kg/L.
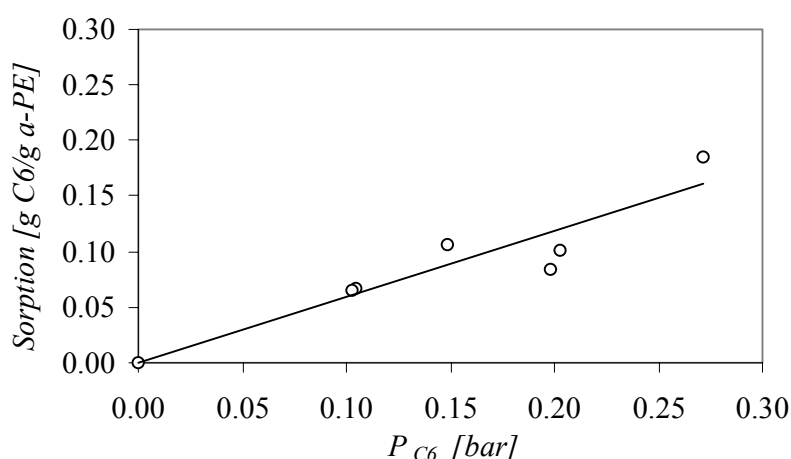

Figure 2: *Sorption of 1-hexene in amorphous polyethylene versus the 1-hexene partial pressure at 90°C, 20 bar and 50mol% ethylene*

It is assumed that 1-hexene is only absorbing in the amorphous part of the polyethylene. Figure 2 shows the amount of 1-hexene, which is absorbed in-situ in the amorphous polyethylene at different partial pressures of 1-hexene. This figure only represents experiments that were executed at 90°C, 20 bar and with 50 mol% ethylene. Within the experimental errors, it is obvious that Henry's law can be used at these low partial pressures of 1-hexene. The obtained value for the Henry constant is 0.59 $g_{C6} \cdot (g_{a\text{-}PE} \cdot bar_{C6})^{-1}$. This in-situ 1-hexene sorption is much higher compared to values reported in literature, which are often obtained ex-situ; i.e. after the polymer has been dried.

Hutchinson and Ray (1990) proposed the correlation presented by Stern *et al.* (1969) as:

$$\log\left(k_{H,i}\right) = -2.38 + 1.08\left(\frac{T_{c,i}}{T}\right)^2 \qquad \textit{[mol/L a-PE/atm]} \qquad (27)$$

This results in a Henry's coefficient for 1-hexene at 90°C of 0.05 $g_{C6}\cdot(g_{a\text{-PE}}\cdot bar_{C6})^{-1}$. This correlation is valid for 1-hexene till a partial pressure of 0.47 bar. Note that the sorption calculated here is at 20 bar in the presence of ethylene and nitrogen. Moore and Wanke (2001) measured 1-hexene solubility in PE pellets, extruded re-crystallized polyethylene; they found non-linear behavior in a wider pressure range. Fitting a Henry's constant in the lower pressure range results in a value proximately 50% lower than obtained here.

Recently Pater *et al.* (2004) showed that propylene sorption behavior in polypropylene is changing irreversibly when the polymer is degassed and/or dried. They saw that the in-situ propylene sorption is much higher than ex-situ. They explained the effect due to a very open polymer network of micro and meso pores: a 'frozen polymer network'. This effect cannot be explained by increased sorption just by a reduced crystallinity during polymerization, even when 100% amorphous polypropylene was assumed.

The sorption effect here is smaller and could be explained by the fact that the in-situ polymer, which is swollen with hydrocarbons, is less able to crystallize during polymerization.

Influence of 1-Hexene

All co-polymerization experiments are presented in Table 3. All experiments have been executed at 90°C, 20 bar and at constant monomer concentrations.
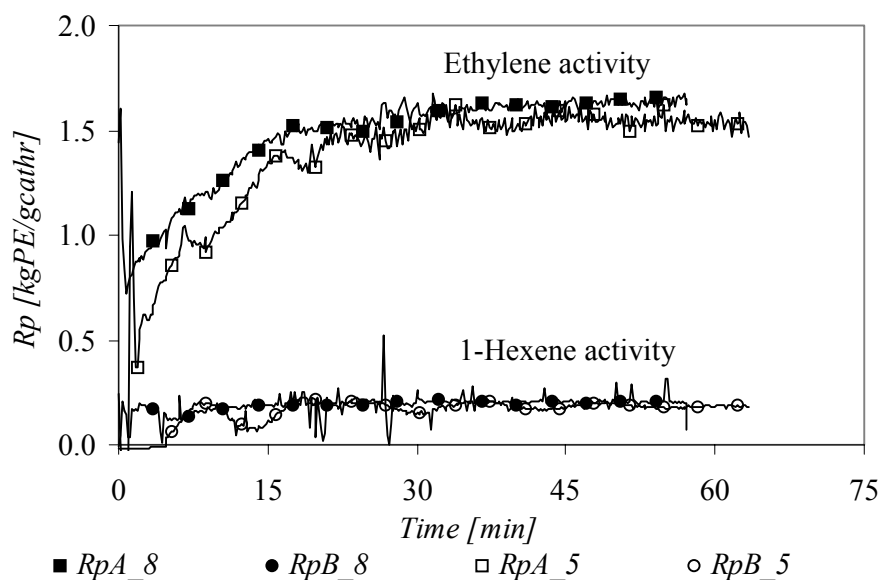

Figure 3: *Ethylene and 1-hexene activity for two gas-phase co-polymerizations (run 5 and 8) at 90°C and 20 bar with 45 mg catalyst (incl. support)*

Runs 5 till 9 have been executed at identical conditions in order to demonstrate reproducibility (see Chapter 2). Figure 3 shows a representative curve for a standard co-polymerization as obtained from the mass balance. The curves have the same typical form as presented by Chakravarti and Ray (2001); a long activation period and slow deactivation.
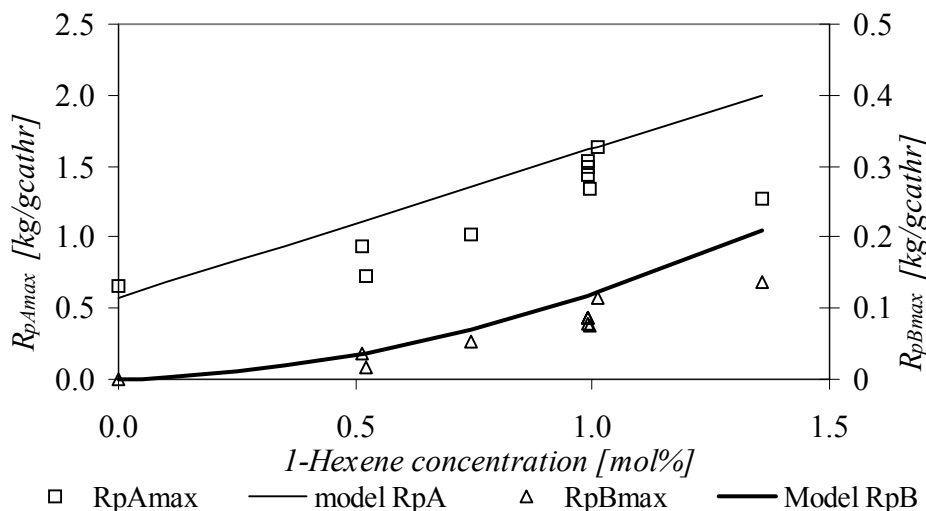

Figure 4: *Maximum reaction rate of ethylene (left) and 1-hexene (right) at different hexene concentration at 90°C, 20 bar and 50 mol% ethylene. The modeled reaction rates are without taken into account deactivation.*

R_{pB} in Table 3 represents the real reaction rates for 1-hexene; mass flow rates have been corrected for the 1-hexene sorption effect. The 1-hexene concentration has been varied between 0.52 and 1.36 mol% in gas phase. The values for the propagation parameters ($k_{pa}C_0$ and $k_{pB}C_0$) are fitted independent from each other; however the values are almost the same.

Figure 4 shows the maximum reaction rates for ethylene (R_{pAmax}) and 1-hexene (R_{pBmax}). The maximum reaction rate for both monomers increases with increasing 1-hexene concentration. So the co-monomer effect is observed. This is in accordance with Chakravarti and Ray (2001). At the highest 1-hexene concentration the maximum activity for ethylene is decreasing. Figures 5 and 6 represent kinetic parameters $k_{pa}C_0$ and $k_{pb}C_0$ for respectively the ethylene and the 1-hexene consumption. These figures show that the propagation rate constants are increasing with increasing 1-hexene concentration. Figure 7 shows the activation and deactivation constants. Although some scattering for the activation and deactivation constants in the measurements is observed, trends can be observed. The activation constant is decreasing with increasing 1-hexene concentration. The deactivation constant is more or less constant, only at high 1-hexene concentration the deactivation is increasing and is almost a factor 10 higher. This explains the lower maximum activity at the highest 1-hexene concentration.

Run	C2 mol%	C6 mol%	N2 mol%	$[C2]$ kg/m^3	$[C6]$ kg/m^3	R_{pA} $kg \cdot g_{cat}^{-1} \cdot hr^{-1}$	R_{pB} $kg \cdot g_{cat}^{-1} \cdot hr^{-1}$	k_i min^{-1}	k_d min^{-1}	$k_{pa}C_0$ $m^3 \cdot g_{cat}^{-1} \cdot hr^{-1}$	$k_{pb}C_0$ $m^3 \cdot g_{cat}^{-1} \cdot hr^{-1}$
0	50	0	50	9.57	0	0.66	0	-	0.0025	0.069	0
1	49.92	0.52	49.55	9.44	0.29	0.73	0.018	0.23	5.1E-04	0.078	0.078
2	50.03	0.52	49.45	9.53	0.29	0.94	0.036	0.11	3.6E-04	0.101	0.101
3	56.63	0.77	42.60	10.85	0.43	1.96	0.067	0.07	1.4E-03	0.195	0.200
4	49.95	0.74	49.31	9.52	0.41	1.02	0.054	0.10	5.5E-03	0.127	0.135
5	50.29	0.989	48.72	9.64	0.55	1.53	0.088	0.14	2.8E-04	0.161	0.161
6	50.06	0.989	48.95	9.58	0.55	1.49	0.086	0.088	5.0E-03	0.185	0.196
7	50.16	0.991	48.85	9.56	0.55	1.44	0.079	0.10	6.0E-03	0.180	0.191
8	50.01	1.012	48.98	9.58	0.57	1.63	0.115	0.11	2.1E-06	0.171	0.171
9	52.77	1.10	46.13	10.60	0.65	1.47	0.089	0.47	2.8E-03	0.143	0.144
10	53.38	0.99	45.63	10.79	0.58	1.43	0.087	0.81	4.4E-04	0.133	0.133
11	51.31	0.99	47.70	9.80	0.55	1.34	0.076	0.10	3.3E-03	0.154	0.159
12	49.84	1.36	48.80	9.51	0.76	1.28	0.136	0.07	1.7E-02	0.209	0.273
13	30.17	0.94	68.89	5.71	0.53	0.75	0.074	0.068	1.4E-02	0.196	0.245
14	72.22	0.96	26.82	13.94	0.54	2.31	0.116	0.12	2.1E-04	0.168	0.168

Table 3: *Experimental data, co-polymerizations at 90°C, 20 bar with 45 mg catalyst (incl. support) and 1280 mg TEA/silica*
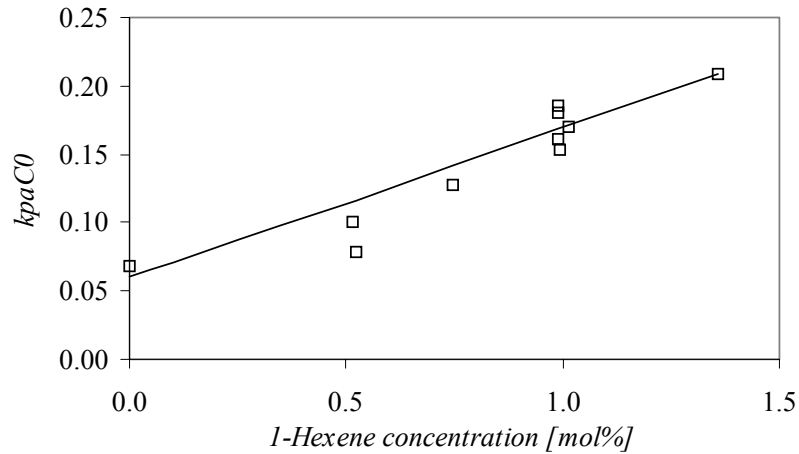
Figure 5: $k_{pa}C_0$ versus 1-hexene concentration at 90°, 20 bar and 50 mol% ethylene, incl. model fit.
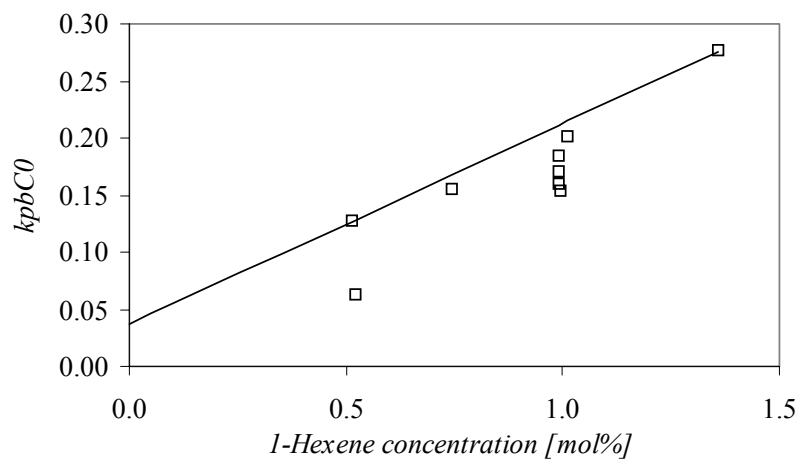

Figure 6: $k_{pb}C_0$ versus 1-hexene concentration at 90°, 20 bar and 50 mol% ethylene, incl. model fit.
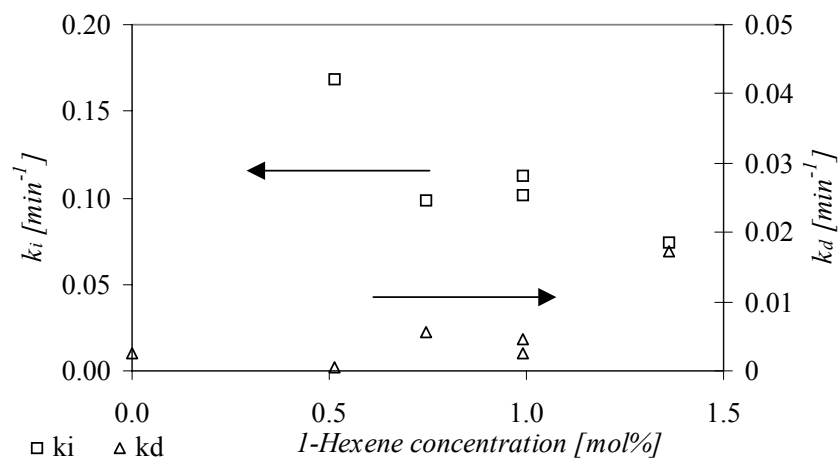

Figure 7: Activation (left) and deactivation (right) constants versus 1-hexene concentration at 90°, 20 bar and 50 mol% ethylene. From the values at 0.5 and 1 mol% an average value is presented.

Influence of Ethylene

The influence of the ethylene concentration in homo-polymerizations was discussed in Chapter 3. Here the influence of a changing ethylene concentration will be examined at constant 1-hexene concentration of 1.0 mol%. The ethylene concentration is varied between 30 and 70 mol%. The nitrogen concentration is varied consequently from 69 till 29 mol%.
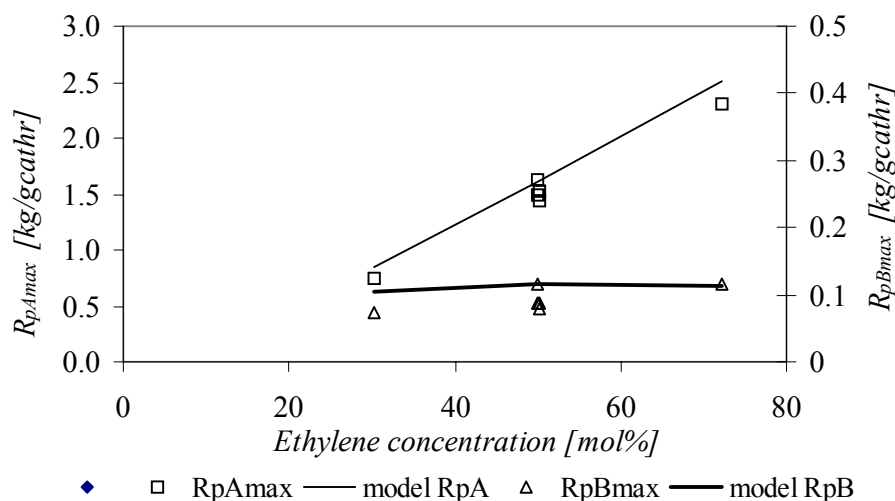

Figure 8: Maximum reaction rate of ethylene (left) and 1-hexene (right) at different ethylene concentrations at 90°C, 20 bar and 1.0 mol% 1-hexene. The modeled reaction rates are without taken into account deactivation.
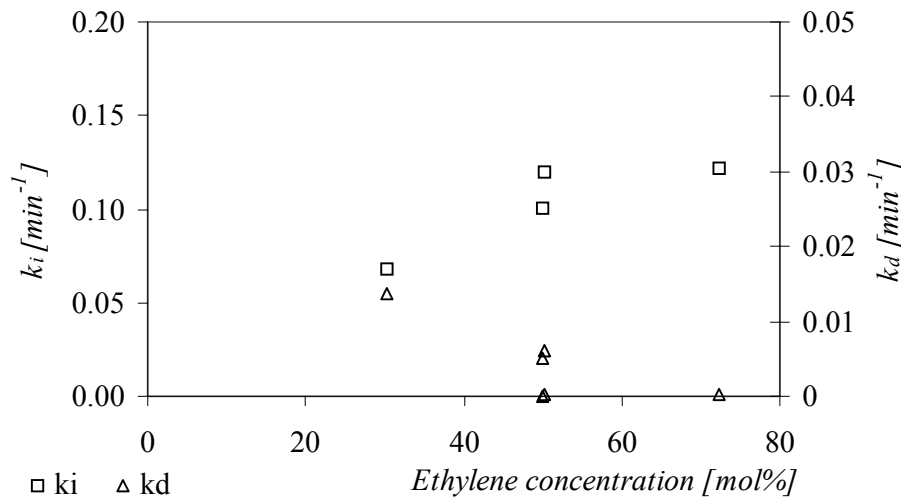

Figure 9: Activation (left) and deactivation (right) constants at different ethylene concentrations at 90°C, 20 bar and 1.0 mol% 1-hexene. From the values for ki at 50 mol% two average values are presented.

Figure 8 represents the maximum reaction rate for ethylene (R_{pAmax}) and 1-hexene (R_{pBmax}). The reaction rate of ethylene is increasing linearly with increasing ethylene concentration; this is corresponding with the homo-polymerizations. Besides the presence of co-monomer, another difference with the homo-polymerizations is the presence of nitrogen. A possible negative effect on the reaction rate, due to

enrichment of inerts in the pores, is not observed within these experiments. The 1-hexene reaction rate is also slightly increasing.

Figure 9 shows the activation and deactivation constants during the ethylene series. The same scattering is observed as in Figure 7 for the activation and deactivation constants. However the activation constant is increasing with increasing ethylene concentration. Figure 9 is consistent with Figure 7; if the ethylene concentration is increasing the relative 1-hexene concentration (C6/(C2+C6)) is decreasing. The deactivation constant in Figure 9 shows a clearer trend compared to the 1-hexene series. Combining both experimental series the conclusion can be drawn that the deactivation constant is increasing with increasing 1-hexene-ethylene ratio.

Run	C6/(C2+C6) mol/mol	CH3 C/1000C	y_{C6} wt%	Mw kg/mol	Mn kg/mol	PDI -	MFI 2.16 g/10 min	MFI 21.6 g/10 min	FRRatio -	Denstity kg/L	Cryst. -	Tm °C
Homo S.	0.000	0.4	0	241.3	71.9	3.35	0.19	3.54	19	0.9547	0.700	138.8
1	0.010	5.6	3.6	113.1	33.2	3.41				0.9296	0.538	124.2
2	0.010	5.0	3.3	100.5	33.6	2.99	3.0			0.9299	0.540	125.1
3	0.013	5.4	3.3	125.7	36.6	3.43	1.63			0.9289	0.533	125.5
4	0.015	7.5	4.4	103.4	34.7	2.98	2.42			0.9246	0.504	122.6
8	0.020	10.3	6.1	92.5	28.0	3.31	2.3	51.3	22	0.9199	0.473	120.0
11	0.019	9.8	6.1	94.0	31.8	2.96	2.9	56.4	19	0.9204	0.476	120.7
12	0.027	13.7	8.5	99.2	31.8	3.12	2.66			0.9140	0.432	116.2
13	0.030	14.9	8.8	76.0	24.8	3.07	7.58			0.9133	0.428	112.6
14	0.013	7.2	4.6	120.3	41.3	2.92	1.4	23.9	17	0.9249	0.506	122.5
ZN-LLDPE[1]		16.4	6.4[1]	166.0	40.1	4.14	0.95	23.8	25	0.9181	0.460	122.0

[1]This ZN-LLDPE is modified with 1-butene

Table 4: *Polymer properties of mPE and ZN-LLDPE*

Polymer Properties

Table 4 represents the polymer properties of nine co-polymers and one homo-polymer produced with the silica supported Ind_2ZrCl_2/MAO catalyst. Also the properties of a commercial butene modified LLDPE produced with a Ziegler-Natta catalyst (ZN-LLDPE) are listed in this table.[1]

GPC

Figure 10 shows the weight average molecular weights of the metallocene produced polymers (mPE). The molecular weight is decreasing with increasing 1-hexene/ethylene ratio; so 1-hexene is acting as chain transfer agent.
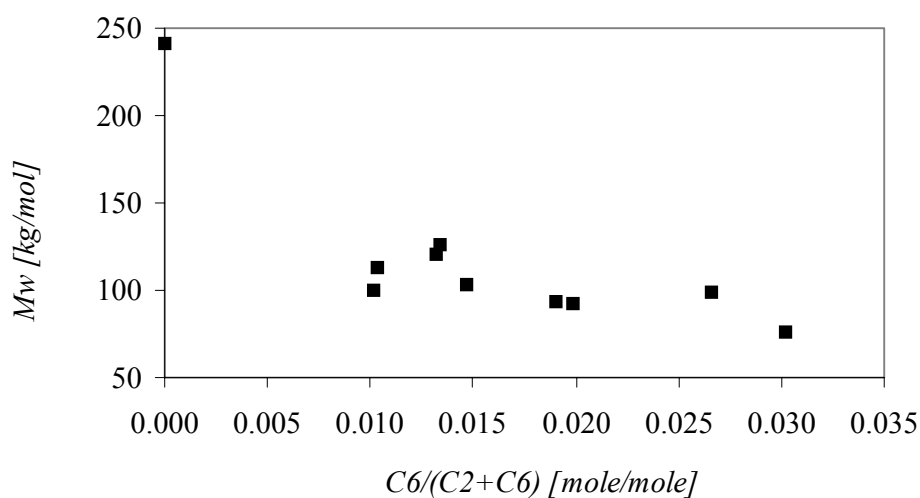

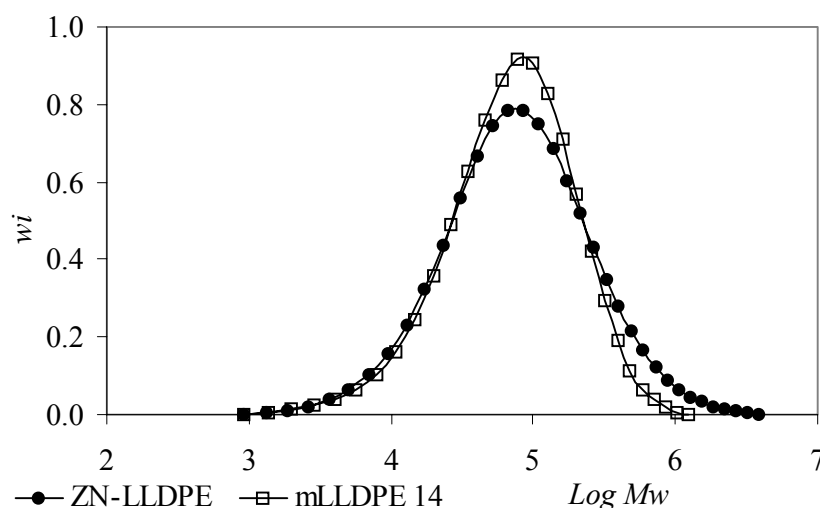***Figure 10:*** *Weight average molecular weight as function of 1-hexene gas fraction*

Figure 11: *Molecular weight distribution of mLLDPE 14 and ZN-LLDPE*

---

[1] All polymer analyzes (GPC, melt index, IR and DSC) have been performed by Basell Polyolefins.

The polydispersity indexes are presented in Table 4. The polydispersity is not changing with the 1-hexene concentration but remains constant with a value of 3.1 ± 10%. An ideal single site catalyst produces polymers with a polydisperity of 2. Higher polydispersities are often observed for supported catalysts. The polydispersity of the ZN-LLDPE is 4.1. Figure 11 shows the molecular weight distribution of mLLDPE from experimental run 14 and the ZN-LLDPE. The number average molecular weights are nearly the same, but the ZN-LLDPE has a 35% higher weight average molecular weight.

Melt Index

Melt flow indexes have been measured with 2.16 kg (MFI 2.16) and 21.6 kg (MFI 21.6) at 190°C. The ratio of these two melt flow rates is the flow rate ratio (FRR). This ratio provides information about the broadness of the molecular weight distribution. Figure 12 shows the two melt indexes as function of the weight average molecular weight. The MFI 2.16 of the ZN-LLDPE (included in the trend line) follows more or less the same trend as the mPE's. However the MFI 21.6 of the ZN-LLDPE (excluded from trend line) is much higher compared to values for mPE with the same molecular weight. This means that at higher shear rates, the apparent viscosity of the ZN-LLDPE polymer is lower. This is due to the broader molecular weight distribution of the ZN-LLDPE.

A common commercial LLDPE with density 0.918 has a MFI 2.16 of 1 g/10 min.
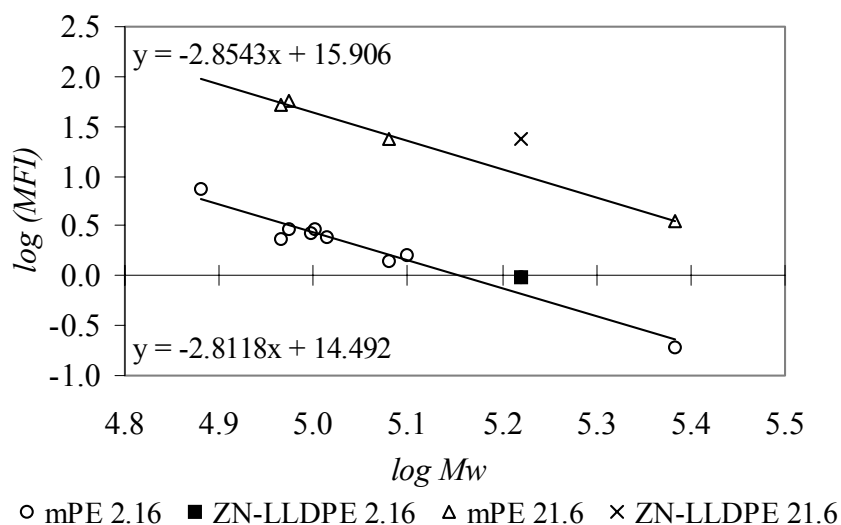

Figure 12: Log Melt flow indexes with 2.16 and 21.6 kg of mPE and ZN-LLDPE vs. Log Mw

IR

IR analyses provides the incorporated weight fraction of co-monomer. Figure 13 shows the hexene weight fraction in the polymer as function of the 1-hexene gas molar ratio. A linear trend can be observed. This confirms that the reaction rate can be assumed to be linearly dependent on the bulk concentration.
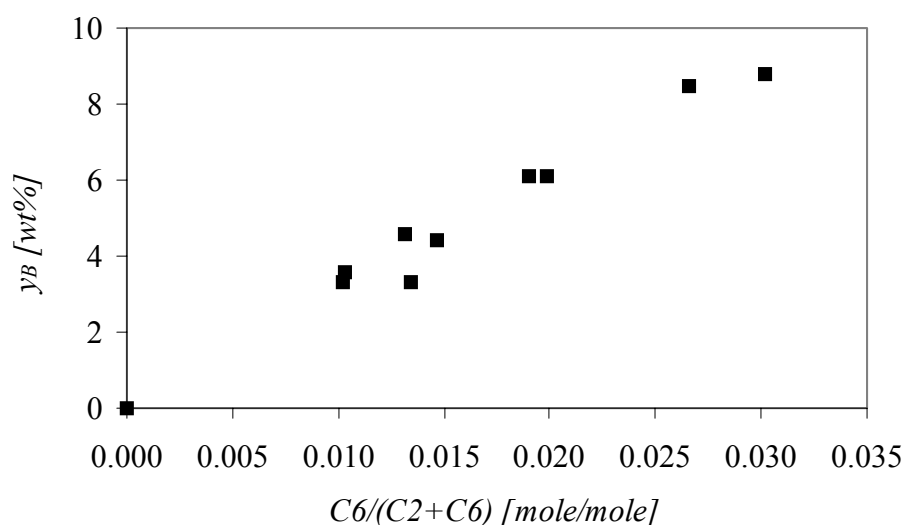
Figure 13: *1-Hexene weight fraction in the produced co-polymers (yB) at different 1-hexene ethylene ratios, hexene and ethylene series combined*
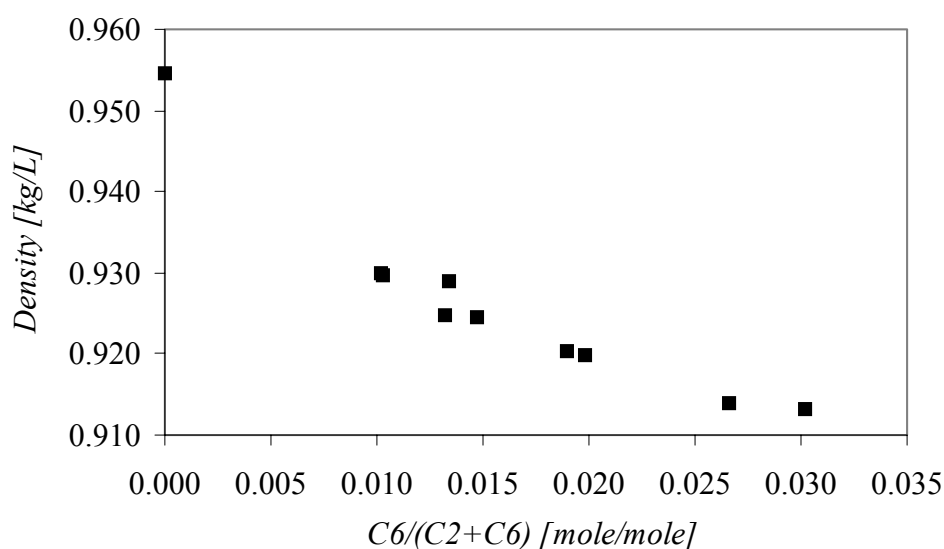

Figure 14: *Density of the produced co-polymers at different 1-hexene ethylene ratios, hexene and ethylene series combined*

LLDPE's are generally classified on their density and melt index. The density is dependent on the weight fraction of incorporated co-monomer, the molecular weight and the molecular weight distribution. Higher molecular weight results in a lower density. A broader molecular weight distribution at the same average molecular weight leads to a higher density.

Figure 14 shows that the density is decreasing with increasing gas phase 1-hexene molar ratio. Figure 15 shows the density as function of the incorporated co-monomer weight fraction. In this figure the ZN-LLDPE data point is following the mPE curve. Note that this ZN-LLDPE is modified with 1-butene. Figure 15 shows that the same co-monomer weight fraction leads in this case to the same density. The slightly higher

molecular weight of the ZN-LLDPE (which has a decreasing effect on the density) and the slightly broader molecular weight distribution (which has an increasing effect on the density) are compensating each other and are probably less important.
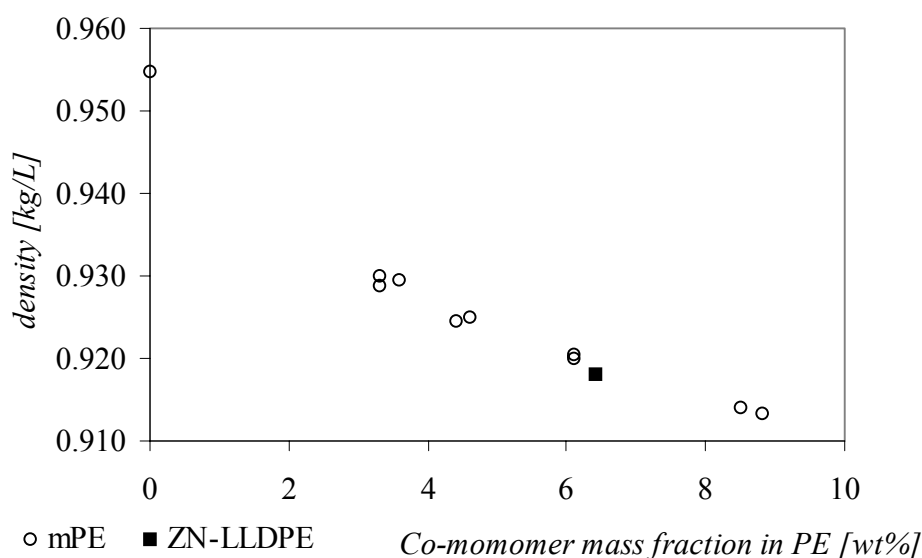

Figure 15: Density of the produced co-polymers plotted versus their incorporated mass fraction co-monomer

DSC

DSC analyses have been executed to show the influence of the co-monomer on the melting point of the polymer. The melting point after re-crystallization is used to eliminate any kind of history in the material. The homo-polymer has a melting point of 138.8°C. The co-polymers have melting points decreasing almost linear from 125°C at low hexene weight fraction (3.3 wt%) till 113°C at the highest hexene weight fraction (8.5 wt%), see Figure 16.
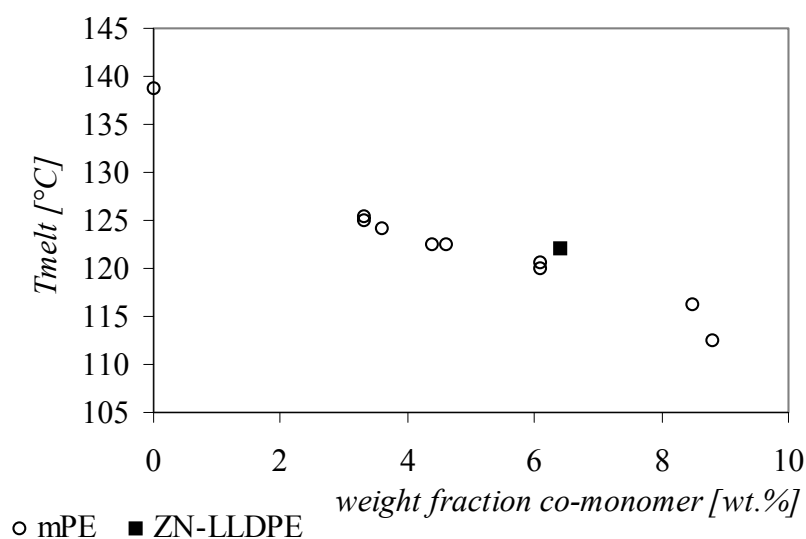

Figure 16: Melting temperature versus incorporated co-monomer weight fraction in PE

This behavior is similar as presented by Quijada *et al.* (1995). The melting point is mainly dependent on the hexene weight fraction, much more than on the molecular weight. Experimental runs 4 and 14 are almost produced at the same co-monomer ratio. However, experiment 14 is executed at a much higher absolute ethylene concentration. Therefore, the molecular weight produced in run 14 is almost 20% higher than in run 4, but the co-monomer weight fractions are the same. The melting points for these two polymers are both 122.5°C.

The ZN-LLDPE has a slightly higher melting point than the metallocene produced polymer at the same co-monomer weight fraction or density (Figure 16 and 17). This is an indirect proof for the better co-monomer distribution of the mPE's. The ZN-LLDPE will contain more non-modified polyethylene chains, especially in the higher molecular weight region. This polyethylene homo-polymer has a higher melting point, giving the ZN-LLDPE a higher overall melting point, than the mLLDPE.
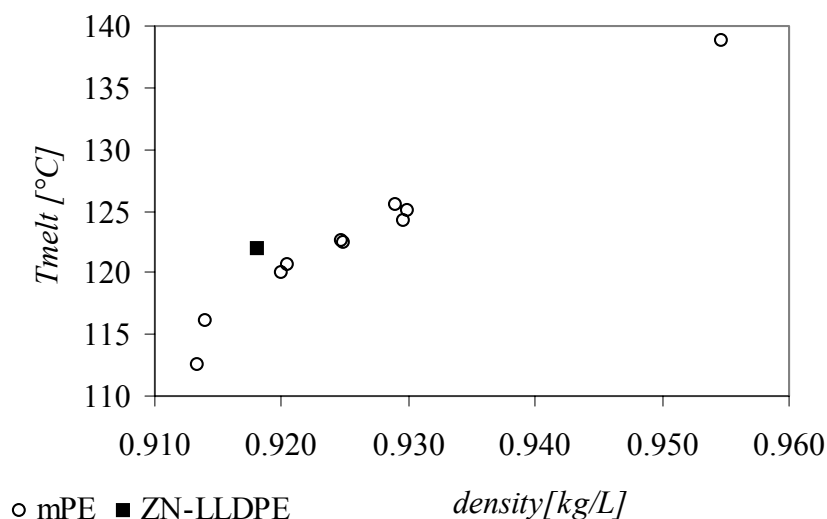

Figure 17: *Melting temperature versus density*

Modeling of Reaction Rate

The measured reaction rate for ethylene has been fitted with an activation, propagation and deactivation constant (equation 23). The measured reaction rate for 1-hexene, corrected for sorption, has been fitted with the same activation and deactivation parameters but with a different kinetic parameter $k_{pb}C_0$. Figures 5 and 6 show that the propagation parameters ($k_{pa}C_0$ and $k_{pb}C_0$) are highly dependent on especially the 1-hexene concentration. The ethylene concentration has less influence on the propagation constants. Equation 25 and 26 are able to describe this dependency only in a linear way if K_B is small and k_{pbb} and k_{pba} are large.

The constants k_{paa} and K_A start with the values obtained from ethylene homo-polymerizations (see Chapter 3). The $k_{pa}C_0$ (propagation for ethylene) dependency on 1-hexene provides the values for K_B and k_{pba}. The $k_{pb}C_0$ (propagation for 1-hexene) dependency on 1-hexene provides the value for k_{pab} and k_{pbb}. These values are further optimized by the $k_{pb}C_0$ (propagation for 1-hexene) dependency on ethylene. The

constants k_{paa} and K_A are optimized by the $k_{pa}C_0$ (propagation for ethylene) dependency on ethylene. The gas bulk concentration is used in the model as the driving force for the reaction, because the 1-hexene gas phase concentration is so low that Henry's law can be used (see Figure 2).

K_A	0.018	0.021^1	$m^3 \cdot kg^{-1}$	K_B	0.0012	$m^3 \cdot kg^{-1}$
$k_{paa}C_0$	0.40	0.41^1	$m^3 \cdot g_{cat}^{-1} \cdot hr^{-1}$	$k_{pbb}C_0$	320	$m^3 \cdot g_{cat}^{-1} \cdot hr^{-1}$
$k_{pab}C_0$	0.25		$m^3 \cdot g_{cat}^{-1} \cdot hr^{-1}$	$k_{pba}C_0$	200	$m^3 \cdot g_{cat}^{-1} \cdot hr^{-1}$
r_A	1.6		-	r_B	1.6	-

[1] values for ethylene homo-polymerization constants at 90°C

Table 5: *Constants for complexation co-polymerization model at 90°C*

Table 5 presents the optimized values for the propagation constants and complexation constants; these constants are valid at 90°C. The optimized values for K_A and k_{paa} within these co-polymerization series deviate respectively 14% and 1.4% from the ethylene homo-polymerization constants.

The constant K_B is small and k_{pba} and k_{pbb} are large. This could be expected in order to obtain increasing reaction rates for ethylene and 1-hexene with increasing 1-hexene concentration. The parameter k_{pab} is more or less arbitrarily fixed. The reactivity ratios for A and B do have the same value.
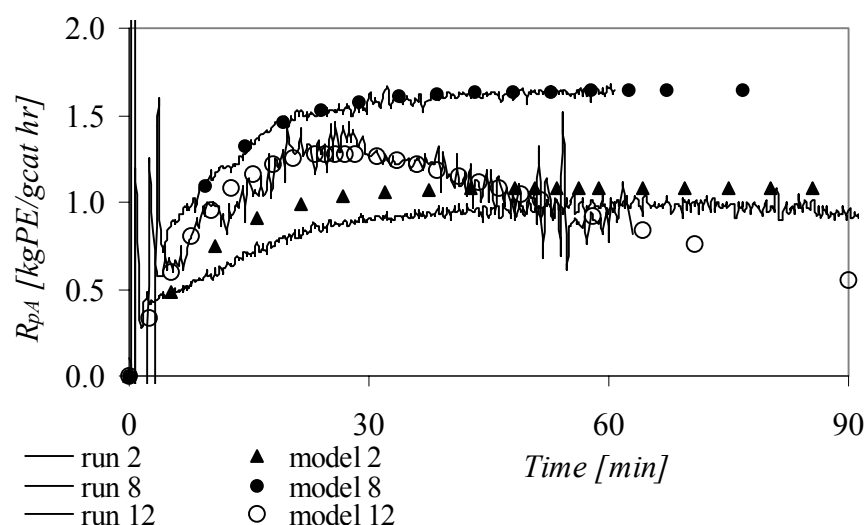

Figure 18: *Ethylene reaction rate runs 2, 8 and 12 with modeled reaction rate.*

Figures 4 and 8 also show with a line the modeled reaction rates for ethylene and 1-hexene. Figures 5 and 6 also include the modeled kinetic parameters $k_{pa}C_0$ and $k_{pb}C_0$. Figure 18 and 19 show the complete reaction rate profiles and the model reaction rate predictions of ethylene and 1-hexene respectively. Figure 18 shows that the maximum reaction rate at the highest 1-hexene concentration (run 12) is not overestimated by the model as was suggested in Figure 4. The maximum reaction rates in Figure 4 are calculated from the propagation parameter without taken into account the

deactivation. When a complete profile is modeled the deactivation and activation behavior of the catalyst is included.
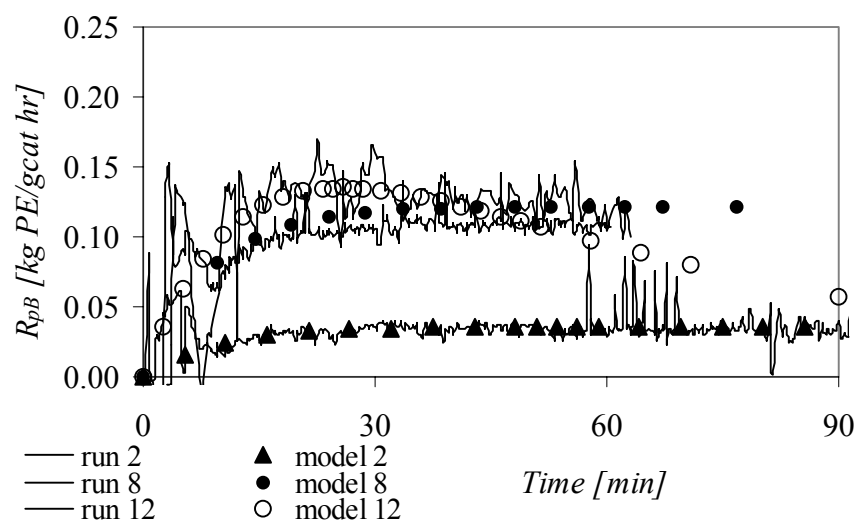

Figure 19: *1-Hexene reaction rate of run 2, 8 and 12 with the modeled rate*

The co-monomer weight fractions are calculated with the estimated kinetic parameters and the co-polymerization equation for the complexation model (equation 20). Figure 20 shows these calculated co-monomer weight fractions versus the measured (with IR) co-monomer weight fractions. The weight fractions calculated from model III fit the measured data rather well.
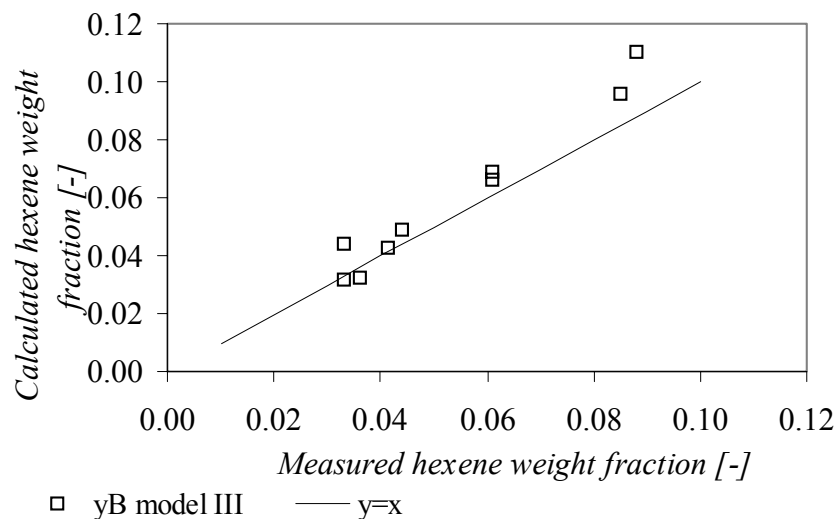

Figure 20: *The hexene weight fraction calculated with complexation model III plotted versus the measured weight fraction with IR.*

Conclusions

The following conclusions can be drawn, taken into consideration that those are valid for the used supported Ind_2ZrCl_2/MAO catalyst under the presented polymerization conditions:

- In-situ 1-hexene sorption has been measured and was found to be much higher as often reported in literature for sorption in degassed dead polymer. At low concentrations Henry's law can be used for 1-hexene sorption. Note that the sorption is calculated under reaction in the presence of ethylene and could be explained by the fact that the in-situ polymer is less able to crystallize during polymerization.
- The ethylene reaction rate is increasing with increasing 1-hexene concentration, the co-monomer effect has been observed.
- The activation constant of the catalyst is decreasing with increasing 1-hexene concentration.
- At high 1-hexene concentrations the deactivation constant is increasing.
- Increasing the 1-hexene weight fraction influences the polymer properties:
    - The density decreases
    - The melting point decreases
    - Molecular weight decreases
    - Melt flow index increases
- The lower melting point of the mLLDPE is an indirect proof for the better co-monomer distribution produced with this catalyst. The ZN-LLDPE contains homo-polymer parts, which increases the melting point
- At the chosen polymerization conditions, this metallocene catalyst is not able to produce a LLDPE with density 0.918 and melt index 1. The chain transfer probability with co-monomer is too high.

The proposed complexation model describes the ethylene 1-hexene co-polymerizations as function of the gas phase bulk concentrations rather well. The co-polymerization effect can be described with this model, even if small amounts of the co-monomer (B) are built in the polymer chains and large reaction rates are obtained for monomer A.

The co-polymerization equation derived from this complexation model is dependent on the reactivity ratios, the monomer bulk concentration ratio and the homo-polymerization kinetic constants ratio (K_X). This in contrast to the standard co-polymerization equation obtained by a first order Markov mechanism, which is only dependent on reactivity ratios and the monomer concentration ratio. The obtained co-polymerization equation is able to describe the incorporated co-monomer weight fractions with the optimized kinetic constants.

This model also describes the ethylene homo-polymerizations, with almost the same kinetic constants. The optimized kinetic constants are fitting the experimental data well.

Acknowledgement

Notation

A	Concentration of monomer A, ethylene	$kg \cdot m^{-3}$
B	Concentration of monomer B, 1-hexene	$kg \cdot m^{-3}$
C	Potential active site	$mol \cdot g_{cat}^{-1}$
C^0	Un-complexed active site	$mol \cdot g_{cat}^{-1}$
C^i	Complexed active site with monomer i	$mol \cdot g_{cat}^{-1}$
C_0	Total amount of potential active sites	$mol \cdot g_{cat}^{-1}$
C_t	Total amount of active sites	$mol \cdot g_{cat}^{-1}$
D	Deactivated sites	$mol \cdot g_{cat}^{-1}$
K_A	Equilibrium constant of complexation with A	$m^3 \cdot kg^{-1}$
K_B	Equilibrium constant of complexation with B	$m^3 \cdot kg^{-1}$
K_X	Ratio of $k_{paa}K_A$ and $k_{pbb}K_B$	-
k_d	Deactivation rate constant	min^{-1}
$k_{H,i}$	Henry's coefficient for monomer i	$g_i \cdot (g_{a-PE} \cdot bar_i)^{-1}$
k_i	Activation rate constant	min^{-1}
k_{i1}	Reaction constant of complex forming with i	$m^3 \cdot kg^{-1} \cdot s^{-1}$
k_{i2}	Reaction constant of de-complexing with i	s^{-1}
k_{pi}	Propagation rate parameter, with i=a,b	$m^3 \cdot mol^{-1} \cdot hr^{-1}$
k_{pij}	Propagation reaction constant with i =a,b j=a,b	$m^3 \cdot mol^{-1} \cdot hr^{-1}$
k_{sij}	Reaction rate constant of start with i =a,b j=a,b	$m^3 \cdot mol^{-1} \cdot hr^{-1}$
P_i	Partial pressure of i	bar
P^*	Active site with last inserted monomer A	$mol \cdot g_{cat}^{-1}$
Q^*	Active site with last inserted monomer B	$mol \cdot g_{cat}^{-1}$
R_{pA}	Polymerization rate (activity) of A, ethylene	$kg(PE) \cdot g_{cat}^{-1} \cdot min^{-1}$
R_{pB}	Polymerization rate (activity) of B, 1-hexene	$kg(PE) \cdot g_{cat}^{-1} \cdot min^{-1}$
r_A	Reactivity ratio of A = k_{paa}/k_{pab}	-
r_B	Reactivity ratio of B = k_{pbb}/k_{pba}	-
S_{M2}	Solubility of 1-hexene	$g \cdot g_{a-PE}^{-1}$
T	Temperature	K
$T_{c,i}$	Critical temperature of monomer I	K
$T_{m,i}$	Melting point, with i = 1,2 for first and second	°C
t	Time	min
X	Ratio of A and B	
y_i^d	Weight fraction of i in polymer	

Sub- and Superscript

A and a	Monomer A, ethylene
B and b	Monomer B, 1-hexene
PE	Polyethylene

Abbreviations

C2	Ethylene
C6	1-Hexene
FRR	Flow Rate Ratio (= MFI 21.6/MFI 2.16)
HDPE	High-density polyethylene
LLDPE	Linear low-density polyethylene
MFI	Melt Flow Index
MFM	Mass Flow Meter
Mn	Number average molecular weight
Mw	Weight average molecular weight
PDI	Polydispersity
PE	Polyethylene
S	Slurry phase experiment
TEA	Tri-ethylaluminum

Literature

Avela, R., Karling, R. and Takaharhu, J. (1998). Borstar- The Enhanced Bimodal Polyethylene Technology. 6th International Workshop on Polymer Reaction Engineering, Berlin, DECHEMA Monographs Wiley-VCH.

Böhm, L. L. (1981). "Zur Copolymerisation von Ethylen und a-Olefinen mit Ziegler-Katalysatoren." *Makromol. Chem.* **182**: 3291-3310.

Böhm, L. L. (1984). "Homo- and Copolymerization with a Highly Active Ziegler-Natta Catalyst." *J. Appl. Polym. Sci.* **29**: 279-289.

Britto, M. L., Galland, G. B., dos Santos, J. H. Z. and Forte, M. C. (2001). "Copolymerization of Ethylene and 1-Hexene with Et(Ind)2ZrCl2 in Hexane." *Polymer* **42**: 6355-6361.

Chakravarti, S. and Ray, W. H. (2001). "Kinetic Study of Olefin Polymerization with a Supported Metallocene Catalyst. II. Ethylene/1-Hexene Copolymerization in Gas Phase." *J. Appl. Polym. Sci.* **80**: 1096-1119.

Covezzi, M. (1995). "The Spherilene Process: Linear Polyethylenes." *Macromol. Symp.* **89**: 577-586.

Covezzi, M. and Mei, G. (2001). "The Multizone Circulating Reactor Technology." *Chem. Eng. Sci.* **56**: 4059-4067.

Fink, G. and Richter, W. J. (1999). "Copolymerization Parameters of Metallocene-Catalyzed Copolymerizations". Polymer Handbook. Brandrup, J., Immergut, E. H. and Grulke, E. A., John Wiley & Sons, Inc**: 329-337.

Hamielec, A. E. and Soares, J. B. P. (1996). "Polymerization Reaction Engineering - Metallocene Catalysts." *Prog. Polym. Sci.* **21**: 651-706.

Han-Adebekun, G. C., Debling, J. A. and Ray, W. H. (1997). "Polymerization of Olefins Through Heterogeneous Catalysis. XVI. Design and Control of a Laboratory Stirred Bed Copolymerization Reactor." *J. Appl. Polym. Sci.* **64**: 373-382.

Hutchinson, R. A. and Ray, W. H. (1990). "Polymerization of Olefin through Heterogeneous Catalysis. VIII. Monomer Sorption Effects." *J. Appl. Polym. Sci.* **41**: 51-81.

Kaminsky, W. (1996). "New Polymers by Metallocene Catalysis." *Macromol. Chem. Phys.* **197**: 3907-3945.

Kappler, B., Tuchbreiter, A., Faller, D., Liebetraut, P., Horbelt, W., Timmer, J., Honerkamp, J. and Mülhaupt, R. (2003). "Real-time Monitoring of Ethylene/1-Hexene Copolymerizations: Determination of Catalyst Activity, Copolymer Composition and Copolymerization Parameters." *Polymer* **44**: 6179-6186.

Kumkaew, P., Wu, L., Praserthdam, P. and Wanke, S. E. (2003). "Rates and Product Properties of Polyethylene Produced by Copolymerization of 1-Hexene and Ethylene in the Gas Phase with (n-BuCp)2ZrCl2 on Supports with Different Pore Sizes." *Polymer* **44**: 4791-4803.

Liu, H. T. D., C.R.; Shirodkar, P.P. (2003). "Bimodal Polyethylene Productc from UNIPOL Single Gas Phase Reactor Using Engineered Catalysts." *Macromol. Symp.* **195**: 309-316.

Meier, G. B., Weickert, G. and Swaaij, W. P. M. v. (2001). "Gas-Phase Polymerization of Propylene: Reaction Kinetics and Molecular Weight Distribution." *J. Polym. Sci. A: Polym. Chem.* **39**: 500-513.

Meier, G. B., Weickert, G. and van Swaaij, W. P. M. (2001). "Comparison of Gas- and Liquid-Phase Polymerization of Propylene with Heterogenous Metallocene Catalyst." *J. Appl. Polym. Sci.* **81**: 1193-1206.

Moore, S. J. and Wanke, S. E. (2001). "Solubility of Ethylene, 1-Butene and 1-Hexene in Polyethylenes." *Chem. Eng. Sci.* **56**: 4121-4129.

Parasu Veera, U., Benes, N. E., Pimplapure, M. S., Swaaij, W. P. M. v. and Weickert, G. (2001). Mass Transport during Olefin Polymerization on Heterogeneous Catalysts. Int. Workshop on Polymer Reaction Engineering, Hamburg, Wiley-VCH, Frankfurt am Main.

Pater, J. T. M., Weickert, G., Fait, A. and Mei, G. (2004). "Measurement of In-Situ Monomer Sorption in Poly(propylene)." *Macromol. Rapid Commun.* **25**: 1638-1642.

Quijada, R., Dupont, J., Miranda, M. S. L., Scipioni, R. B. and Galland, G. B. (1995). "Copolymerization of Ethylene with 1-Hexene and 1-Octene: Correlation between type of Catalyst and Comonomer Incorporated." *Macromol. Chem. Phys.* **196**: 3991-4000.

Samson, J. J. C., Weickert, G., Heerze, A. E. and Westerterp, K. R. (1998). "Liquid-Phase Polymerization of Propylene with a Highly Active Catalyst." *AIChE Journal* **44**(6): 1424-1437.

Schnauss, A. and Reichert, K.-H. (1990). "Modeling the Kinetics of Ethylene Polymerization with Ziegler-Natta Catalysts." *Makromol. Chem., Rapid Commun.* **11**: 315-320.

Shaffer, W. K. A. and Ray, W. H. (1997). "Polymerization of Olefins Through Heterogeneous Catalysis. XVIII. A Kinetic Explanation for Unusual Effects." *J. Appl. Polym. Sci.* **65**: 1053-1080.

Shimizu, F. (2001). Liquid Pool Polymerization of Propylene and Ethylene Using a Highly Active Ziegler-Natta Catalyst - Kinetics and Polymerization Mechanism. Enschede, University of Twente**:** 77-91.

Stern, S. A., Mullhaupt, J. T. and Gareis, P. J. (1969). "The Effect of Pressure on the Permeation of Gases and Vapors through Polyethylene. Usefulness of the Corresponding States Principle." *AIChE Journal* **15**(1): 64-73.

Weickert, G. (2003). High Precision Polymerization Rate Profiles. Ziegler Natta Catalysts. Busico, V. Kanazawa, JAIST.

Ystenes, M. (1991). "The Trigger Mechanism for Polymerization of a-Olefins with Ziegler-Natta Catalysts: A New Model Based on Interaction of Tweo Monomers at the Transition State and Monomer Activation of the Catalytic Center." *J. Catal.* **129**: 338-401.

Zhou, J. M., Li, N. H., Bu, N. Y., Lynch, D. T. and Wanke, S. E. (2003). "Gas Phase Ethylene Polymerization over Polymer Supported Metallocene Catalysts." *J. Appl. Polym. Sci.* **90**: 1319-1330.

Chapter 5

Catalytic Ethylene Solution Polymerization:

Precise Kinetic Measurements

Abstract

An experimental setup and kinetic study of high temperature solution homo- and co-polymerization of ethylene and 1-octene with a highly active and fast deactivating catalyst are presented. The reaction temperature has been controlled with isothermal-isoperibolic heat-compensation. The concept of this temperature control, the hardware and experimental procedures are described in detail. A catalyst was used with initial polymerization rates up to 30.000 $kg \cdot g_{cat}^{-1} \cdot hr^{-1}$ losing more than 80% of it's activity within 2 minutes at 180°C reaction temperature and 30 bar pressure. Reproducible polymerization rate profiles were measured with this new reactor within a few seconds after catalyst injection even at initial heat production rates of 3.8 kW at isothermal (±1 K) and isobaric (±0.05 bar) conditions. Catalyst decay could be described as second order deactivation.

Chapter 5

Introduction

A number of solution polymerization processes for ethylene have been commercialized since ICI started her high-pressure free radical polymerization process for LDPE production in 1938. Solution processes for <u>catalyzed</u> ethylene polymerizations were originally introduced for low-pressure manufacture of PE resins in the late 1950s and have been commercialized by DuPont, NOVA Chemicals, Dow, DSM, DEX Plastomers, Mitsui and Sumitomo Chemical (Whiteley 2002). Today a number of different slurry, gas phase and solution processes are economically competitive.

In the early 1990s, solution polymerization processes acquired new importance because of their shorter residence times and ability for using modern homogeneous catalysts exhibiting improved co-monomer incorporation, like single site catalysts. Many heterogeneous multi-center Ziegler-Natta catalysts produce superior LLDPE resins with a better branching uniformity if the catalyst residence time in a reactor is short. Catalytic solution polymerization processes usually operate at residence times of around 5 till 10 min or less and are ideal for these high active and thermally unstable catalysts. Catalyst design for solution processes does not require supporting of the catalyst on carriers like silica. Supporting often broadens molecular weight distributions and lowers catalyst activity. These solution processes can operate in a wide range of co-monomer types and concentrations providing a wide range of product densities. They are highly suitable for the production of lower molecular weight resins, which can cause fouling in gas and slurry phase reactors. The major drawbacks are: a solvent is necessary, which should be recovered in a commercial continuous process, and the high viscosity of the reaction mixture especially for high molecular weight products. State-of-the-art processes operate at temperatures between 130°C and 250°C. Because of low feeding temperatures, the high temperature level compensates a large part of the enormous polymerization heat by convective heat transfer. Operation temperatures above 230°C would lead to easier solvent removal and would lower the solution viscosity.

State of the art

Most catalytic ethylene polymerization kinetic studies are dealing with low temperature and low pressure; only few kinetic studies are published on catalytic high-temperature solution polymerization of ethylene. Machon *et al.* (1975) have presented kinetic data, propagation constants and deactivation constants, for semi batch experiments, using a Ziegler-Natta catalyst with varying temperature and different aluminum alkyls up to pressures of 10 bar and 220°C. Temperature profiles or temperature rises were not reported. Also continuous experiments were executed in a tubular isothermal reactor (up to 200 bar, 180°C with a residence time of 5-20 s) and in autoclave adiabatic reactor (up to 600 bar, 280°C with residence times of 20-40 s).

Kissin and Beach (1984) presented a kinetic study including rate-time profiles and temperature-time profiles for different Ziegler-Natta catalyst systems. The reaction rate was calculated from the pressure drop. The temperature control during the polymerizations was difficult, temperature increases of 15 till 20°C were observed for

10-15 min. Maximum polymerization rates were observed from 30 g/g(Ti)min until 2.6 kg/g(Ti)min at 14.8 bar and 180°C.

Jaber and Ray (1993a; 1993b; 1993c; 1993d) used a high-activity $TiCl_4/MgCl_2$ catalyst in a semi-batch reactor. They varied the hydrogen ratio (3.48-10.66 10^{-3} molar ratio H_2/C_2), the co-monomer ratio for 1-hexene (0.16-0.67 molar ratio C_6/C_2), and 1-octene (0.14-0.83 molar ratio C_8/C_2), temperature (145-200°C) and pressure (6.9 - 27.6 bar). Maximum reaction rates were reported in a range of 20 up to 150 kg/g(Ti)min. The catalysts showed a fast first order decay, the maximum reaction rate was reached after about 60 seconds. Jaber and Ray believed that mass transfer of ethylene is playing a major role in causing the very fast deactivation as observed in their presented solution polymerizations. Temperature profiles were not presented.

Some researchers (Adisson *et al.* 1993; Ribeiro *et al.* 1996) used vanadium based Ziegler-Natta catalysts at high temperature (160°C and 5 bar). The observed maximum reaction rates, calculated from the pressure drop, were low (7 kg/g(V)min, 0.25 gPE/s). Despite this low activity temperature increases of 8°C were observed[1].

Hasegawa *et al.* (2000) presented semi batch experiments at constant ethylene pressure of 20 bar at 150-200°C. The polymerization time was 20 min, reaction rates were derived from yield and varied between 1 and 35 kgPE/g(Zr)min, depending on catalyst type and temperature.

Continuous solution polymerizations (Charpentier *et al.* 1997; Wang *et al.* 1998; 1999) were carried out in a CSTR up to pressures of 206 bar and 300°C. Charpentier used a metallocene catalyst and residence times of 5 min, resulting in overall yields of maximum 250 kgPE/g(Zr) at 103 bar and 160°C. Wang *et al.*, using a constrained geometry catalyst, carried out experiments at 34.5 bar and temperatures between 140 and 190°C with residence times of 4 min. The authors improved the temperature and pressure control, steady state was reached after four mean residence times. Yields were observed up to 80 kgPE/g(Ti).

A few articles report polymer yields and polymer properties produced at high temperature and high pressure in (LDPE like) solvent-free processes (above 1000 bar) using Ziegler-Natta catalysts (Machon 1976; Grünig and Luft 1986) and metallocene catalysts (Luft *et al.* 1993; Bergemann *et al.* 1995). Machon produced polyethylenes at different temperatures (200-280°C) and pressures (1000-1500 bar), but did not show kinetic data of these experiments. Grünig and Luft presented productivities in a range of 400 kgPE/g(Ti) (at 500 bar, 230°C) till 2000 kg PE/g(Ti) (at 1500 bar, 150°C); the performed experiments were batch-wise with a polymerization time of 1 to 2 min. Both publications did not report temperature profiles or temperature rises. Bergemann *et al.* used a continuous stirred tank reactor at 1000-1500 bar and 120-220°C with a residence time of 4 min for homo- and co-polymerizations. For homo-polymerizations reaction rates were measured of 4400 kgPE/gMetal at 1500 bar and 180°C, <u>calculated from the polymer yield</u>. Luft *et al.* presented catalyst productivities of 13300 kgPE/gMe at 80°C till 3400 kgPE/gMe at 210°C, measured batch wise at 1500 bar with a residence time of 2 min. The used catalyst showed a decreasing yield with

---

[1] This work: activity 1 PEg/s; temperature ±1K

increasing temperature. This can be explained with a higher activation energy of the catalyst decay than the activation energy of the propagation. Furthermore, the initial thermal behavior – directly after catalyst injection – is most important for interpretation of kinetic results. An enormous initial temperature increase can lead to chemical instability and dramatic deactivation of active sites. Therefore, most attention has to be given to temperature control of the reactors used.

In continuous processes with high active fast deactivating catalysts the polymer production is kept constant by controlling the catalyst feed. A constant polymer production causes a constant chemical heat production; therefore the temperature can be controlled easily (Hasegawa *et al.* 2000). However, continuous operation needs a much higher experimental effort, provides much less kinetic data. Kinetics of batch versus continuous processes can differ in presence of inhibiting or retarding components. For batch experiments the heat production is not constant. Isothermal calorimetric reactors for slurry and bulk catalytic polymerizations at low temperature are usually controlled with the jacket temperature. A temperature control by a cooling medium through the jacket is slow. This leads often to temperature oscillations over more than 5 minutes; especially when the initial heat production is higher than 500 W in lab-scale reactors. Samson *et al.* (1998) and Pater *et al.* (2003) presented the temperature control for deriving kinetics by means of isothermal calorimetry for catalytic propylene bulk polymerizations in a 5-L steel reactor based on a constant-heat-transfer assumption. This assumption was verified experimentally for the liquid pool slurry up to a solid phase concentration of about 25 wt%. Due to temperature oscillations they were not able to measure 'real' kinetics within the first 5 till 10 minutes. Using the same reactor equipment, Weickert (2003) showed, by means of an isoperibolic calorimetric method, quasi steady state could be reached within 1.5 min. However, this is not fast enough if one uses catalysts deactivating by more than 80% within the first two minutes. Furthermore, the initial temperature rise should be small enough to keep the system "quasi-isothermal". Under conditions described above, calorimetric measurements of the complete polymerization rate profile for catalytic high temperature solution processes are not possible, due to two reasons

1. The quickly increasing viscosity leads to a drop of the heat transfer coefficient.
2. The catalyst decay is too fast compared to other processes, which are dominating heat storage and heat transfer.

This paper

Weickert (2003) showed the importance of knowing the complete kinetic profile of a catalyst; especially two arguments mentioned there are important for solution polymerization kinetic studies:

- Yield measurements, often used to characterize the catalyst performance, are not sufficient, as very different polymerization rate profiles can result in the same yield
- The reaction conditions during the first seconds after contacting active sites with monomer should be analyzed very carefully,

especially in terms of physical and chemical changes around the active sites, see also Weickert (2004).

Especially in polymerizations with highly active and fast deactivating catalysts, resulting in shorter residence times, the reaction should be controlled a few seconds after catalyst injection. Due to the enormous instantaneous heat production, the temperature control is getting more difficult and important. Mixing of the injected catalyst within the reaction volume, local overheating, and mass transfer effects are to be analyzed.

Continuous catalytic solution polymerizations in well mixed reactors result in accurate temperature control. Local mixing and overheating can be avoided by dilution of the catalyst solution. Gas-liquid mass transfer can be neglected when the monomer is pre-solved, but getting a complete set of kinetic information (rate time profile) is very costly and time consuming. The reaction rate should be determined for different residence times after reaching the steady-state operation of the reactor. Downscaling is more difficult and can lead to low scalability and reproducibility; the use of very small amounts of catalyst causes more problems with impurities due to the continuous feed of monomer and solvent.

Isothermal and isobaric experiments are required in order to obtain kinetic parameters, like propagation rate constants and deactivation constants. Isothermal and isobaric experiments are also required for obtaining relations between proces conditions and polymer properties, like molecular weight distribution and copolymer composition. The temperature and pressure control should be accurate and fast, because a temperature increase of 10°C can lead to a significant change of the polymerization rate and can cause a 10% decrease in molecular weight (Jaber and Ray 1993c). Due to the short residence time, the amount of polymer produced under non-isothermal conditions cannot be neglected. So an impropriate temperature control with a highly active and fast deactivating catalyst with exothermal reaction leads to broadening of the molecular weight distribution. Up to now no isothermal temperature profiles for batch and semi-batch high-temperature solution polymerizations were reported in literature.

Temperature increases have also a physical effect. A temperature increase leads to an instantaneous expansion of the gas within the reactor and desorption of gas from the solvent. If mass flow meter techniques are used, the detected flow of the gas feed required for keeping the pressure constant will be lower. So temperature changes can cause apparent rate changes.

New reactors are required which guarantee fast mass transfer combined with good mixing behavior and a superb temperature control. These new reactors should measure polymerization reaction rates reproducibly and accurately within a very short time (<10 s). In this chapter the Isothermal-Isoperibolic Compensation Reactor (IICR) is presented for catalytic olefin polymerizations in liquid phase, which fulfill these demands. High temperature solution ethylene homo- and co-1-octene polymerizations are used as model reactions.

Experimental

Setup

The experimental setup for solution-phase polymerizations is represented in Figure 1. The reactor, equipped with a special designed electrical 4-kW heating element, is a jacketed, stainless steel 5-liter reactor from Büchi, which operates up to pressures of 40 bar and temperatures till 220°C. The operation mode is "semi batch", this means that the catalyst is only injected once each experiment, whereas the pressure drop by monomer consumption is compensated by feeding fresh monomer gas. Solvent and co-monomer are fed only once before starting the experiment via a liquid thermal mass flow controller (Bronkhorst Hi-Tec). Also hydrogen is fed batch wise by a thermal mass flow controller (Bronkhorst Hi-Tec). The pressure is kept constant by feeding ethylene continuously over an electronic reducer (Bronkhorst Hi-Tec) by a coriolis mass flow meter (Elite sensor, Micro Motion).
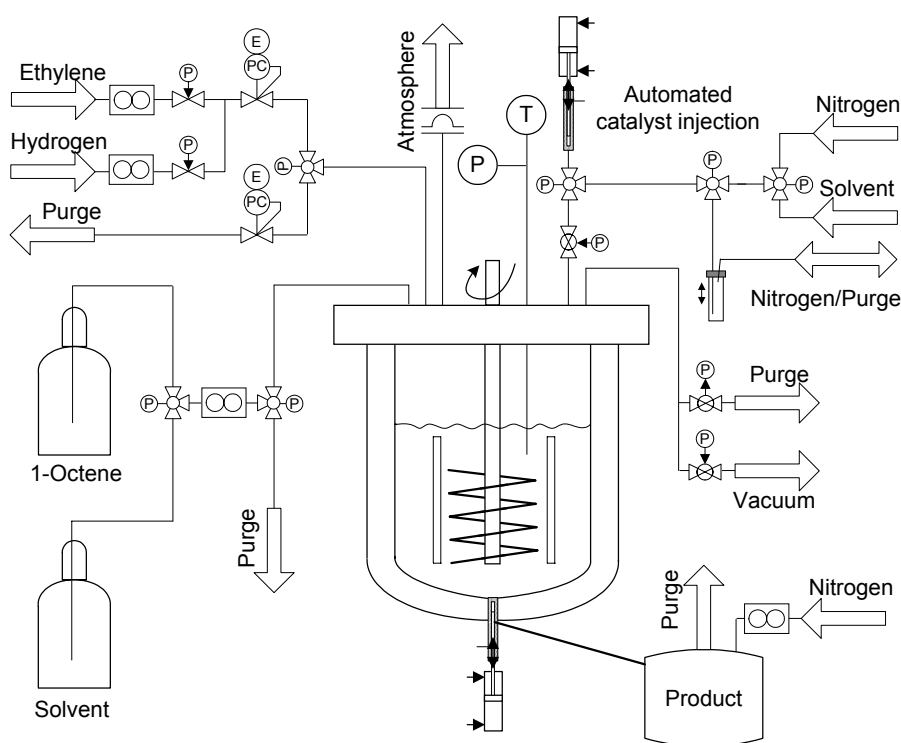

Figure 1: Isothermal-Isoperibolic Compensation Reactor

The catalyst is injected by an automated suspended injection system (Samson *et al.* 1998; Bergstra and Weickert 2004) with Schlenck technique. The reactor is designed in such a way that opening of the reactor is not required after each experiment; therefore a vessel is connected to the reactor that collects the product and solvent after an experiment. This vessel is equipped with a large open purge connection and is continuously flushed with a small nitrogen flow, in order to guarantee an inert atmosphere in the product collection vessel. A magnetic coupled drive rotates the stirrer, comprising a hollow shaft with helix and propeller, in the reactor with a variable speed of maximum 4000 rpm. The reactor is furthermore equipped with a

rupture disc, a connection to a central purge system and a central vacuum system. The complete setup is placed in a concrete box.

Temperature control system

The temperature in the reactor has to be constant before and after catalyst injection, so with starting and during the reaction. In this way the temperature profiles and heat storage are not disturbed and the kinetics are measured immediately after catalyst injection.
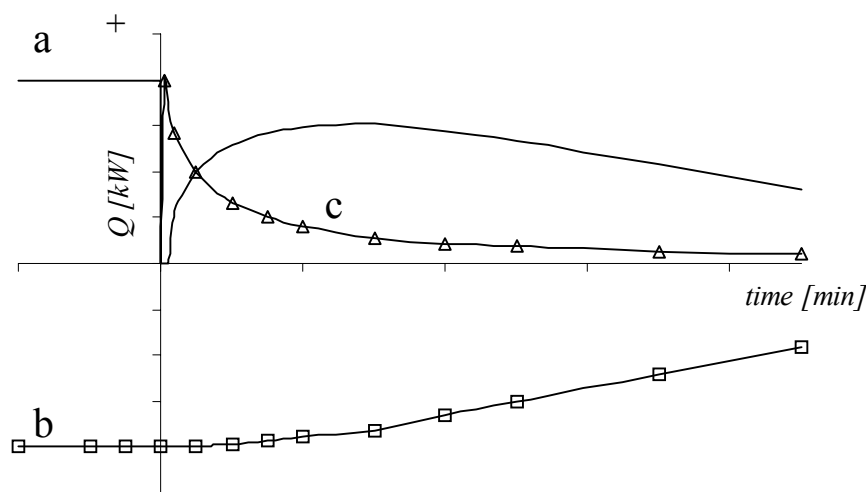

Figure 2: IICR principles, a - electrical heating element, b - cooling heat, c - chemical reaction heat

To achieve this the jacket and cover plate have to be kept initially at constant temperature (isoperibolic). The reactor is equipped with an internal electrical heating element. This element is a helical coil, which combines a large heat exchanging surface and minimized mass, resulting in a low heat capacity. The temperature is reversely controlled by this heating element, in such a way that the total heat production in the reactor, chemical and electrical heat, is kept constant before and after catalyst injection. Figure 2 gives a schematic representation. Injecting the catalyst results in starting the reaction, the exothermic polymerization reaction is giving a maximum heat flux. The maximum heat flux should not exceed the power of the heating element (3.8 kW), which is switched to zero during catalyst injection. Subsequently, corresponding to the catalyst decay, the temperature is kept constant by increasing the power of the heating element compensating the decrease in chemical heat production. The temperature in the cooling jacket will decrease over the reaction time due to polymer production, which increases the viscosity and lowers the heat transfer coefficient. By means of this electrical heater the response time is decreased enormously, an accurate and fast temperature control is achieved.

Figure 3 shows the scheme of the temperature control of this Isothermal Isoperibolic Compensation Reactor (IICR). The connection tube from reactor to product collection vessel and the cover plate are heated with an oil bath (Unistat T326 HT, huber) at a

constant temperature. Oil is continuously circulated by pump 1 through the jacket maintaining a high flow rate; this oil loop has a minimized volume and contains no heating. Inside the reactor the electrical heating element is placed (maximum power 1.9 kW during the first experiments, upgraded to 3.8 kW currently), the power is monitored (Programmable AC Power Monitor & Display, Moore Industries) and the temperature of the electrical heater is watched (Eurotherm Alarmunit & Indicator). The electrical heating element is controlled by a PID controller (Eurotherm 2408). The temperature of the oil loop is kept initially constant and is controlled by adding cold oil by pump 2 via a control valve (ABB Automation), which is operated by a PID controller (Eurotherm 2408). After catalyst injection the temperature of the cooling jacket can decrease due to the increased viscosity and lowered heat transfer coefficient. The cold oil is kept in a reservoir at a constant temperature of 30°C by cooling with cold water (Eurotherm Alarm Unit & Indicator).

A Data Acquisition/Control Unit (DACU, HP 3852A) measures all temperatures, pressures, mass flows and the power of the heating element and controls the pneumatic valves, the mass flow controllers, backpressure and reducer. This data is stored every three seconds on a PC (HP), which contains the operating software (in HPVEE).
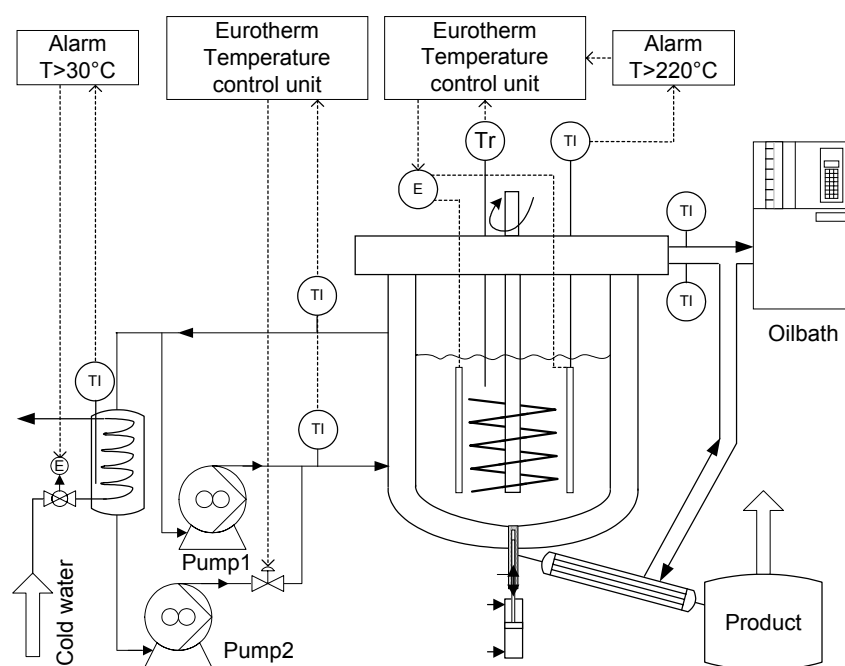

Figure 3: *Temperature control of Isothermal-Isoperibolic Compensation Reactor*

Reaction-rate measurements

The ethylene reaction rate is determined with mass flow technique. By keeping the pressure and the temperature in the reactor constant, the polymerization rate-time profile is achieved by the mass flow meter already within 10 seconds.

Mass balance of ethylene for the gas cap:

$$\frac{\partial m_{C2}}{\partial t} = \Phi_{m,in,C2} - \Phi_{m,liq,C2} \tag{1}$$

Under isothermal and isobaric conditions, with no significant accumulation or change in gas volume and assuming no mass transfer limitations, the reaction rate can be estimated from the mass flow directly:

$$R_{p,C2} = \Phi_{m,in,C2} \qquad\qquad (2)$$

Chemicals and monomer purification

The used catalyst in this work is obtained from Dow. This titanium-based catalyst was provided in suspension. Triethylaluminum (TEA) is used as co-catalyst. The catalyst is stored and handled in a glove box (Braun MB 150BGII).

Ethylene (purity > 99.9%, C_2H_2 < 7 ppm, Hoekloos) is further purified over oxidized BASF R3-16 catalyst, reduced BASF R3-16 catalyst, molecular sieves (13X, 4A and 3A) and Selexsorb® COS (Alcoa). Nitrogen (purity >99.999%, O_2 < 1-10 ppm, H_2O < 1-10 ppm, Praxair) and hydrogen (purity >99.999%, Praxair) are purified over reduced BASF R3-11 catalyst and molecular sieves (13X, 4A, 3A). Co-monomer (1-octene) and solvent (Exxsol), both delivered by Dow, are stored under low nitrogen overpressure and are not further purified.

Solution Polymerization procedure

The reactor is purified by performing a polymerization experiment. The reactor is not opened afterwards, so baking-out or washing with aluminum alkyls is not required.

The standard procedure is as follows:
1. Before each experiment the reactor is pressurized with nitrogen till 20 bars and checked for any leakage during 3 minutes. Afterwards the reactor is purged and evacuated (< 70 mbar).
2. Solvent is added to the reactor by means of the liquid flow controller, in case of homo-polymerizations 3000 Nml is added, for co-polymerizations 2500 Nml.
3. In case of a co-polymerization around 440 Nml of co-monomer, 1-octene, is fed to the reactor. The total liquid volume should be at least 3 L; the liquid level should immerse the heating element.
4. The stirring speed is installed at the desired value, in most cases at 2000 rpm.
5. The reactor is heated up until the desired set point of 180°C by switching on the heating element, pump 1 and pump 2 (see Figure 2); the temperature of the cooling oil is set to typically 140°C for this stirring speed.
6. If a stable temperature close to the set point is reached, 300 Nml of hydrogen is added.
7. The reactor is pressurized with ethylene until 30 bar.
8. The power of the heating element is maximized to 1.9 kW (or to 3.8 kW, depending on catalyst amount) by changing the cooling oil temperature at constant reactor temperature.
9. Meanwhile the catalyst is weighed and the desired amount of TEA is added to the catalyst. Table 1 shows the real amounts of Ti and TEA. During some experiments TIBA was used as scavenger and was added 10 minutes before

catalyst injection into the reactor. TIBA decomposes at these high temperatures faster then TEA.

10. The catalyst vial is connected to the needles and suspended/diluted with solvent. Just before the injection the heating element is switched off. The catalyst is injected; the catalyst vial is refilled with solvent and injected again into the reactor for two times. The heating element is switched on and the Eurotherm PID controller is keeping the reactor temperature constant by controlling the power.

11. After the desired polymerization time the ethylene supply is stopped and the heating element is switched off. Due to the fast deactivation only the first minutes of the polymerization experiment are interesting, for a good estimation of the deactivation constant the polymerization can be continued for 20 minutes.

12. The pressure starts dropping, at 25 bars the bottom valve is opened. Due to the pressure difference the viscous polymer-solvent mixture is flashed into the product collection vessel, which is at atmospheric pressure.

13. The bottom valve is closed again and next experiment can be started.

14. After a few minutes the product collection vessel is opened, the precipitated polymer is dried and the solvent is collected.

Results and Discussion

Method

A typical example of results is given in Figures 4 to 9 for the co-polymerization of ethylene with 1-octene. Figure 4 shows the reaction temperature profile during the complete reaction time of co-polymerization experimental run 1. The real ethylene consumption is represented in Figure 7.
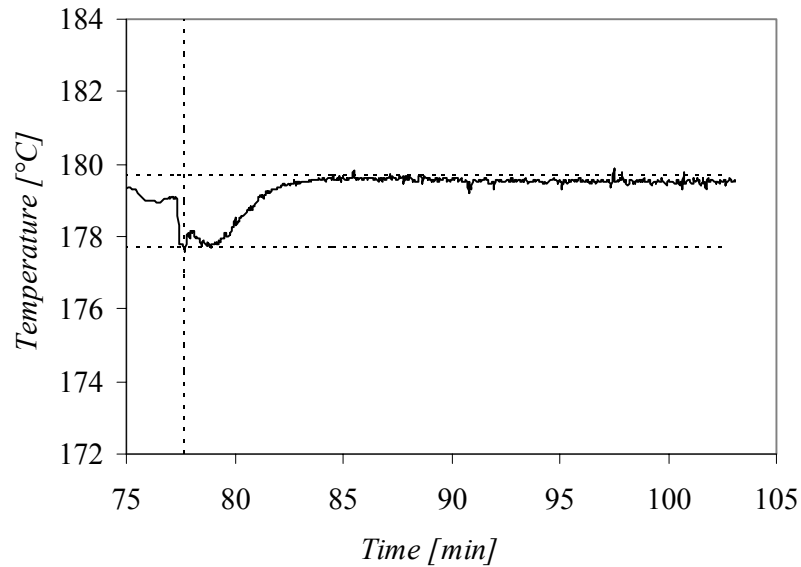

Figure 4: *Temperature vs. time plot of run 1. The vertical dotted line indicates the injection of the catalyst, the two horizontal dotted lines indicate the interval ±1°C.*
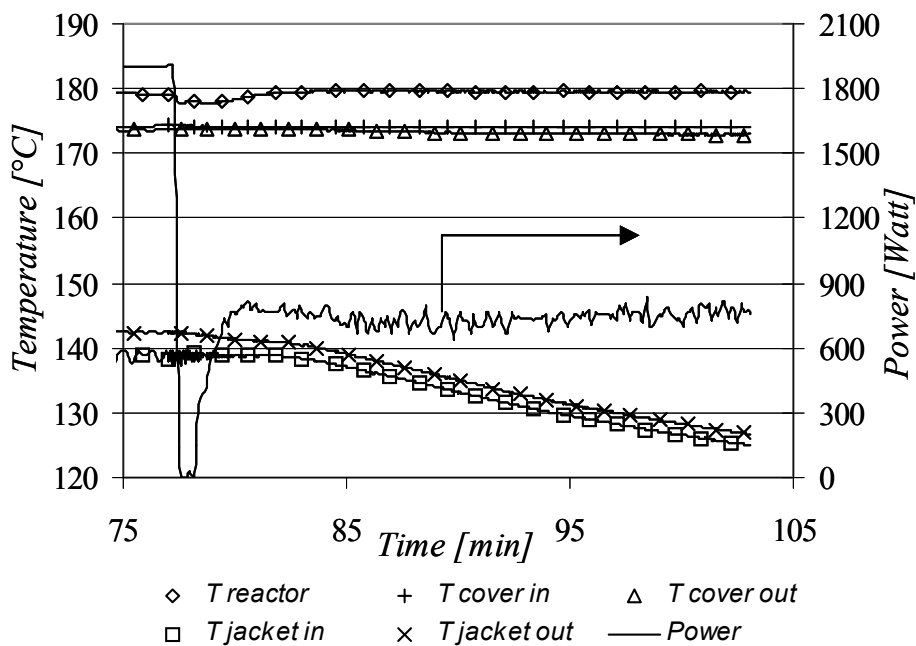

Figure 5: *Temperature of reactor, cover plate and cooling jacket and electrical power vs. time of run 1.*

The reaction temperature decreases 1 degree before catalyst injection, because the heating element is switched off. During the complete experiment, the reaction temperature remains constant within 1 degree: $T_{reactor} = 178.7 \pm 1.0$ °C. Figure 5 shows the temperatures of the cooling oil through the jacket, the cover plate, reactor and the power of the electrical heating element during this experiment. The temperature of the cover plate is kept constant during the complete experiment. As soon as the polymer production starts, the viscosity increases. As a consequence the heat transfer decreases and the cooling oil temperature decreases. In this experiment, the electrical power is initially 1900 Watt. Just before catalyst injection the power is switched to zero. After this catalyst injection the power is switched on again and is compensating for the deactivation of the reaction. As result of the decreased heat transfer through the reactor wall the electrical power is not returning to the initial maximum power at the end of the experiment.
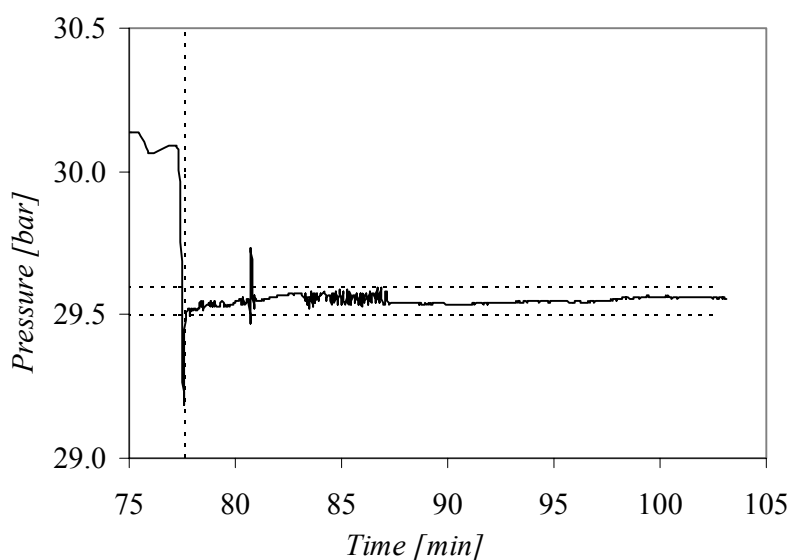

Figure 6: *Pressure vs. time plot of run 1.*

The pressure control within a complete experiment (run 1) is presented in Figure 6. Just before the catalyst injection the pressure drops due to the temperature decrease. After this decrease and after catalyst injection the pressure is kept constant by the mass flow meter at 29.55 bar within a range of 0.05 bar.

Figure 7 represents the real polymerization rate. Due to inaccuracy of the flow meter below 10 g/min a small part of the reaction rate curve is missing (at t = 81 min) until the flow is below 6 g/min. From that point another flow meter was recording the polymerization rate.
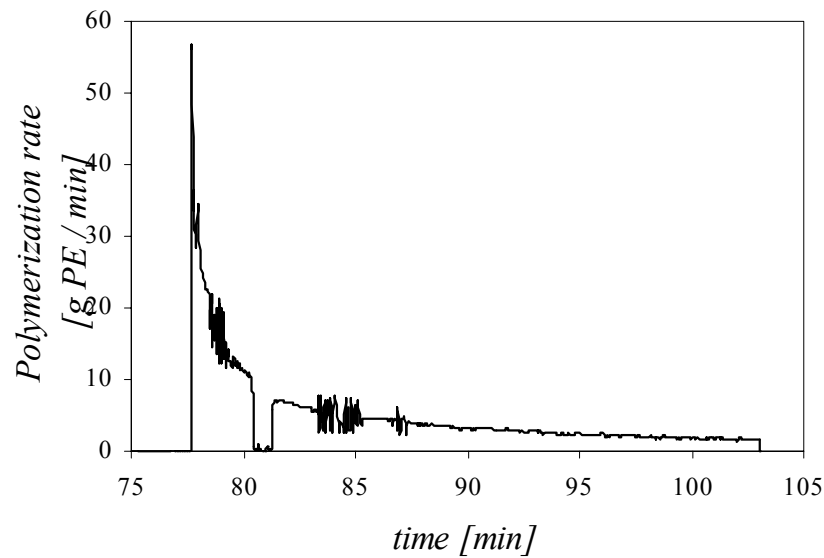
Figure 7: Run 1 real polymerization rate vs. time.

The catalyst shows instantaneously a high activity of 370 kgPE·g(Ti)$^{-1}$·min^{-1}, twice as high as reported by Jaber and Ray (1993a), and shows a very fast deactivation, within one minute the catalyst looses 50% of the initial activity. One of the major objectives of the new reactor design was to measure the real polymerization rate within ten seconds after catalyst injection at constant temperature and pressure.
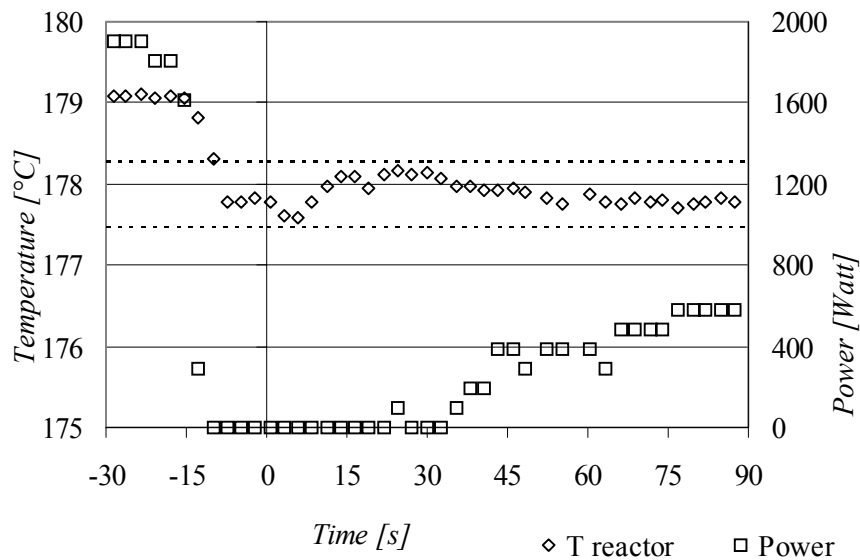

Figure 8: Enlargement of Figure 5, temperature (left) and electrical power (right) during the first two minutes of run 1

Figure 8 shows the reactor temperature and the electrical power of the heating element of experimental run 1 during the two most important minutes of the experiment, i.e. 30 seconds before injection and the first 90 seconds of the polymerization. Figure 9 shows the ethylene mass flow, which stands for the polymerization rate, and pressure of run 1 during the same two minutes. About fifteen seconds before catalyst injection, the

heating element is switched from maximum power (1900 W) to zero for several seconds. These timings are determined by experience and valid under these reaction conditions and with this reaction rate. A drop in temperature of one degree can be observed and also the pressure drops (0.5 bar). The catalyst is injected (at time zero) resulting in a small initial decrease in temperature due to the cold solvent, which is injected with the catalyst. Then a small increase in temperature can be observed caused by reaction, and the mass flow meter is starting with the registration of the polymerization rate (see Figure 9). Afterwards, the heating element is switched on via the controller and is keeping the temperature constant (see Figure 8). Within the first 90 seconds, the temperature is kept constant at $177.9 \pm 0.4°C$ and the pressure is kept constant at 29.55 ± 0.05 bar. So within this period already isothermal and isobaric conditions are reached despite the dramatic changes caused by the polymerization rate. The mass flow meter is giving a signal after 5 seconds. One can conclude from these figures that kinetics can be measured already after five/ten seconds at isothermal and isobaric conditions with a highly active and fast deactivating catalyst.
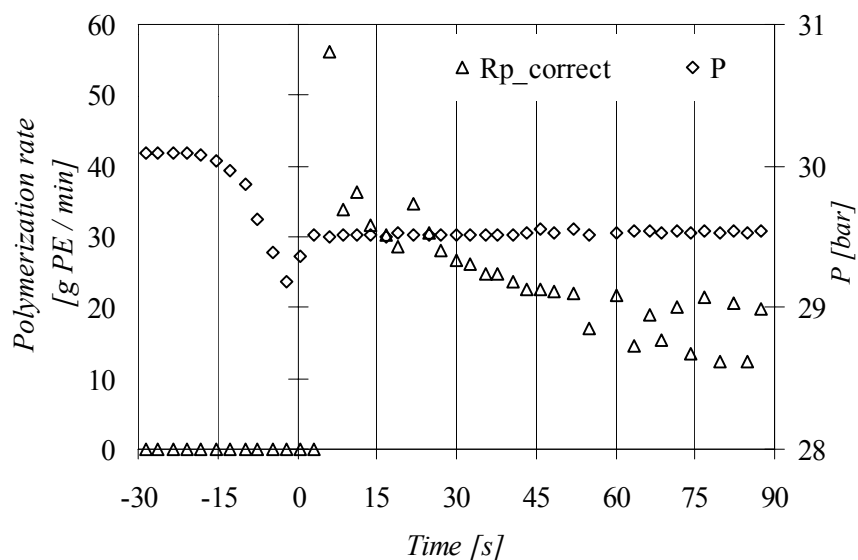

Figure 9: *Enlargement of Figure 6 and 7, polymerization rate (left) and pressure (right) during the first two minutes run 1*

Reproducibility

The reproducibility is tested for standard homo-polymerization experiments, at 179°C, with 300 Nml of hydrogen and at a total pressure of 30 bars. The reactor is purified by a polymerization experiment. A consequence is that the first experiment in a series has only a small chance on high kinetic accuracy. This loss is compensated by the possibility to run up to 7 experiments per day.

One should take into consideration that an estimation should be made for the expected polymerization rate; the expected heat production should not exceed the maximum electrical power to obtain isothermal conditions.

Run	Catalyst	TEA	TIBA	H2	C8	Yield	τ	R_{p0}	k_dC_0	Yield $\tau=10min$
-	mg	mg	mg	Nml	Nml	kg/g_{cat}	min	$\frac{kg/g_{cat}}{min}$	min^{-1}	kg/g_{cat}
1	0.112	1.71	-	300	440	1062	25.4	369	1.06	852
2	0.196	3.14	112.5	300	0	253	7.4	369	2.25	517
3	0.168	2.85	106.6	300	0	550	14.0	376	1.63	656
4	0.168	2.85	78.1	300	0	405	10.0	368	2.05	551
5	0.168	2.85	-	300	0	319	10.5	391	2.31	539
6	0.084	2.85	-	300	0	833	12.0	678	1.82	1103
7	0.084	1.43	105.1	300	0	735	27.3	773	3.12	860
8	0.140	2.28	-	300	440	553	15.3	267	1.38	520
9	0.140	2.85	-	300	440	759	17.1	318	1.43	608
10	0.168	4.43	-	206	0	522	10.7	380	2.34	518
11	0.168	4.49	-	203	0	619	15.0	363	2.00	552

Table 1: *Experimental results at 180°C and 30 bar, homo-polymerizations with 3150 NmL and co-polymerizations with 2490 NmL solvent*

The reproducibility of four successful experiments (run 2-5) is shown in Figure 10. The average initial polymerization rate for these experiments is 376 kgPE·g(Ti)$^{-1}$·min^{-1}, the maximum deviation is only 4%. Again, the measured activities are twice as high as the maximum activities reported by Jaber and Ray. Table 1 summarizes the reaction conditions of all presented experiments.
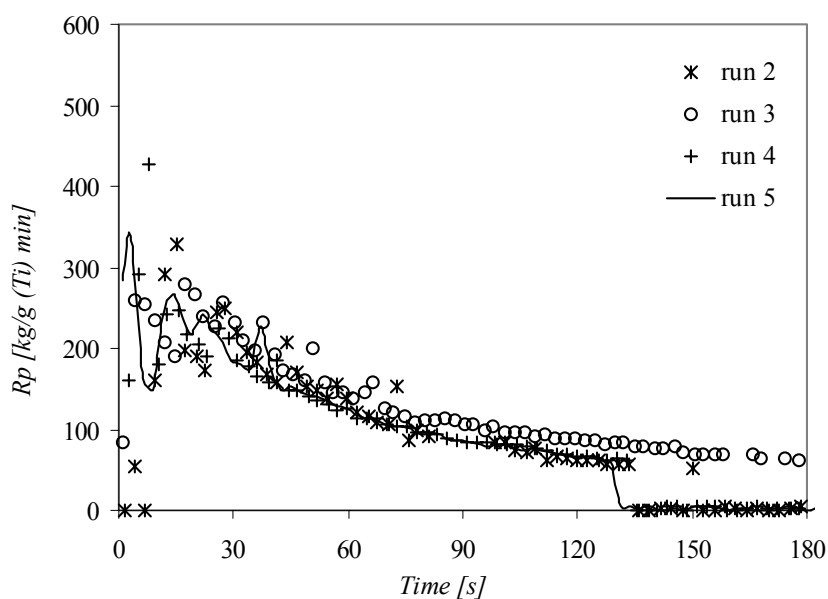

Figure 10: *Polymerization rate for homo-polymerization runs 2, 3, 4 and 5 with 0.168 mg Ti*

Figure 11 shows two standard co-polymerization experiments (run 8 and 9) at 180°C. The activity for these experiments is somewhat lower than for the homo-polymerizations; this is in agreement with findings of Jaber and Ray (1993b). Co-monomers often contain impurities; higher activities could be reached by optimizing scavenger and catalyst amount. But also concentrations of ethylene and/or hydrogen could be different compared to the homo-polymerizations due to the presence of the

co-monomer. Also the reactivity of the co-monomer under these conditions is not yet clear and should be analyzed within further investigations.
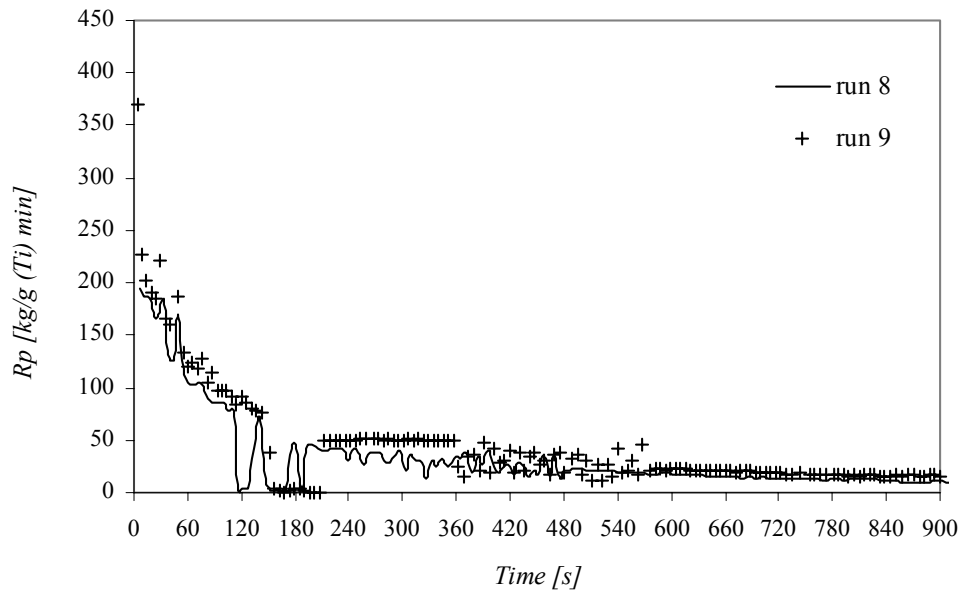

Figure 11: *Polymerization rate in time for co-polymerization runs 8 and 9 with 0.140 mg Ti*

Mass transport limitations

Figure 12 represents two homo-polymerization experiments (run 6 and 7) at standard test conditions but with 50% less catalyst compared to Figure 10 (run 2-5). This plot shows that the specific activity is almost twice as high (780 kgPE·g(Ti)$^{-1}$·min^{-1}) as with the doubled amount of catalyst (376 kgPE·g(Ti)$^{-1}$·min^{-1}).
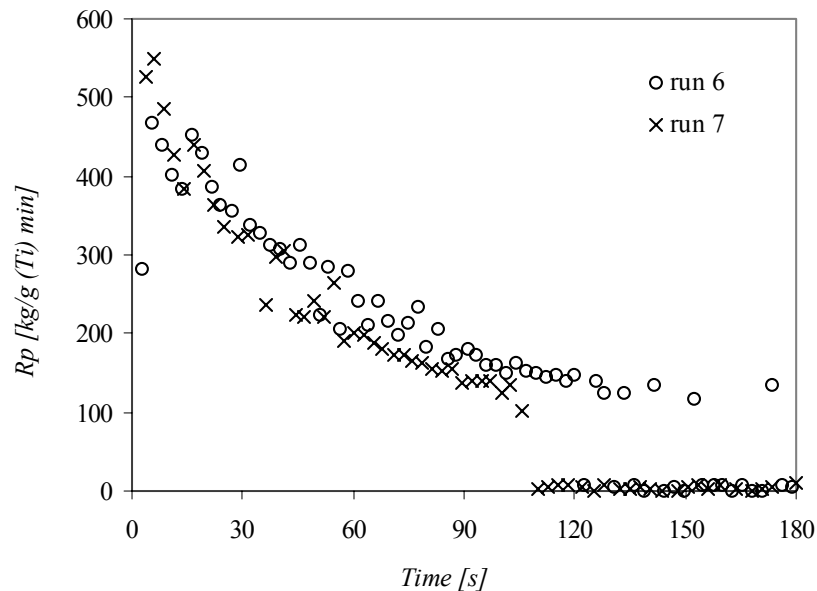

Figure 12: *Polymerization rate for homo-polymerization runs 6 and 7 with 0.084 mg Ti*

Due to the enormous high activity the viscosity increases during the very early stage of polymerization, limiting mass transfer from the gas cap to the liquid phase. The

solubility of ethylene in the solvent at these high temperatures is much lower compared to low temperature slurry polymerizations, additionally the polymer production will change the gas-liquid mass transfer. The question arises if mass transport limitations from the gas cap to the liquid phase might occur. Jaber and Ray (1993b) compared activities measured in solution phase co-polymerization with slurry polymerizations, which were assumed by Dumas and Hsu (1989) having mass transfer limitations and resulting in a 25% decrease of monomer concentration. The activities in the presented experiments and the experiments by Jaber and Ray show much higher activities compared to slurry phase polymerizations. Jaber and Ray measured rates of 6 - 7 g/min, whereas in this study reaction rates were measured of 40 - 60 g/min. Reactor geometry, gas inlet, stirring velocity and stirrer geometry play an important role beside the reaction conditions used.

Determination of kinetic parameters

The reaction rate can be modeled with a first order deactivation model using three parameters, R_{p0}, k_d and a R_{p_end}, as proposed by Jaber and Ray.

Here a 2nd order deactivation model is suggested with only two fitting parameters, being R_{p0} and k_dC_0, that can be derived as follows:

Catalyst deactivation:
$$\frac{dC}{dt} = -k_d C^2 \qquad\qquad t = 0, C = C_0 \qquad (3)$$

Integrating results in:
$$C(t) = \frac{1}{k_d t + \dfrac{1}{C_0}} \qquad (4)$$

Polymerization rate is assumed to be dependent on the catalyst concentration and the monomer concentration, assuming no mass transport limitation:
$$R_P{}'(t) = k_p \cdot C(t) \cdot C_M \cdot V \qquad (5)$$

The specific reaction rate can be expressed as:
$$R_P(t) = \frac{R_P{}'(t)}{m_{cat}} = k_p \cdot C(t) \cdot C_M \cdot \frac{V}{m_{cat}} \qquad (6)$$

Combining (4) and (5):
$$R_p(t) = \frac{k_p C_0 C_M}{k_d C_0 \cdot t + 1} \cdot \frac{V}{m_{cat}} = \frac{R_{p,0}}{k_d C_0 \cdot t + 1} \qquad (7)$$

Table 1 shows the values for the parameters R_{p0} and k_dC_0, which describe the polymerization rate based on equation (7). Figures 13, 14 and 15 give representations of the model fit with the measured reaction rate (all at 180°C) for co-polymerization run 1 and homo-polymerization runs 10 and 11 respectively. These figures show clearly that the proposed model, with only two parameters, is fitting the experimental data.
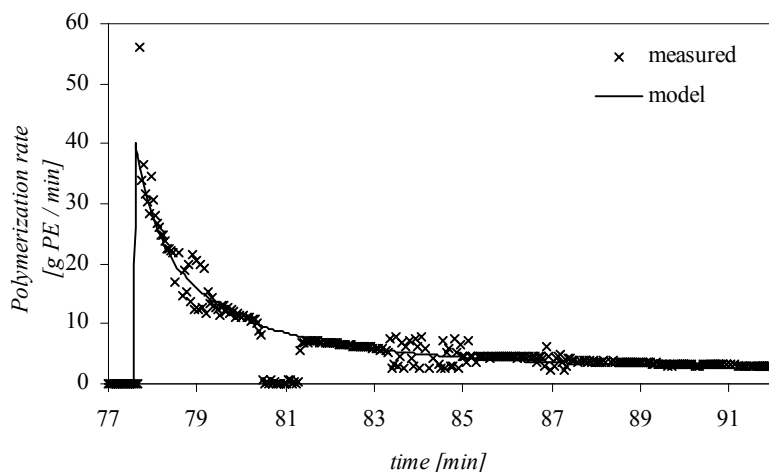
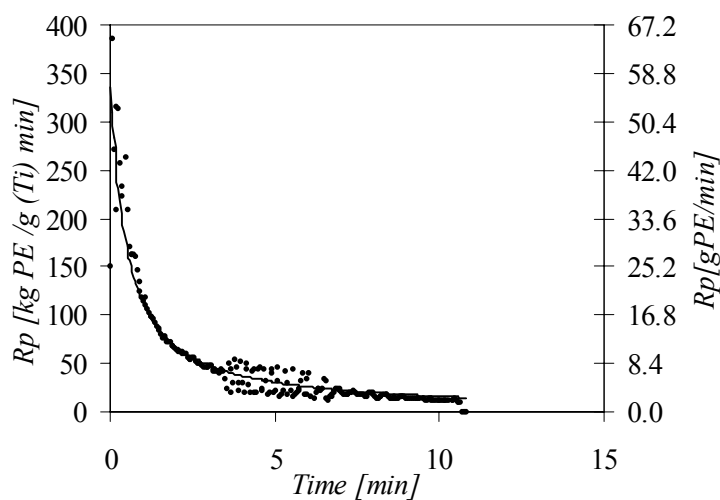*Figure 13: Co-polymerization Run 1 with modeled reaction rate*

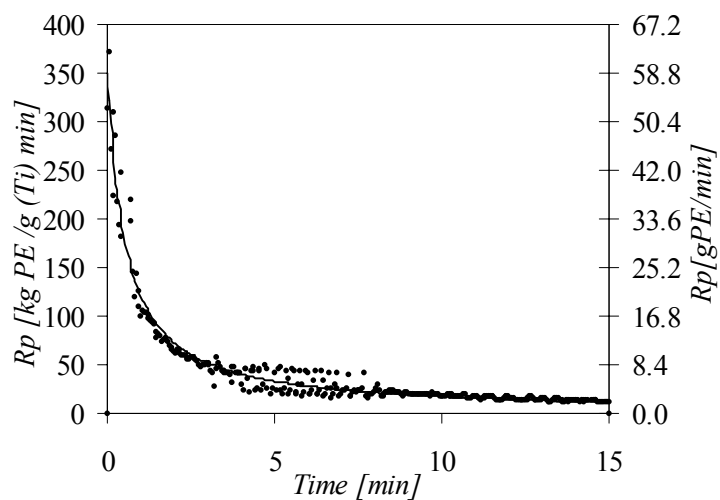*Figure 14: Homo-polymerization Run 10, 0.168 mg catalyst*

Figure 15: Duplication measurement Homo-polymerization Run 11, 0.168 mg catalyst

Conclusions

An experimental setup for high temperature solution ethylene homo- and co-polymerizations has been presented. Polymerization rate profiles could be measured already some seconds after catalyst injection at isothermal and isobaric conditions with highly active and fast deactivating catalysts in solution homo- and co-polymerizations of ethylene with 1-octene.

The accuracy and reproducibility of the experimental results is good for both homo- and co-polymerization. The obtained polymerization rates are very high, however mass transfer limitation cannot be excluded. For the co-polymerizations a lower activity was observed.

A 2nd order deactivation model was proposed for describing the reaction rate, this requires only two parameters, a lumped deactivation constant, $k_d C_0$, and the initial polymerization rate, R_{p0}.

Acknowledgements

Notation

C	Active catalyst concentration	$[kg \cdot m^{-3}]$
C_M	Monomer concentration	$[kg \cdot m^{-3}]$
m	Mass	$[g]$
k_d	Deactivation reaction rate constant	$[m^3 \cdot kg^{-1} \cdot min^{-1}]$
k_p	Propagation reaction rate constant	$[m^3 \cdot kg^{-1} \cdot min^{-1}]$
P	Pressure	$[bara]$
R_P	Specific polymerization rate	$[kg(PE) \cdot g(Ti)^{-1} \cdot min^{-1}]$
R_P'	Polymerization rate	$[g(PE) \cdot min^{-1}]$
R_{P0}	Specific polymerization rate at t=0	$[kg(PE) \cdot g(Ti)^{-1} \cdot min^{-1}]$
T	Temperature	$[°C]$
t	Time	$[min]$
V	Volume of liquid	$[m^3]$
Yield	Catalyst efficiency	$[kg(PE) \cdot g(Ti)^{-1}]$

Greek letters

τ	Residence time	$[min]$
Φ_m	Mass flow	$[g \cdot min^{-1}]$

Subscript

0	Initial condition at time zero
cat	Catalyst
end	Time at the end of experiment
in	In flowing
liq	Flowing to liquid phase
M	Monomer

Abbreviations

C2	Ethylene
C8	1-Octene
H2	Hydrogen
LDPE	Low density polyethylene
LLDPE	Linear low-density polyethylene
PE	Polyethylene
TEA	Tri-ethylaluminum
TIBA	Tri-isobutylaluminum

Literature

Adisson, E., Deffieux, A. and Fontanille, M. (1993). "Polymerization of Ethylene at High Temperature by Vanadium-Based Heterogeneous Ziegler-Natta Catalysts. I. Study of Deactivation Process." *J. Polym. Sci. A: Polym. Chem.* **31**: 831-839.

Bergemann, C., Cropp, R. and Luft, G. (1995). "Copolymerization of Ethylene and Linear 1-Olefins with a Metallocene Catalyst System under High Pressure. Part

I. Copolymerization of Ethylene and Propylene." *J. Mol. Cat. A: Chem.* **102**: 1-5.

Bergstra, M. F. and Weickert, G. (2004). Gas-Phase Polymerization of Ethylene and 1-Hexene with a Heterogeneous Metallocene Catalyst. <u>Ziegler Natta Catalysts</u>. Terano, M. and Busico, V. Kanazawa, JAIST.

Charpentier, P. A., Zhu, S., Hamielec, A. E. and Brook, M. A. (1997). "Continous Solution Polymerization of Ethylene Using Metallocene Catalyst System, Zirconocene Dicloride/Methylaluminoxane/Trimethylaluminum." *Ind. Eng. Chem. Res.* **36**(12): 5074-5082.

Dumas, C. and Hsu, C. C. (1989). "Propylene Polymerization in a Semibatch Slurry Reactor over Supported TiCl4/MgCl2/Ethylbenzoate/Triethyl Aluminum Catalyst. I. Catalytic Behavior." *J. Appl. Polym. Sci.* **37**: 1605-1623.

Grünig, H. and Luft, G. (1986). Polymerization of Ethylene with Ziegler-Natta Catalysts under High Pressure. <u>Polymer Reaction Engineering</u>. Reichert, K.-H. and Geiseler, W. Heidelberg, Hüthig and Wepf**:** 293-297.

Hasegawa, S., Sone, M., Tanabiki, M., Sato, M. and Yano, A. (2000). "High Temperature Ethylene/a-Olefin Copolymerization with a Zirconocene Catalyst: Effect of the Zirconocene Ligand and Polymerization Conditions on Copolymerization Behavior." *J. Polym. Sci. A: Polym. Chem.* **38**: 4641-4648.

Jaber, I. A. and Ray, W. H. (1993a). "Polymerization of Olefins through Heterogeneous Catalysis. XII. The Influence of Hydrogen in the Solution Copolymerization of Ethylene." *J. Appl. Polym. Sci.* **49**: 1695-1707.

Jaber, I. A. and Ray, W. H. (1993b). "Polymerization of Olefins through Heterogeneous Catalysis. XIII. The Influence of Comonomer in the Solution Copolymerization of Ethylene." *J. Appl. Polym. Sci.* **49**: 1709-1724.

Jaber, I. A. and Ray, W. H. (1993c). "Polymerization of Olefins through Heterogeneous Catalysis. XIV. The Influence of Temperature in the Solution Copolymerization of Ethylene." *J. Appl. Polym. Sci.* **50**: 201-215.

Jaber, I. A. and Ray, W. H. (1993d). "Polymerization of Olefins through Heterogeneous Catalysis. XV. The Influence of Pressure in the Solution Copolymerization of Ethylene." *J. Appl. Polym. Sci.* **50**: 217-231.

Kissin, Y. V. and Beach, D. L. (1984). "Kinetics of Ethylene Polymerization at High Temperature with Ziegler-Natta Catalysts." *J. Appl. Polym. Sci.* **29**: 1171-1182.

Luft, G., Bataraseh, B. and Cropp, R. (1993). "High Pressure Polymerization of Ethylene with a Homogeneous Metallocene Catalyst." *Angew. Makromol. Chem.* **212**: 157-166.

Machon, J. P. (1976). "Polyéthylènes Preparés par Catalyse Ziegler a Haute Température." *Eur. Polym. J.* **12**: 805-811.

Machon, J. P., Hermant, R. and Houzeaux, J. P. (1975). "Etude des Activités Catalytique du Triclorure de Titane Violet dans la Polymérisation Haute Température de l'Ethylène." *J. Polym. Sci.: Symp.* **52**: 107-117.

Pater, J. T. M., Weickert, G. and van Swaaij, W. P. M. (2003). "Propene Bulk Polymerization Kinetics: Role of Prepolymerization and Hydrogen." *AIChE Journal* **49**(1): 180-193.

Ribeiro, M. R., Deffieux, A., Fontanille, M. and Portela, M. F. (1996). "Kinetic Investigation of Parameters Governing the High-Temperature Polymerization of Ethylene Initiated by Supported VCl3 Catalytic Systems." *Eur. Polym. J.* **32**(7): 811-819.

Samson, J. J. C., Weickert, G., Heerze, A. E. and Westerterp, K. R. (1998). "Liquid-Phase Polymerization of Propylene with a Highly Active Catalyst." *AIChE Journal* **44**(6): 1424-1437.

Wang, W. J., Kolodka, E., Zhu, S. and Hamielec, A. E. (1999). "Continous Solution Copolymerization of Ethylene and Octene-1 with Constrained Geometry Metallocene Catalyst." *J. Polym. Sci. A: Polym. Chem.* **37**: 2949-2957.

Wang, W. J., Yan, D., Zhu, S. and Hamielec, A. E. (1998). "Kinetics of Long Chain Branching in Continuous Solution Polymerization of Ethylene Using Constrained Geometry Metallocene." *Macromolecules* **31**: 8677-8683.

Weickert, G. (2003). High Precision Polymerization Rate Profiles. Ziegler Natta Catalysts. Terano, M. and Busico, V. Kanazawa, JAIST.

Weickert, G. (2004). The First Seconds in the Life of Active Sites. MOSPOL, Moskou.

Whiteley, K. S. (2002). Polyolefins - Polyethylene. Ullmann's Encyclopedia of Industrial Chemistry, InterScience Wiley-VCH Verlag GmbH.

Chapter 5

Samenvatting

De jaarlijkse wereldwijde productie polyethyleen bestaat tegenwoordig uit ongeveer 31 miljoen ton hoge-dichtheid polyethyleen (HDPE) en 19,6 miljoen ton lineaire lage-dichtheid polyethyleen (LLDPE). Beide polymeren worden met behulp van katalytische polymerisatieprocessen geproduceerd. Veel polyethyleen (PE) producten worden gebruikt in de verpakkingsindustrie (film, tassen, afdichtingen, flessen, drums, etc.) vanwege de lage kostprijs van het PE. Andere belangrijke markten zijn de auto-industrie en buizen en pijpen (voor water, gas etc.), omdat PE een goede chemische resistentie en sterkte heeft. Deze en meer geavanceerde producten vereisen superieure polymeereigenschappen, die in hoge mate bepaald worden door de procescondities tijdens de polymerisatiereactie, door de reactiekinetiek en door de katalysator. Ondanks vele jaren onderzoek is slechts een beperkt aantal onderzoeksgroepen in staat om informatie over de polymerisatiekinetiek en polymeereigenschappen onder industriële en constante procescondities te verschaffen.

Dit werk beschrijft een opstelling die is ontwikkeld voor homo- en co-polymerisaties van ethyleen en 1-hexeen in slurry- en gasfase. Polymerisatie-experimenten zijn uitgevoerd in semi-batch mode met een heterogene metalloceenkatalysator onder industriële procescondities. Tijdens de polymerisaties in gasfase zijn de concentraties monomeer online gemeten en gestuurd. De activiteit van beide monomeren is gemeten met flowmeter techniek.

De gepresenteerde polymerisatiekinetiek is op een zeer nauwkeurige manier gemeten onder isotherme ($\pm$ 0,2 K) en isobare condities ($\pm$ 0,15 bar). De concentraties monomeer en co-monomeer zijn constant gehouden binnen 5% van het betreffende setpoint. De metingen van de polymerisatiekinetiek zijn met hoge reproduceerbaarheid gedaan. De reactiviteit van ethyleen was 50% hoger in de aanwezigheid van 1 mol% 1-hexeen vergeleken met een homo-polymerisatie: dit is 'het co-monomeer effect'.

Homo-polymerisaties

Ethyleen homo-polymerisaties zijn uitgevoerd met de Ind_2ZrCl_2/MAO op silica gedragen katalysator met behulp van de 'Reactieve Bed Preparatie' methode. Deze RBP methode combineert een slurryfase polymerisatie met een gasfase polymerisatie, met dezelfde polymeriserende deeltjes, d.w.z. een reactief bed.

De polymerisatiekinetiek is met hoge nauwkeurigheid en reproduceerbaarheid gemeten. De slurry- en gasfase polymerisatiesnelheden lieten dezelfde afhankelijkheid van de concentratie monomeer zien. Een complexatiemodel is voorgesteld om de waargenomen niet-eerste orde afhankelijkheid van de bulkconcentratie van de monomeer te beschrijven. Dit model kan ook de niet-Arrhenius afhankelijkheid van de temperatuur verklaren. Als gebruik wordt gemaakt van een standaard

polymerisatiesnelheidsmodel: $R_p = k_p \cdot C^* \cdot M$, wordt de activativeringsenergie afhankelijk van de bulkconcentratie.

Gasfase co-polymerisaties

Ethyleen/1-hexeen co-polymerisaties zijn uitgevoerd met dezelfde Ind_2ZrCl_2/MAO op silica gedragen katalysator in gasfase. De invloed van de co-monomeer is onderzocht onder industriële condities. De profielen van de reactiesnelheid zijn gemeten voor beide monomeren, en deze vertonen een stijgende activiteit met stijgende concentratie co-monomeer. Het complexatiemodel is uitgebreid voor de co-monomeer. Dit uitgebreide model kan de grote stijging van de reactiesnelheid verklaren, zelfs als slechts een kleine hoeveelheid co-monomeer wordt ingebouwd in het polymeer. De co-polymerisatievergelijking, afgeleid van het complexatiemechanisme, is afhankelijk van de twee reactiviteitsratio's, van de monomeerratio en van een ratio van de homo-polymerisatieconstanten. Dit is in tegenstelling tot de co-polymerisatievergelijking afgeleid van een eerste orde Markov mechanisme, die slechts afhankelijk is van de reactiviteitsratio's en van de monomeerratio. Het complexatiemodel beschreef de gemeten reactiesnelheden voor beide monomeren en ook de gewichtsfractie van de ingebouwde 1-hexeen redelijk goed. De geproduceerde polymeren zijn geanalyseerd op eigenschappen zoals dichtheid, molekuulgewicht, smeltpunt en gewichtsfractie van de ingebouwde co-monomeer, die alle zeer afhankelijk bleken te zijn van de concentratie 1-hexeen in gasfase en derhalve van de gewichtsfractie van 1-hexeen in het polymeer.

In-situ absorptie van de co-monomeer kon worden bepaald door de kinetische informatie te combineren met de werkelijk ingebouwde co-monomeergewichtsfractie in het polymeer. De polymeereigenschappen zijn vergeleken met een LLDPE geproduceerd door een Ziegler-Natta katalysator.

Solutiefase polymerisaties

Naast de opstelling voor slurry- en gasfase ethyleen-polymerisaties is een experimentele opstelling ontwikkeld voor solutiefase polymerisaties bij hoge temperatuur, d.w.z. boven het smeltpunt van polyethyleen. Deze opstelling is uitgerust met een isotherme-isoperibole warmtecompensatie-temperatuurregeling. Dit houdt in dat de temperatuur in de reactor wordt geregeld door een intern verwarmingselement zodanig dat de totale warmteproductie, dus de chemische en elektrische warmte, in de reactor constant wordt gehouden voor en na injectie van de katalysator.

Een kinetische studie is uitgevoerd van de hoge-temperatuur ethyleen homo- en co-octeen-polymerisaties in solutiefase met een zeer actieve en snel deactiverende katalysator. De katalysator had een initiële polymerisatiesnelheid tot maximaal 30.000 kg·g(kat)$^{-1}$·h^{-1} en de activiteit daalde binnen 2 minuten met 80% bij 180°C en 30 bar. Deze nieuwe reactor maakt het mogelijk om reproduceerbaar polymerisatiesnelheidscurven te meten enkele seconden na injectie van de katalysator bij een initiële warmteproductie van 3,8 kW onder isotherme (±1 K) en isobare condities (±0,05 bar). De activiteitsafname van de katalysator kon beschreven worden met een tweede-orde deactivatiemodel.

Dankwoord

Ruim 5 jaar geleden werd mij door Günter Weickert de kans aangeboden om binnen drie jaar te gaan promoveren. Ik zou wel hard moeten werken, maar er was al wat voorwerk gedaan. Dat pakte even anders uit. Nu, 5 jaar later en veel ervaring rijker, heb ik mijn proefschrift afgerond en hiermee is ook een periode van 10 jaar aan de Universiteit Twente afgesloten.

Günter, ik wil je heel hartelijk bedanken voor de kans en het vertrouwen die je me hebt gegeven. Eind 2001 zag het project er niet zo rooskleurig uit. Echter, na een bezoek in Ferrara zijn we er achter gekomen dat 3 jaar te kort was en heb je me de mogelijkheid gegeven om binnen de staf mijn promotiewerk te voltooien, met dit proefschrift als resultaat.
Tijdens de vele discussies heb ik veel van je opgestoken en veel geleerd van je ideeën over experimenteren en modellen. En natuurlijk ben ik ook een beetje besmet geraakt met het enthousiasme over polyolefinen. Je stimulerende enthousiasme en creativiteit hebben in zeer hoge mate bijgedragen tot dit resultaat.
Gedurende de laatste 2 jaar hebben we nog nauwer samengewerkt en hebben we ook onvergetelijke reizen gemaakt. Vooral de reis naar China en Japan was bijzonder. Die reis heeft tot het complexatiemodel geleid, dat we in het vliegtuig van Shanghai naar Osaka hebben afgeleid. (Waar een reis al wel niet goed voor is!)

I would like to thank the commission for their participation, their interest in my work and for their time: professor L.L. Böhm, professor K.H. Reichert, G. Mei, F. van Buren, professor W.P.M. van Swaaij, professor J. Noordermeer, and professor U. Karst.

Within my Ph.D. project I have been working in a cooperation with Basell Polyolefins. I would like to thank M. Schopf, H. Schmitz and G.B. Meier for the discussions and interest. Also I would like to thank C. Gabriel and D. Lilge for the polymer analyses and the interpretation.
During the last year I have also worked in a project with Dow Benelux. I would like to thank Pim Hagemans, Tonnie Vink, Frits van Buren and Henk Hagen for their contribution in the discussions.

Aangezien ik veel experimenteel werk heb gedaan, heb ik veel van mijn tijd doorgebracht in het Hogedruklaboratorium. Ik wil iedereen van het HDL graag hartelijk bedanken voor alles wat jullie voor mij hebben gedaan. Daar ik redelijk lang in de groep ben geweest hebben jullie allemaal veel voor mij gedaan. Gert Banis, Karst van Bree, Johan Agterhorst, Jeffry Karstenberg, Fred ter Borg en Geert Monnink hartelijk dank voor alle hulp, koffie en taart!

In het bijzonder wil ik Fred bedanken. Zonder jouw technische vaardigheden en inzicht was dit werk niet tot stand gekomen. Je hebt beide reactoren opgebouwd en ik mag nu wel zeggen dat dat tot een goed resultaat geleid heeft. Dank je wel!

De solutiefase experimenten zijn grotendeels door Geert uitgevoerd. Ik vond het een plezierige samenwerking en ik wil je bedanken voor je hulp.

Tijdens de opbouwfases van de reactoren en als staflid heb ik ook veel samengewerkt met Gert Banis. Ik heb hier veel van geleerd over veiligheid. Daarnaast hadden we ook vaak leuke gesprekken, en niet te vergeten de BBQ's en de uitjes!

I had a great help from my graduate students: Marçal Carmaniu Fàbrega, Neus Comas Roma, Roger Bringue Tomas and Shankara N. Keelapandal Ramamoorthy. Although not all your work is in this thesis I have learned a lot during your graduation projects. Thank you for your help.

Furthermore I would like to thank my (ex-)colleagues from the IPP group: my room mate Makarand Pimplapure, Rob Emonds, Yayha Banat, Ravi Tupe, Mohammad Al-haj Ali, Parasu Veera, Inge van Putten, Bert Koning and Arthur Iordanidi. Ik wil ook graag Wies Elfers en Annet Rip bedanken voor de samenwerking gedurende mijn periode als staflid.

Verder hebben een heel aantal mensen binnen de voormalige CT-faculteit mij geholpen met allerlei zaken. Ook hen wil ik graag bedanken: van inkoop Wim Platvoet en Nellie Vos; van SGA Jan Heezen, Joachim Olde Bolhaar, Gilbert van den Dobbelsteen en Mark Hulshof; en van PA&O Odette Scholten (voor de hulp bij alle contracten).

Twee oud-collega's wil ik extra hartelijk danken voor al hun discussies en hulp tijdens mijn gehele promotie. Gerben Meier, dank je wel voor alle hulp, vooral bij hoofdstuk 4, jouw inzet heeft geleid tot de polymeeranalyses en hun interpretatie en tot het goed op papier krijgen hiervan. Jochem Pater dank je wel voor alle discussies, voor goede raad en voor het zoeken naar fouten in mijn proefschrift.

Mijn paranimfen Jelmer 'Fudd' Scholte en Shankara N. Keelapandal Ramamoorthy wil ik graag bedanken voor hun inzet en hulp. Fudd bedankt voor het corrigeren van de samenvatting! Shankar thanx so much for all your help!

Ik wil graag mijn ouders bedanken voor alle steun gedurende mijn studie en promotie, en omdat jullie er altijd voor me zijn. Tenslotte wil ik Roxane bedanken. Roxane, bedankt voor je steun, je begrip en je vertrouwen in de toekomst.

<div align="right">

Michiel F. Bergstra

Helsinki, oktober 2004

</div>

Curriculum Vitae

Michiel F. Bergstra was born in Ede at the 23rd of March 1976. After completing the primary school O.B.S. Poalsbrêge in Drachten in 1988, he went to 'O.S.G. Het Drachtster Lyceum', where he got the VWO diploma in 1994.

Next Michiel started studying Chemical Engineering at the Universiteit Twente. During his studies he did an internship at Clariant A.G. in Basel, Switzerland. In September 1999 he finished his studies by defending his master thesis: 'Gas Phase Polymerization of Propylene with a Heterogeneous Metallocene Catalyst - Influence of Hydrogen'.

In November 1999 Michiel started as Ph.D. student in the group of professor Weickert and professor van Swaaij, Industrial Polymerization Processes. The already running Ph.D. project was a cooperation between Elenac (now Basell Polyolefins) and the UT. In May 2002 Michiel became partly member of the scientific staff of the research group IPP of professor Weickert at the University Twente.

Since September 2004 Michiel has been employed at Polyolefins R&D of Borealis Polymers Oy in Porvoo, Finland.